



DIGITAL ACCESS TO SCHOLARSHIP AT HARVARD

Functional and genomic analysis of MEF2 transcription factors in neural development

The Harvard community has made this article openly available.
[Please share](#) how this access benefits you. Your story matters.

Citation	No citation.
Accessed	February 17, 2015 1:07:09 AM EST
Citable Link	http://nrs.harvard.edu/urn-3:HUL.InstRepos:13070059
Terms of Use	This article was downloaded from Harvard University's DASH repository, and is made available under the terms and conditions applicable to Other Posted Material, as set forth at http://nrs.harvard.edu/urn-3:HUL.InstRepos:dash.current.terms-of-use#LAA

(Article begins on next page)

HARVARD UNIVERSITY
Graduate School of Arts and Sciences

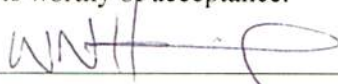


DISSERTATION ACCEPTANCE CERTIFICATE

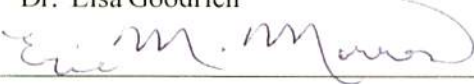
The undersigned, appointed by the
Division of Medical Sciences
Committee on Immunology
have examined a dissertation entitled

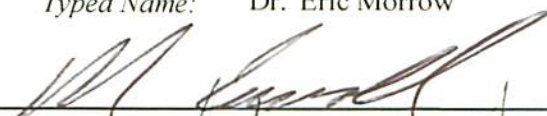
*Functional and genomic analysis of MEF2 transcription
factors in neural development*

presented by Milena Maria Andzelm
candidate for the degree of Doctor of Philosophy and hereby
certify that it is worthy of acceptance.

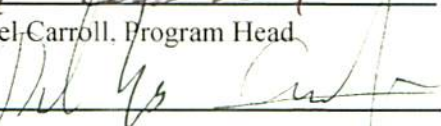
Signature: 
Typed Name: Dr. Nick Haining

Signature: 
Typed Name: Dr. Lisa Goodrich

Signature: 
Typed Name: Dr. Eric Morrow


Dr. Michael Carroll, Program Head

Date: June 26, 2014


Dr. David Lopes Cardozo, Director of Graduate Studies

Functional and genomic analysis of MEF2 transcription factors in neural development

A dissertation presented

by

Milena Maria Andzelm

to

The Division of Medical Sciences

in partial fulfillment of the requirements

for the degree of

Doctor of Philosophy

in the subject of

Immunology

Harvard University

Cambridge, Massachusetts

June 2014

© 2014 Milena Maria Andzelm

All rights reserved.

Functional and genomic analysis of MEF2 transcription factors in neural development

Abstract

Development of the central nervous system requires the precise coordination of intrinsic genetic programs to instruct cell fate, synaptic connectivity and function. The MEF2 family of transcription factors (TFs) plays many essential roles in neural development; however, the mechanisms of gene regulation by MEF2 in neurons remain unclear. This dissertation focuses on the molecular mechanisms by which MEF2 binds to the genome, activates enhancers, and regulates gene expression within the developing nervous system.

We find that one MEF2 family member in particular, MEF2D, is an essential regulator of the development and function of retinal photoreceptors, the primary sensory neurons responsible for vision. Despite being expressed broadly across many tissues, in the retina MEF2D binds to retina-specific enhancers and regulates photoreceptor-specific transcripts, including critical retinal disease genes. Functional genome-wide analyses demonstrate that MEF2D achieves tissue-specific binding and action through cooperation with a retina-specific TF, CRX. CRX recruits MEF2D away from canonical MEF2 binding sites by promoting MEF2D binding to retina-specific enhancers that lack a strong consensus MEF2 binding sequence. MEF2D and CRX then synergistically co-activate these enhancers to regulate a cohort of genes critical for normal photoreceptor development. These findings demonstrate that MEF2D, a broadly expressed TF, contributes to retina-specific gene expression in photoreceptor development by binding to and activating tissue-specific enhancers cooperatively with CRX, a tissue-specific co-

factor.

A major unresolved feature of MEF2D function in the retina is that the number of MEF2D binding sites significantly exceeds the number of genes that are dependent on MEF2D for expression. We investigated causes of this discrepancy in an unbiased manner by characterizing the activity of MEF2D-bound enhancers genome-wide. We find that many MEF2D-bound enhancers are inactive. Furthermore, less than half of active MEF2D-bound enhancers require MEF2D for activity, suggesting that significant redundancies exist for TF function within enhancers. These findings demonstrate that observed TF binding significantly overestimates direct TF regulation of gene expression. Taken together, our results suggest that the broadly expressed TF MEF2D achieves tissue specificity through competitive recruitment to enhancers by tissue-specific TFs and activates a small subset of enhancers to regulate genes.

Table of Contents

Abstract	iii
List of Figures	vi
List of Tables	vii
Acknowledgments	viii
Attributions	x
Chapter 1	
Introduction	1
Preface	
1.1 Cell type-specific gene regulation	
1.2 Introduction to MEF2 transcription factors	
1.3 MEF2 transcription factors in muscle	
1.4 MEF2 transcription factors in the hematopoietic system	
1.5 MEF2 transcription factors in the nervous system	
1.6 Gene regulation in photoreceptor development	
1.7 Summary of the dissertation	
Chapter 2	
MEF2 regulates retinal photoreceptor development through synergistic binding and selective activation of tissue-specific enhancers	48
2.1 Abstract	
2.2 Background & Rationale	
2.3 Results	
2.4 Discussion	
2.5 Experimental Procedures	
Chapter 3	
Features of widespread MEF2D binding and differential function at enhancers	135
3.1 Abstract	
3.2 Background & Rationale	
3.3 Results	
3.4 Discussion	
3.5 Experimental Procedures	
Chapter 4	
Conclusion	165
Bibliography	171

List of Figures

Figure 1.1. Indirect mechanisms of TF cooperativity at enhancers	10
Figure 1.2. Models of enhancer activation	12
Figure 1.3. Basic structure and conservation of MEF2 family members	18
Figure 1.4. Dual functions of MEF2 as both activator and repressor	20
Figure 1.5. Diverse mechanisms of MEF2 regulation	21
Figure 1.6 Structure of the retina and retinal photoreceptors	40
Figure 1.7. Timeline of retinal development	42
Figure 2.1. Expression of MEF2 family members in the retina	55
Figure 2.2. Generation and validation of new <i>Mef2d</i> knockout and conditional mice	58
Figure 2.3. <i>Mef2d</i> KO mice have defects in retinal photoreceptor development	63
Figure 2.4. <i>Mef2d</i> KO mice are functionally blind	66
Figure 2.5. <i>Mef2d</i> is required cell autonomously for photoreceptor development	68
Figure 2.6. MEF2D regulates critical cell type-specific targets and disease genes in the retina ..	73
Figure 2.7. MEF2D binds broadly throughout the retinal genome	83
Figure 2.8. MEF2D binds tissue-specific enhancers	89
Figure 2.9. CRX mediates a genome-wide competition for MEF2D binding to retina-specific sites	93
Figure 2.10. MEF2D regulates retinal gene expression by selective activation of enhancers	99
Figure 2.11. CRX determines the selective activation of MEF2D-bound enhancers	103
Figure 2.12. MEF2D and CRX coordinate gene expression through enhancer co-binding and co-activation	108
Figure 2.13. Model of MEF2D-CRX co-regulation of photoreceptor target genes	110
Figure 3.1. MEF2D predominantly binds enhancers throughout the retinal genome	141
Figure 3.2. Identification of active MEF2D-bound enhancers genome-wide	144
Figure 3.3. Motif enrichment in active versus inactive MEF2D-bound enhancers	147
Figure 3.4. Properties of active and inactive enhancers normalized by size of MEF2D peak ...	150
Figure 3.5. MEF2D is required for enhancer activity at a subset of its bound enhancers	154
Figure 3.6. MEF2D-dependent regulatory elements are enriched for conserved MREs	157

List of Tables

Table 2.1. Significantly misregulated genes in MEF2D KO versus WT retinae	76
Table 2.2. Direct MEF2D target genes and associated MEF2D-bound regulatory elements	85

Acknowledgements

I have been fortunate to have extensive support from many individuals during graduate school. First and foremost, I would like to thank Michael Greenberg for his constant support and mentorship even as my project veered in unexpected directions. Being in his lab has been an amazing experience and I have learned an incredible amount from him about how to do science as well as how to be a scientist. Talking with Mike inevitably yields either great experiment ideas, or helpful advice on how to give presentations or write papers, or insightful career advice. Often all three result from one conversation. I hope to continue to have many such conversations with him in the future.

One of the great strengths of the Greenberg lab is its members, who have been great colleagues and friends and from whom I have learned a great deal. In particular, Steve Flavell was very helpful and a great teacher at the beginning of my time in the lab. I would like to especially thank Eric Griffith, Yanni Salogiannis and Emi Ling for helpful advice in the writing of this thesis. I would also like to thank Sonia Cohen, Athar Malik, and Shannon Robichaud for always being willing to answer any of my numerous questions.

Finally, I would like to thank the eye team for making the lab a particularly exciting and fun place to be over the past few years. I have learned a tremendous amount from Tim Cherry and consider myself very lucky that he came to this lab. Annabel Boeke and Charlotte Lee were also essential to pushing our project forward and fantastic to work with. David Harmin was instrumental in helping us analyze and think about our data and was always willing to answer my many questions and help me learn to analyze the data myself.

My Dissertation Advisory Committee –Beth Stevens, Vijay Kuchroo and Connie Cepko- always provided me with valuable advice and insights. I would especially like to thank Connie Cepko for serving as my thesis defense chair. I am also very grateful to Lisa Goodrich, Eric Morrow and Nick Haining for finding time in their busy schedules to serve on my thesis defense committee. Several faculty members have also been very generous with time and knowledge in less formal capacities. Elio Raviola impressed upon me the value of aesthetics in science. Chinfei Chen has been a wonderful role model in her enthusiasm for science and mentoring.

My first in-depth research experience was in college, and this provided me with a solid foundation for graduate school as well as an enduring love for NK cells. For this I am extremely grateful to Jordan Orange and Jack Strominger, who took the time to teach me and build my confidence as a scientist with incredible patience and enthusiasm.

I would like to thank Dominico Vigil for his unwavering faith in me and his encouragement throughout this writing process. I would also like to thank my parents, Jan Andzelm & Elżbieta Radzio-Andzelm for always supporting me and seeking to provide me with every opportunity possible. Their hard work and sacrifices have made it possible for me to be in this position. Finally, I would like to thank my grandparents, Leon & Leokadia Andzelm and Czesław & Celina Radzio, who worked equally hard to support my parents in their educational and life goals and were excellent role models in perseverance and demonstrating great strength of character in difficult circumstances. In particular, this thesis is dedicated to my grandfather Czesław, who was my first role model in medicine and continues to be a great source of inspiration today.

Attributions

In Chapter 1, **Figure 1.1** and **Figure 1.2** are adapted from (Spitz and Furlong, 2012). **Figure 1.3** is from (Potthoff and Olson, 2007). **Figure 1.4** is from (McKinsey et al., 2002). **Figure 1.5** is from (Rashid et al., 2014). **Figure 1.6** and **Figure 1.7A** are from (Swaroop et al., 2010).

Chapters 2 and 3 are the result of an equal collaboration between Milena Andzelm and Timothy Cherry under the supervision of Michael Greenberg.

MEF2D knockout mice were generated by Milena Andzelm, Athar Malik and Steve Flavell. Histology was performed by Milena Andzelm with the help of Elio Raviola. Basil Pawlyk performed and analyzed the electroretinograms. Charlotte Lee analyzed cell-autonomous development of photoreceptors *in vivo* with help from Milena Andzelm and Timothy Cherry. Milena Andzelm performed all other immunohistochemistry and western experiments. Timothy Cherry and Annabel Boeke generated the luciferase reporters and quantified their activity in retinal explants *in vitro*.

ChIP and RNA experiments were performed by Timothy Cherry with help from Milena Andzelm and Annabel Boeke. David Harmin processed the RNA-seq data and determined gene exon density. He also developed the programs to analyze eRNAs with help from Milena Andzelm. Martin Hemberg performed initial processing of MEF2D ChIP-Seq experiments. Processing of all other ChIP-Seq data, bioinformatics data analysis and figure generation from RNA-Seq and ChIP-Seq experiments (in Figures 2.7-2.12, as well as all figures in Chapter 3) was performed by Milena Andzelm. Figure 2.13 was produced with the help of Janine Zieg.

Chapter 1

Introduction

Preface

How a single cell develops into a complex multicellular organism is a remarkable process mediated by extensive cell division and differentiation into a diverse array of cell types. The specification of unique cell types, their subsequent differentiation, and their acquisition of varied functions is fundamentally determined by distinct gene expression programs. These programs of gene expression are orchestrated by transcription factors (TFs), which combinatorially regulate genes by acting on associated DNA regulatory elements, promoters and enhancers. The expression of some transcription factors is limited to one or a few cell types, and their presence may lead to expression of cell type-specific genes. Many other transcription factors, however, are widely expressed, and so how they contribute to cell type-specific gene expression programs is less clear. Advances in molecular biology, which allow genome-wide analyses of transcription factor function, have provided new insights into tissue-specific mechanisms of gene regulation, including the central role of enhancers. How broadly expressed TFs work to selectively regulate enhancers and genes in a tissue-specific manner remains a question of great interest, and insights into this process should shed light on how cells acquire specific functions and how this might be disrupted in human disease.

The myocyte enhancer factor-2 (MEF2) family of broadly expressed transcription factors is made up of four family members in vertebrates, MEF2A, B, C, and D. MEF2 family members are highly conserved and important for a variety of functions across cell types, including differentiation and response to extracellular stimuli. In the nervous system, MEF2 factors are critical for neuronal survival, synaptic plasticity and memory formation; their importance is underscored by the discovery that mutations in MEF2 factors cause inherited neurological

disease (Bienvenu et al., 2013; Novara et al., 2010). Furthermore, the function of MEF2 family members in neurons can be regulated by stimuli critical to neuronal development and synaptic maturation, for example growth factors or synaptic activity (Flavell et al., 2006). Given the importance of MEF2 transcription factors in the nervous system, elucidating how MEF2 regulates neuronal-specific gene expression is of great interest. However, insight into MEF2 transcriptional mechanisms in a biologically significant context in the CNS has remained challenging, largely due to the difficulties of studying transcriptional mechanisms in the heterogeneous neuronal populations of the CNS, as well as the overlap in MEF2 family member expression patterns throughout the nervous system.

The molecular mechanisms by which MEF2 transcription factors regulate gene expression have however been studied in myocytes and lymphocytes. Although these studies were generally limited to *in vitro* paradigms using reporters and MEF2 overexpression, they have nonetheless provided insight into how the function of MEF2 might be specified in a given cell type. This work found that MEF2 family members both repress and activate target genes through interactions with co-factors, which can differ across cell types (Molkentin et al., 1995; Morin et al., 2000). MEF2 family members regulate these co-factor interactions as well as their DNA binding affinity in multiple ways, but most commonly through differential posttranslational modifications. Whether these or other mechanisms contribute to how MEF2 family members regulate gene expression in neurons is not yet well elucidated.

In this introduction, I first provide an overview of the molecular mechanisms of gene regulation, particularly mechanisms by which TFs achieve tissue-specific function (Chapter 1.1). Next, I provide an overview of research related to the MEF2 family members, including studies of MEF2 function in muscle

and hematopoietic cells that highlight mechanistic knowledge of how MEF2 family members regulate gene expression and achieve tissue-specific function in non-neural systems (Chapters 1.2-1.4). I then review the key roles of MEF2 family members in neuronal biology, and the limited mechanistic information known for how MEF2 family members regulate gene expression in the nervous system (Chapter 1.5).

Finally, I will introduce retinal photoreceptors, one neuronal cell type in the CNS that we have found specifically expresses a single MEF2 family member, MEF2D. I review the development of photoreceptors and how they have emerged as an excellent paradigm for studying transcriptional mechanisms in neural development (Chapter 1.6). This dissertation focuses on applying genome-wide analyses to elucidate the molecular mechanisms of MEF2-mediated gene expression in the nervous system, using retinal photoreceptors as our model for neural development.

1.1 Cell type-specific gene regulation

While each cell begins with essentially the same DNA sequence, an extensive array of distinct cell types is generated in the development of an organism. Elucidating how cell type-specific programs of gene expression are established is currently an area of extensive research, including in the nervous system. In recent years, distal DNA regulatory elements known as enhancers and their interactions with transcriptional promoters as well as other co-regulatory regions have been suggested to be major contributors to cell type specificity (Bulger and Groudine, 2011).

Characterization of regulatory elements

Transcription factors bind to regulatory elements within the genome to drive gene expression. These elements include promoters, which are located at the transcriptional start site of genes, and enhancers, which act over a greater distance in an orientation-independent manner (Banerji et al., 1981; Moreau et al., 1981). These regulatory elements are hubs that allow transcription factors to dock to the genome, to interact with one another and to recruit components of the basal transcriptional complex (Spitz and Furlong, 2012). These regions of DNA are also powerful substrates for evolutionary change because changes in the DNA sequence can modify the regulation of a gene without compromising its coding sequence (Baker et al., 2012). How transcription factors identify and regulate these regions of DNA in neurons is only beginning to be understood and is hampered in part by the cellular heterogeneity that makes up the CNS. A better understanding of these regulatory elements would do a great deal to unlock

the gene regulatory logic that drives specific expression programs in neurons.

The first step toward understanding the role of DNA regulatory elements in the nervous system is their identification. Promoters can be identified by their proximity to target genes. Enhancer elements have been harder to identify because they may act at a great distance from their target genes (Lettice et al., 2003). However, the task of identifying enhancers on a genome-wide scale has recently become possible through the advances of high-throughput DNA sequencing technology coupled to both chromatin immunoprecipitation (ChIP-Seq) and DNase-hypersensitivity assays (DNase-Seq) (Johnson et al., 2007; Mikkelsen et al., 2007; Robertson et al., 2007). Enhancer elements can now be exhaustively identified throughout the genome of a given cell type or tissue using these assays according to their epigenetic signatures. Nucleosomes bordering enhancer elements are enriched for mono-methylation at lysine 4 of histone 3 (H3K4me1) while promoters tend to have tri-methylated H3K4 (H3K4me3) (Heintzman et al., 2007). Furthermore, active enhancers and promoters can be distinguished from inactive ones by ChIP-Seq for acetylation or methylation at lysine 27 of histone 3, modifications that correlate with either active or inactive loci, respectively (Rada-Iglesias et al., 2011). Lastly, active enhancers and promoters may also be distinguished from inactive ones by their transcription of bi-directional enhancer RNAs (eRNAs) or promoter anti-sense RNAs (pasRs) (Kim et al., 2010; Li et al., 2013; Wang et al., 2011). The discovery that eRNAs and H3K27Ac are robust markers of enhancer activation has allowed a new level of insight by allowing the evaluation of regulatory element activity in the context of the endogenous genome. Together these tools facilitate the identification of how transcription factors bind to enhancers and promoters, regulate their activity and influence target gene expression.

Competition for TF binding

One important modulator of TF binding is the existence of competition for TFs in the nucleus. In general, there are 10,000 to 50,000 molecules of each TF in a cell, although some can be as high as 300,000 (Biggin, 2011). There is still controversy over whether TF concentration is limiting with respect to the number of available binding sites (Biggin, 2011), however studies suggest that for any single TF, >90% of molecules are bound to DNA. A large portion of this binding is suggested to be non-functional and designed to limit the concentration of free TF molecules in the nucleus (Kao-Huang et al., 1977; Liu et al., 2007).

A recent study has explored the interplay between TF number and binding site number at promoters. Brewster and colleagues titrated the concentration of TFs in *E.coli* and varied whether the TF binding site was within a chromosome or on multi-copy plasmids (Brewster et al., 2014). They found complex dosage responses to TF and plasmid copy numbers suggesting the number of binding sites for a TF can have strong effects on how a TF controls gene expression. This has important implications for previous research done examining TF activity in the context of high copy reporters and overexpression of the TF protein. The effect of limiting TF expression would certainly be lost in an artificial system of overexpressing TFs. In addition, reporter assays with high plasmid copy number would likely not reflect competitive aspects of TF binding as well. Therefore, loss of function studies at endogenous loci will be particularly important for teasing apart the endogenous function of a TF and the cooperative mechanisms it uses to drive gene expression.

Molecular mechanisms to specify function of broadly expressed TFs

There are several ways in which transcription factors may regulate cell type-specific gene expression programs in neurons. In the simplest model a lineage specific transcription factor may bind to promoters or enhancers and directly regulate a battery of proximal target genes (Hobert, 2008). For example, the homeodomain transcription factor Crx is highly enriched in photoreceptors and regulates expression of photoreceptor-specific genes (Chen et al., 1997; Freund et al., 1997; Furukawa et al., 1997). Human mutations in CRX can lead to blindness, underscoring the importance of such cell type-specific factors (Swain et al., 1997). Alternatively, a transcription factor could be differentially modified in different cell types or in response to different extrinsic stimuli in a manner that affects target gene expression. This model is powerful in that allows a single factor to regulate gene programs in more than one way. A third model of regulation requires that two or more transcription factors act cooperatively or sequentially to activate gene expression. This type of regulation allows for a diversity of transcriptional outputs. For example, if two transcription factors have overlapping but distinct expression domains then three different modes of regulation are possible; two modes where each transcription factor is working alone and a third where they regulate gene expression together. This model helps explain how a broadly expressed transcription factor may have very different roles in two distinct cell types. For example, the overlapping patterns of dorsal-ventral and rostral-caudal Hox gene expression in the developing spinal cord exemplify this type of intersectional regulation (reviewed in (Dasen and Jessell, 2009)). This type of combinatorial regulation allows for a great deal of flexibility and precision, and is likely a common mechanism for specifying gene expression in a given cell-type.

Diverse molecular mechanisms of TF cooperativity

To understand how a TF regulates a cell type-specific program of gene expression, it is critical to understand where it binds in the genome and how it is recruited to specific DNA regulatory elements. One method to identify possible sites of TF binding is by searching for known transcription factor binding motifs throughout the genome. The presence of a consensus DNA binding motif alone however is not predictive of transcription factor binding (White et al., 2013). How therefore does a transcription factor decide where to bind? Chromatin availability is one factor that limits binding. Many transcription factors can only bind their consensus motifs within open chromatin. Such a protein may therefore first require a pioneer factor to sit down and remodel the chromatin landscape (**Figure 1.1**). Another limiting factor may be the affinity of a transcription factor to a given binding motif. Transcription factors typically bind 6-12bp DNA sequences with varying degrees of degeneracy. This affinity can be increased however through cooperative binding at an enhancer. For example, multiple TFs may co-activate an enhancer and this may stabilize their binding through the formation of a larger activating complex. For example, TFs may co-recruit HATs and HDACs (Spitz and Furlong, 2012). P300 and CBP in particular have been suggested to act as bridges between TFs and have been shown to have multiple TF interaction domains (Chan and La Thangue, 2001). In these two examples the cooperativity between TFs is indirect. However, the cooperativity between TFs may also be direct. For example, direct binding between TFs may increase their affinity for DNA, allowing them to bind where they would have previously been unable to, such as to lower affinity motifs

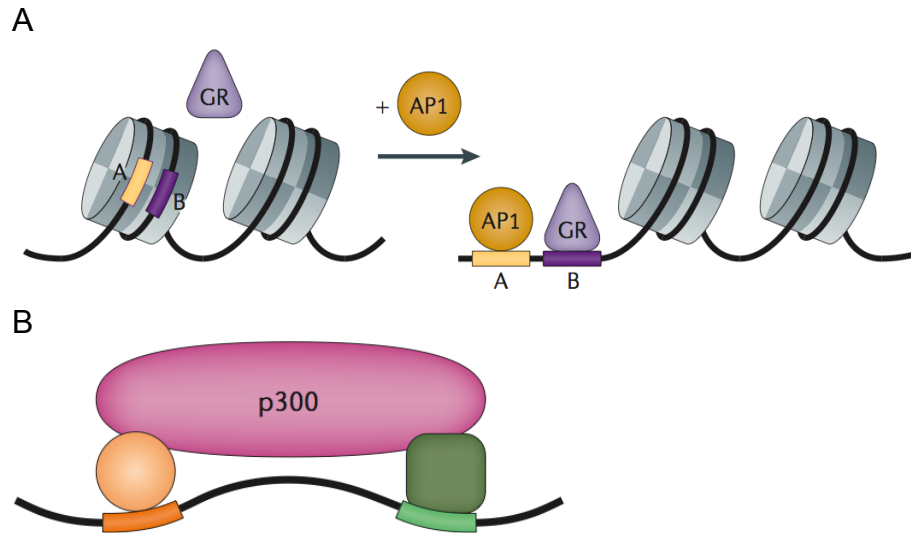


Figure 1.1. Indirect mechanisms of TF cooperativity at enhancers.

(A) Activator protein 1 (AP-1) functions as a pioneer factor for glucocorticoid receptor (GR). In the absence of AP-1, GR cannot bind its binding motif as it is in a nucleosome-bound region of DNA and inaccessible. AP-1 binding to its proximal binding motif (A) repositions the nucleosome, exposing the GR motif (B) and allowing GR to bind (Biddie et al., 2011).

(B) Co-recruitment of a co-factor may stabilize TF binding. Two TFs may initially bind DNA independently and then recruit a HAT such as CBP/p300. CBP/p300 may directly interact with both TFs at two distinct domains, and this tripartite complex may stabilize binding of the original TFs (Merika et al., 1998). References and images from (Spitz and Furlong, 2012).

or to motifs in less accessible DNA. In all of these scenarios, the consensus binding motifs of the cooperating TFs may be clustered together at enhancers.

Within a given enhancer, several possibilities for binding of many transcription factors exist (**Figure 1.2**). There may be an established motif grammar constant to all sets of a particular enhancer type, suggesting that a specific cohort of required transcription factors always binds together in a fixed arrangement to provide a consistent protein interface (Spitz and Furlong, 2012) (**Figure 1.2A**). Alternatively, a group of transcription factors may function cooperatively to activate an enhancer but with more flexibility. Not all TFs in the group may be required at an enhancer, and the position of motifs may not be consistent. In this scenario, each TF adds toward the activation of an enhancer but a strict arrangement is not required (**Figure 1.2B**). An example of this can be found in a recent study where the binding motifs for CREB, MEF2 and SRF cluster together in an enhancer regulatory element termed the synaptic-activity responsive element (SARE), but not necessarily in the same configuration at each enhancer. This set of motifs is however found proximal to many activity-regulated genes and is hypothesized to mediate a coordinated gene expression response to neuronal activity (Rodriguez-Tornos et al., 2013). Whether all three TFs are required at each of these SAREs remains to be determined. Finally, not all TFs may need to bind to the DNA directly but may interact with other TFs in the group. In this case, binding is highly cooperative and the motifs present in the enhancer are variable (**Figure 1.2C**).

Examples of co-factors facilitating binding have provided examples of TF cooperativity and illustrate the power of genome-wide analyses in assessing determinants of TF binding and cooperativity. Recent work showed that SMAD proteins have highly cell type-specific binding,

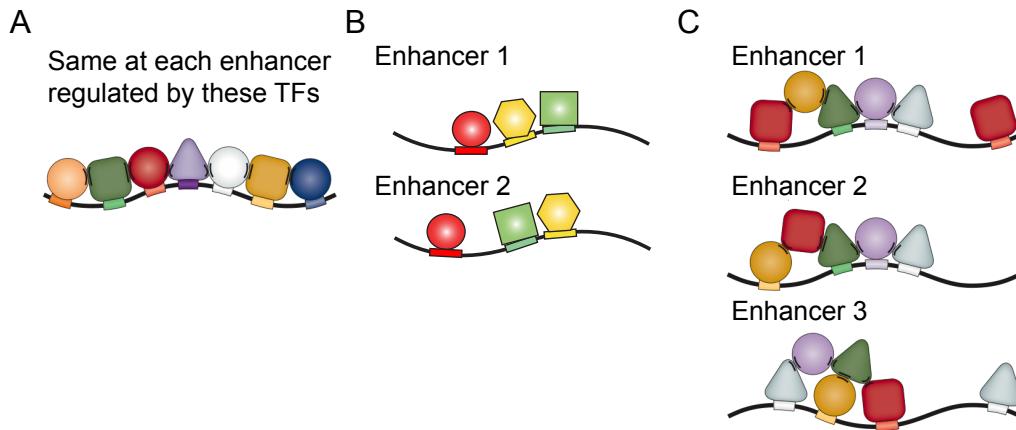


Figure 1.2. Models of enhancer activation.

Multiple models have been proposed for how TFs might cooperate to activate enhancers. These models include the following:

(A) Binding of all TFs in a set is required to form a higher-order protein interface for enhancer activation. DNA motif composition and positioning is identical at all enhancers regulated by this “enhanceosome” (Merika and Thanos, 2001).

(B) Motif positioning is flexible. All TFs bind their motifs and cooperatively contribute to enhancer activation but their specific location on the DNA relative to each other is not critical.

(C) A consistent group of TFs binds many enhancers but motif composition and positioning is variable. Not all TFs need to directly bind DNA, and not all members of the TF group are required at each enhancer for activation (Junion et al., 2012).

References and images adapted from (Spitz and Furlong, 2012).

and that this was mediated by pioneer factors which provided tissue specific DNA accessibility that revealed SMAD binding sites to specify SMAD binding as part of the TGF β response (Mullen et al., 2011). SMADs have a short, degenerate consensus binding sequence and therefore likely have a high requirement for DNA accessibility provided by pioneer factors. Additionally, recent work has examined the binding dynamics of Sox2 and Oct4 with single molecule imaging in ES cells and demonstrated that Sox2 searches the DNA, binds, and then assists Oct4 in more directed binding, which leads to a stabilized Sox2-Oct4 complex bound to DNA (Chen et al., 2014). Finally, a recent paper demonstrated sequence-independent binding of estrogen receptor alpha (ER α) (Gertz et al., 2013). ER α binds to shared sites with high-affinity response elements (EREs) or at cell type specific sites without EREs that are more accessible and co-bound by other factors. A model was proposed for estrogen receptor alpha at sites without high-affinity response elements (EREs), where ER α is tethered to the DNA by protein-protein interactions with other TFs (Gertz et al., 2013). Taken together, these examples illustrate how TFs can function as co-factors to provide DNA accessibility, facilitate other TF binding, or tether other TFs at a regulatory element where they do not have a binding site.

The genome-wide patterns of transcription factor cooperation and TF function specification are just beginning to be revealed in the nervous system. In induced cultured neurons, specification of cranial versus spinal motor neurons was shown to require cooperative binding of two different sets of homeodomain factors, Isl1-Phox2a or Isl1-Lhx3. The different outcomes in neuronal cell types was found to be mediated by differential binding of Isl1 to the genome, due to specific sets of motif co-occurrences which helped specify the different binding of the two pairs of TFs (Mazzoni et al., 2013). However, these mechanisms have not been

carefully investigated *in vivo* and further work to elucidate how these mechanisms function in the nervous system is required.

1.2 Introduction to MEF2 transcription factors

MEF2 family members have critical functions in development and disease

Vertebrates have 4 MEF2 family members, MEF2A-MEF2D, which are homologous to three MEF2 isoforms in *Xenopus laevis* (MEF2A, MEF2C and MEF2D) as well as single MEF2 proteins in *Saccharomyces cerevisiae*, *Drosophila melanogaster* and *Caenorhabditis elegans*. These 4 family members are expressed in distinct though overlapping patterns across cell types (Black and Olson, 1998; Potthoff and Olson, 2007). While MEF2 transcription factors were initially characterized in muscle, they are widely expressed and are important in cell survival, differentiation and response to stimulus in many other tissues (Potthoff and Olson, 2007). For example, MEF2 family members are critical for numerous functions in the nervous system as well as important in T cell, bone and neural crest development (Arnold et al., 2007; Rashid et al., 2014; Savignac et al., 2007; Verzi et al., 2007), and endothelial cell organization and vascular integrity (Lin et al., 1997). Furthermore, MEF2 family members have been implicated in human diseases in multiple organ systems, including neurodevelopmental defects (Bienvenu et al., 2013; Novara et al., 2010), coronary artery disease (Bhagavatula et al., 2004; Wang et al., 2003) and migraines (Chasman et al., 2014; Freilinger et al., 2012).

Discovery of MEF2

In 1989, Myocyte enhancer factor 2 (MEF2) was discovered as a factor expressed early after the induction of myocyte differentiation and bound to regulatory elements for muscle-specific genes (Gossett et al., 1989). In 1991, a separate line of inquiry also led to the discovery of MEF2, in a search for homologues of Serum Response Factor (SRF), a transcription factor that was beginning to be characterized at growth factor inducible promoters (Pollock and Treisman, 1991). MEF2 was discovered because it shared a domain with SRF, the MADS domain. This DNA-binding domain is highly conserved throughout eukaryotes, as demonstrated by its namesakes, several of the earliest factors characterized with it: Minichromosome Maintenance 1 (MCM1), Agamous, Deficiens and SRF (Gramzow and Theissen, 2010). MCM1 is a protein characterized in *Saccharomyces cerevisiae* as important for viability and pheromone response, among other functions (Shore and Sharrocks, 1995; Treisman and Ammerer, 1992). Agamous and Deficiens are proteins expressed in the plants *Arabidopsis thaliana* and *Antirrhinum majus*, respectively, and mediate floral organogenesis and morphogenesis (Gramzow and Theissen, 2010). Finally, SRF was initially characterized in human cell lines as being expressed in response to serum and growth factors, and was shown to have an important role in directly promoting *fos* transcription (Norman et al., 1988; Rivera et al., 1990). SRF has since been found to have broader functions in stimulus responsive gene expression across many cell types (e.g., (Mylona et al., 2011; Ramanan et al., 2005; Xia et al., 1996)).

These two approaches that led to the discovery of MEF2 illustrate two of the main features of MEF2 TFs that were immediately apparent. First, they are critical in muscle differentiation and stimulus response. Secondly, they have highly conserved domains, and members of their family of MADS-box TFs had important functions across phyla. We now know they play similarly important roles in cell differentiation and response to stimuli across many cell types, and these functions are conserved across organisms as well (Potthoff and Olson, 2007).

Basic structure of MEF2 TFs

The MADS domain comprises the first 57 amino acids of the N terminus of MEF2 TFs, and is a minimal DNA binding domain (**Figure 1.3**) (Black and Olson, 1998). This is followed by a 29 amino acid MEF2 domain, which is also highly conserved among MEF2 family members and is responsible for high affinity DNA binding and homo and heterodimerization among MEF2 family members (Molkentin et al., 1996a). The MADS and MEF2 domains mediate high affinity DNA binding to the consensus MEF2 Response Element (MRE) which is YTAWWWTAR (Flavell et al., 2008; Potthoff and Olson, 2007). This A/T rich sequence is similar to the sequence bound by SRF (CCWWAWWWGG) and previous work has shown that this specificity in binding sites is primarily due to three differing amino acids in the MADS DNA binding domain (Nurrish and Treisman, 1995). While the DNA binding domains of MEF2 family members are well conserved, the C terminus of MEF2 proteins, which contains transactivation domains, is highly divergent between family members. While some areas of homology and parallels in regulation exist, often the divergent C termini provide the opportunity for differential post-translational regulation of the different MEF2s (see below).

Key mechanisms of MEF2 regulation

The MADS and MEF2 domains at the N terminus have additional functions beyond DNA binding and dimerization. The majority of characterized interactions between MEF2 and other TFs that serve as co-factors are mediated by regions within the MADS domain (McKinsey et al., 2002). The MADS domain is also critical for the interaction of MEF2 with Histone acetyltransferases (HATs) and Histone deacetylases (HDACs) (Lu et al., 2000; Sartorelli et al., 1997).

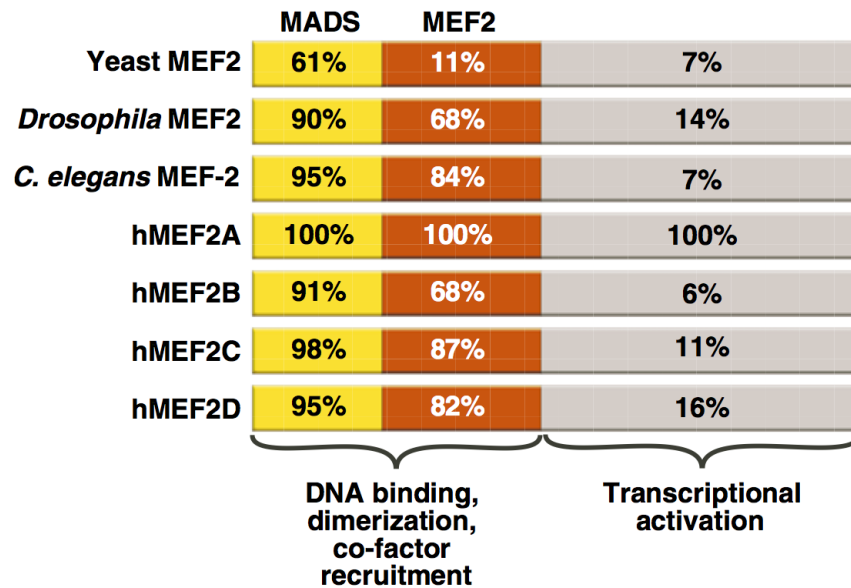


Figure 1.3. Basic structure and conservation of MEF2 family members.

MEF2 family members have highly conserved N-terminal MADS/MEF2 domains and a divergent C-terminus. Image is from (Potthoff and Olson, 2007).

As MEF2 interacts with both activating HATs and repressing HDACs, a model of dual functions for MEF2 has been proposed (McKinsey et al., 2002). In this model, MEF2 binds DNA and associates with class IIa HDACs, which recruit class I HDACs, and this represses gene expression (**Figure 1.4**). Signaling upon a differentiation stimulus in myocytes or TCR engagement in thymocytes leads to dissociation of HDACs, which allows MEF2 to now bind p300/CBP and activate gene expression (Haberland et al., 2007; McKinsey et al., 2000; Youn et al., 2000b). HDAC and p300/CBP binding with MEF2 is thought to be mutually exclusive and a major mechanism for how MEF2 contributes to the repression or activation, respectively, of a regulatory element.

There are also numerous mechanisms of regulation of the MEF2 family members at post-transcriptional and post-translational levels. These modifications occur predominantly through phosphorylation and dephosphorylation of serine/threonine residues across the body of the protein (**Figure 1.5**). For example, phosphorylation of serine 59 in the MADS/MEF2 domains by casein kinase II (CKII) increases DNA binding affinity in cultured cells (Molkentin et al., 1996b). There are also critical sites of phosphorylation in the transactivation domains of MEF2, which are often regulated in a cell type specific manner and which also modulate the transcriptional activity of MEF2 (McKinsey et al., 2002). Finally, alternative splicing in the transactivation domains of MEF2 family members changes how the MEF2s are regulated and produces a greater diversity of MEF2 functions (Lyons et al., 2012; Sebastian et al., 2013).

MEF2 transcription factors have been most thoroughly investigated in muscle, hematopoietic, and neural lineages (Potthoff and Olson, 2007). Examples of tissue-specific mechanisms of MEF2 regulation and function for these best characterized cell types will be discussed further in Chapters 1.3-1.5.

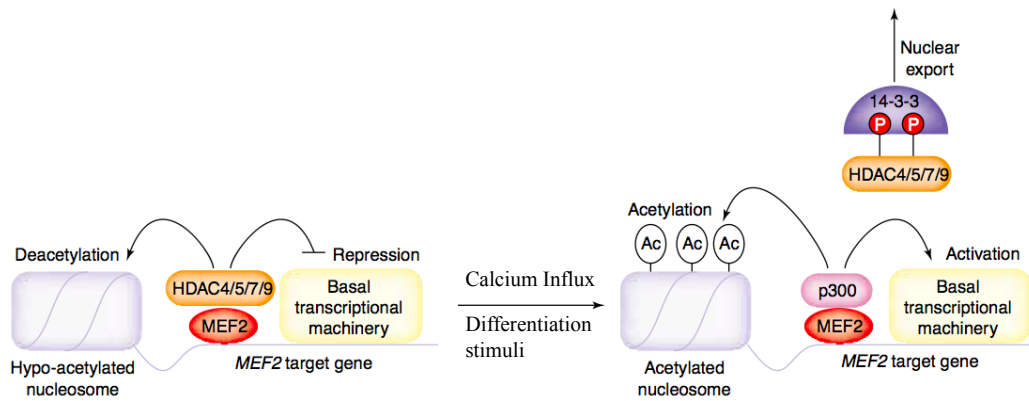


Figure 1.4. Dual functions of MEF2 as both activator and repressor.

In some systems, MEF2 sits on DNA and associates with HDACs to repress gene expression under baseline conditions. Various stimuli can activate Ca^{2+} /Calmodulin-dependent protein kinase signaling, which phosphorylates the HDACs, promoting their association with 14-3-3 and export from the nucleus. MEF2, still bound to the DNA, can now associate with HATs such as p300 and become an activator of gene expression instead of a repressor. Image adapted from (McKinsey et al., 2002).

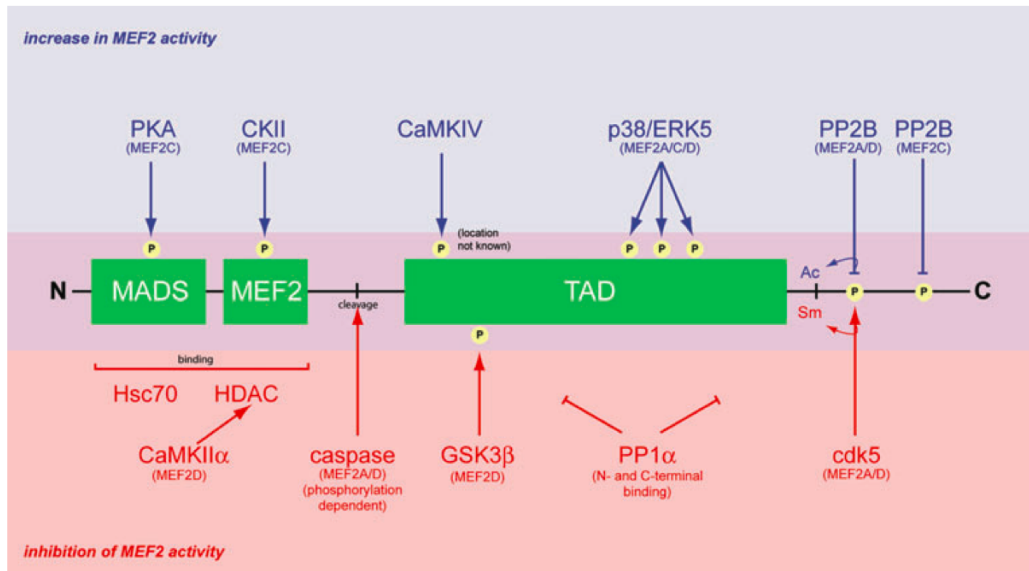


Figure 1.5. Diverse mechanisms of MEF2 regulation.

MEF2 family members are extensively modified throughout the body of the protein to regulate their functions. This diagram demonstrates modifications in neurons but many happen in other tissues as well, for example CKII phosphorylation of MEF2 in the MEF2 domain. Modulatory events in blue increase MEF2 activity whereas those in red decrease MEF2 activity. Apart from phosphorylation of MEF2, other modulations include acetylation (Ac)/sumoylation (Sm) as well as degradation. Image adapted from (Rashid et al., 2014).

1.3 MEF2 transcription factors in muscle

MEF2 factors in muscle development

The MEF2 family members were first characterized as factors able to promote myogenic differentiation *in vitro* (Gossett et al., 1989). In this experimental paradigm, serum withdrawal prompted conversion of cultured fibroblasts into developing myocytes and expression of myocytes genes such as myosin heavy chain (MHC) (Edmondson and Olson, 1989). Alternatively, this conversion could be initiated by the overexpression of the bHLH factor myocyte enhancer factor 1 (MEF1), now known as MyoD (Buskin and Hauschka, 1989; Davis et al., 1987; Lassar et al., 1989; Tapscott et al., 1988). In searching for additional myocyte-promoting factors, MEF2 was discovered as able to potentiate the conversion into myocytes. It was also proposed to be able to induce the myogenic lineage alone as MYOD can (Kaushal et al., 1994), though this was controversial and disputed by other papers (Molkentin et al., 1995). However, expression of a MEF2 dominant negative protein blocked myocyte differentiation (Ornatsky et al., 1997), establishing that MEF2 factors were critical for this process. The importance of MEF2 family members in muscle has now been demonstrated across many organisms, including *Drosophila melanogaster* (Bour et al., 1995; Lilly et al., 1995) *Xenopus laevis* (Della Gaspera et al., 2012; Kolpakova et al., 2013), *Mus musculus* (Lin et al., 1997), and *Homo sapiens* (Bhagavatula et al., 2004; Wang et al., 2003).

The first evidence for the importance of MEF2 function in muscle *in vivo* came from *Drosophila*. MEF2 is expressed in myogenic lineages in *Drosophila* embryogenesis (Lilly et al., 1994). D-mef2 mutant *Drosophila* embryos demonstrate abnormal differentiation of all myogenic lineages (cardiac, skeletal, visceral) (Bour et al., 1995; Lilly et al., 1995). These

findings were extended to vertebrates with the generation of the first MEF2 knockout mice. These confirmed the importance of MEF2 family members in muscle development, most notably in the development of cardiac muscle. MEF2C total knockout mice are embryonic lethal due to severe defects in early cardiac development (Lin et al., 1997). MEF2A total knockout mice are born but die by P7, also due to cardiac defects (Lin et al., 1997; Naya et al., 2002). Previously published MEF2D knockout mice appear phenotypically normal but still have cardiac abnormalities, specifically resistance to stress-induced cardiac remodeling (Kim et al., 2008; Potthoff et al., 2007). Finally, there is evidence for the importance of MEF2 in human muscle development as well, as mutations in MEF2A have been linked to cardiac disease (Bhagavatula et al., 2004; Wang et al., 2003).

Molecular mechanisms of MEF2 function in muscle

In striated muscle, MEF2 family members are transcriptionally activated by MYOD and other muscle-specific bHLH family members. They then co-bind with these family members to activate the expression of genes critical for muscle differentiation. Over the past twenty years, significant gains in understanding these molecular mechanisms of MEF2-mediated gene expression have been made through studying the interactions of MEF2 factors and MYOD or MYOG in myocyte cell lines, primarily through the use of reporter systems (Black and Olson, 1998).

The interaction of MEF2 and the myogenic bHLH factors is mediated by regions in their respective DNA-binding domains (Molkentin et al., 1995). Experiments in cultured myocytes have suggested that the direct interaction between MEF2 and MYOD is sufficient to allow both proteins to regulate gene expression even if only one DNA binding site is present. One of the earliest investigations of this cooperativity demonstrated that myogenic bHLH factors can

activate a *Myog* promoter reporter with MEF2 factors where there is an MRE but no E-box (Edmondson et al., 1992). Furthermore, in a GAL4 reporter system, the motif for bHLH heterodimer binding, an E-box, is dispensable as long as MEF2 is able to bind to its MEF2 response element (MRE), and the converse is true as well (Molkentin et al., 1995). In addition, a MEF2C mutant with the single amino acid mutation R24L, which renders it unable to bind DNA (Molkentin et al., 1996a) is able to effectively co-activate reporters with MYOD (Molkentin et al., 1995). However, when this was investigated in the context of endogenous gene expression, both DNA binding motifs were required for MYOG and MEF2 co-activation of the *Mrf4* promoter in myogenesis (Naidu et al., 1995). Thus, whether MEF2 and MYOD both need to bind to DNA to effectively co-activate gene expression remains unclear.

Further research has examined how MYOD and MEF2 may co-activate gene expression once bound to the DNA. Initial studies found that p300/CBP interact with MYOD through its N terminal domain to amplify myogenic conversion of fibroblasts (Sartorelli et al., 1997). This N terminal activation domain of MYOD is unavailable for p300 binding when just MYOD is bound to DNA. It was proposed that cofactor binding might induce a change in conformation that would then make this domain of MYOD functional (Davis et al., 1990; Huang et al., 1998). MEF2C was also found to interact with CBP/p300 through its MADS domain, and this potentiated MEF2C's transcriptional activating ability, though how MEF2, MYOD and p300/CBP may form a complex to regulate transcription was not tested (Sartorelli et al., 1997). In addition, overexpressing MYOD and p300 alone was sufficient to induce synergistic activation, suggesting that MEF2 family members are not necessary cofactors for MYOD interactions with p300 (Sartorelli et al., 1997). Taken together, these results have suggested

multiple mechanisms of interaction between MEF2 and myogenic bHLH factors for co-binding and co-activation. How these happen *in vivo* remains to be elucidated.

Beyond MYOD, MEF2s have been suggested to work with several other cofactors in myocytes, including thyroid hormone receptor (De Luca et al., 2003; Lee et al., 1997), SMADs (Quinn et al., 2001), and LMD in *Drosophila* (Cunha et al., 2010). In cardiac muscle, a key cofactor for MEF2 is the zinc finger protein GATA4. Using similar strategies as those to characterize MEF2 interactions with MYOD, it was shown that GATA4 can recruit MEF2 to cardiac target gene promoters to potentiate GATA4's activity (Morin et al., 2000). Similar to MYOD, GATA4 can recruit MEF2 in an MRE-independent manner (Morin et al., 2000). However in contrast to MYOD, in cardiac myocytes MEF2D alone bound to p300 whereas GATA4 did not (Slepek et al., 2001). This MEF2D-p300 interaction was sufficient to drive the alpha-actin promoter in cardiac myocytes. How these mechanisms work in an endogenous context remains to be examined.

The co-factor binding and transcriptional activity of MEF2 family members are also regulated by posttranslational modifications of MEF2, many of which were first identified in muscle. For example, MEF2 binding to p300/CBP not only serves to recruit these HATs to the DNA, but MEF2 is also directly acetylated in its transactivation domain by p300, which further activates MEF2 (Ma et al., 2005).

Phosphorylation of MEF2 family members also mediates MEF2 function in muscle. For example, Protein kinase A (PKA) is known to phosphorylate MEF2D at S121/S190, which inhibits MEF2D function and represses myogenesis (Du et al., 2008). There is a myocyte-specific, developmentally controlled alternate splice form of MEF2D that does not contain these

two serines, rendering MEF2D insensitive to PKA-mediated inhibition and able to promote myocyte differentiation (Sebastian et al., 2013). A recent study has demonstrated that these differentially modified splice forms do not differ in their binding of DNA. However, this modification does affect the co-factors MEF2D associates with, as in the phosphorylated form, MEF2D associates with co-repressors HDAC4/HDAC9, whereas in the later non-phosphorylated form, MEF2D associates with the Ash12 co-activator complex, likely accounting for the switch in MEF2D function from inhibitor to promoter of myogenesis (Sebastian et al., 2013).

Global gene regulation in muscle by MEF2

The majority of work done to investigate MEF2-mediated global mechanisms of gene regulation has been done in the context of *Drosophila* mesoderm development. MEF2 ChIP-ChIP throughout *Drosophila* development demonstrated that MEF2 binds proximally to muscle genes throughout embryonic development, and binds near genes misregulated in MEF2 mutant embryos (Sandmann et al., 2006). When combined with data for binding of other key myogenic factors, it was observed that MEF2 participates in a feed forward loop in *Drosophila* muscle development, where the bHLH factor Twist regulates the expression of Mef2 and then binds to the genome in overlapping patterns with MEF2 (Sandmann et al., 2007).

Studies of how MEF2 globally mediates gene expression in vertebrates are now beginning to emerge. Two studies have characterized MEF2A binding in the context of the cardiac muscle differentiation transcriptional network. These studies demonstrated that MEF2A binding overlapped with other transcriptional network components and that regulatory elements with multiple TFs present are more likely to be active (He et al., 2011; Schlesinger et al., 2011).

These studies underscore the importance of MEF2 in muscle development and that it cooperates with co-factors in muscle differentiation. While MEF2 has been best characterized in muscle, some of these molecular mechanisms occur in the hematopoietic system as well, suggesting some universal principles in how MEF2 family members function.

1.4 MEF2 transcription factors in the hematopoietic system

MEF2 in T lymphocytes

T cells have well defined calcium-dependent responses to stimuli using mechanisms parallel to those used in muscle or neurons (Savignac et al., 2007). Briefly, when T cells encounter an MHC-peptide bearing cell with sufficient affinity to their T cell receptor (TCR), engagement of the TCR triggers a signaling cascade that involves calcium influx from both the ER as well as external calcium via CRAC channels. This calcium influx regulates the transcriptional activity of MEF2 family members, which then play an important role in regulating several aspects of T cell development and function (Savignac et al., 2007).

Developing T cells (thymocytes) with a T cell receptor (TCR) that reacts too strongly to an MHC-self peptide complex undergo apoptosis in a process known as negative selection. Strong TCR engagement in this process triggers calcium influx, which activates MEF2 and lead to the expression of *nur77*, which mediates thymocyte apoptosis (Youn et al., 1999). Prior to activation, MEF2 is bound by its co-repressor Cabin1. Calcium influx prompts the binding of Cabin1 to calmodulin, which dissociates it from MEF2.

To further test whether the interaction of Cabin1 with MEF2 is important for thymocyte negative selection, a mouse with a mutant form of Cabin1 that could not bind MEF2 was created. This mouse however did not have defects in negative selection, which suggested other regulatory mechanisms must also be involved (Esau et al., 2001). Calcium influx also activates CamKIV and Calcineurin, which can directly phosphorylate and dephosphorylate MEF2, respectively, at different residues to activate it (Blaeser et al., 2000; Rashid et al., 2014). Calcineurin also

dephosphorylates NFATp and allows it to translocate into the nucleus, where it associates with MEF2. NFATp and MEF2 then co-recruit p300/CBP to activate the *nur77* promoter and promote *nur77* expression (Blaeser et al., 2000; Youn et al., 2000a; Youn and Liu, 2000; Youn et al., 1999). In this paradigm, MEF2D is bound directly to the *nur77* promoter but NFATp does not require its DNA recognition site, and instead was thought to bind directly to MEF2D through its MADS domain (Youn et al., 2000a).

Beyond negative selection, MEF2 has also been suggested to have a parallel role in mature T cells in regulating cytokine expression (Savignac et al., 2007). In this case, the mutant mouse where Cabin1 could no longer interact with MEF2 supported these findings, as these mice had increased cytokine expression (Esau et al., 2001). Furthermore, MEF2 binding sites were found in the promoter of IL-2, and MEF2 was shown to promote calcium-mediated expression of IL-2, also together with NFATp (Pan et al., 2004). Further work remains to examine how MEF2D works in T cells *in vivo*.

MEF2C in early lymphopoiesis

While MEF2D has a role in thymocyte development and T cell activation, MEF2C is expressed earlier in lymphoid development, in particular in hematopoietic stem cells, common lymphoid progenitors, and common myeloid progenitors (Stehling-Sun et al., 2009). A recent study suggested that MEF2C regulates a key choice in hematopoietic development between lymphoid and myeloid differentiation. Early deletion of *Mef2c* in hematopoietic development led to impaired pan-lymphocyte differentiation (Stehling-Sun et al., 2009). This regulation of earlier

lymphopoiesis by MEF2C may have implications for human disease as well. Translocations leading to the upregulation of *Mef2c* expression have been found in subtypes of acute myeloid leukemia and T-cell acute lymphoblastic leukemia (Cante-Barrett et al., 2014).

Taken together, the data in Chapters 1.3 and 1.4 highlight the critical function of MEF2 factors in lymphocyte and myocyte biology as well as human disease. They also illustrate the diverse array of co-factors as well as signaling mechanisms employed to regulate MEF2 function. MEF2 transcription factors have also been found to have critical roles in neuronal biology and human neurological disease and investigation into MEF2 transcription factor function in the nervous system is an area of ongoing intensive research.

1.5 MEF2 transcription factors in the nervous system

MEF2 transcription factors play critical roles in the nervous system. While several examples of MEF2 co-factors exist in non-neural tissues as discussed in Chapters 1.3 and 1.4, investigating these kinds of interactions has been limited in the nervous system. MEF2 has been suggested to interact with the neurogenic bHLH factor MASH1 (Black et al., 1996; Mao and Nadal-Ginard, 1996), however demonstrating a biological function for this interaction has remained elusive. Beyond this, co-factors for MEF2 family members in the nervous system have not yet been described, likely due to limitations in examining the molecular function of MEF2s in the nervous system. However, the critical role of MEF2 transcription factors in neuronal biology at multiple levels has been well established.

Role of MEF2 in neuronal differentiation

The MEF2 family members are expressed throughout the nervous system in different but overlapping patterns. Expression of MEF2 family members often begins once a neuron begins to differentiate, suggesting that MEF2 plays a role in this process (Heidenreich and Linseman, 2004; Ikeshima et al., 1995; Lam and Chawla, 2007; Lyons et al., 1995). MEF2 may also play an active role in neural differentiation, as it has been shown to promote the expression of neural genes in P19 embryonic carcinoma cells, including the neurogenic bHLH factor MASH1 (Skerjanc and Wilton, 2000). Furthermore, MEF2C may have a neurogenic role in murine ES cells (Li et al., 2008b), and enhance neuron generation in hESC-derived neural stem progenitor cell (Cho et al., 2011). However, perhaps the best evidence that MEF2 factors play a role in

neuronal differentiation comes from a study of mice with conditional loss of MEF2C in neuronal progenitor cells. These mice had cortical layering defects and deficits in neuronal maturation (Li et al., 2008a). However, mice with a similar loss of MEF2C in early neural progenitors were not reported as having neuronal maturation defects but rather later developmental synaptic defects (Barbosa et al., 2008), and while these synaptic defects could be secondary to more subtle earlier defects in neuronal maturation, these results remain unclear. Further investigation of the role that MEF2s play in neural differentiation in an endogenous context is required.

MEF2 mediates neuronal survival

Most initial studies that explored mechanisms of MEF2 regulation in neurons studied the role of MEF2 in promoting neuronal survival and preventing apoptosis. MEF2 was first shown to be important for the survival of cerebellar granule cells (Mao et al., 1999). Cultured cerebellar granule cells normally undergo apoptosis when neuronal activity is withdrawn (Mao et al., 1999). Expressing a constitutively active form of MEF2 was found to rescue these cells from apoptosis; however expressing a dominant negative form accelerated this process (Mao et al., 1999). This was suggested to be a process based on activation of p38 MAPK that would then phosphorylate and activate MEF2C. Further experiments extended these findings to implicate other MEF2 family members MEF2A and MEF2D (Gaudilliere et al., 2002; Wang et al., 2009).

Other stimuli and modifications of MEF2 regulate its role in neuronal survival as well. Several kinases have been identified that phosphorylate MEF2 family members and inhibit their function, leading to neuronal apoptosis. For example, GSK3 β phosphorylates 3 residues in

MEF2D that inhibit MEF2D activity, which leads to cerebellar granule cell apoptosis (Wang et al., 2009). Activation of Protein kinase A (PKA) by cAMP leads to PKA-mediated inhibitory phosphorylation of MEF2D at S121/S190, which results in hippocampal neuron apoptosis (Salma and McDermott, 2012). Finally, neurotoxic stimuli induce Cdk5-mediated inhibitory phosphorylation of MEF2A and MEF2D at S408 or S444, respectively, which results in apoptosis of cortical neurons (Gong et al., 2003).

The importance of MEF2 factors in neuronal survival has also been observed *in vivo*. Mice with expression in the nervous system of MEF2A, MEF2C and MEF2D mutants missing DNA binding domains instead of wildtype proteins demonstrated defects in neuronal survival (Akhtar et al., 2012). However, mice where only one or two of the MEF2 family members were mutated did not have such defects, likely due to the ability of co-expressed MEF2 factors to compensate for each other (Akhtar et al., 2012).

MEF2 regulates synapse number

MEF2 family members have been implicated in later stages of neuronal development as well, particularly in modulating synapse number through regulation of synapse formation and/or synapse elimination. Excitatory synapses are the primary form of communication between neurons in the CNS, and during development they undergo a period of exuberant growth followed by selective refinement. Simultaneous MEF2A and MEF2D knockdown in rat hippocampal neuron culture increases excitatory synapse density. MEF2-VP16, a hyperactivated version of MEF2, can lead to a decrease in synapse density (Flavell et al., 2006). Furthermore, MEF2A and MEF2D are activated

by neuronal depolarization. MEF2A and MEF2D have a homologous serine on their transactivation domains, S408 and S444, respectively, whose phosphorylation inhibits MEF2 activity, as described above. Neuronal activity activates calcineurin, and activity-dependent dephosphorylation of MEF2 by calcineurin at S408/444 can activate MEF2A/MEF2D and alter the transcription of hundreds of genes. These studies have demonstrated that MEF2A/MEF2D regulate synapse number by controlling the expression of a cohort of immediate early genes that mediate the response to activity (e.g. *fos*, *egr1*) as well as genes with clear synaptic and neurological functions (e.g. *homer1*, *arc*, *bdnf*) (Flavell et al., 2008).

The observation that MEF2 factors regulate synapse number has been extended beyond *in vitro* cultured neurons as well. In hippocampal organotypic culture, expressing an overactive MEF2-VP16 decreased excitatory synapses and dendritic spines in CA1 hippocampal neurons, whereas expressing the dominant negative MEF2-Engrailed led to an increase in synapses and dendritic spines (Pfeiffer et al., 2010). Furthermore, these studies have been extended *in vivo* through the use of conditional knockout mice. MEF2C conditional knockout mice have an increase in excitatory synapses onto dentate granule cells in the hippocampus, though these mice lose MEF2C early in development so it is difficult to identify the cause as direct or indirect due to defects in neuronal health or differentiation (Barbosa et al., 2008).

Role of MEF2 in neural circuit development

Most recently, the study of MEF2 factors in neurons has been extended to investigating their role *in vivo* in brain circuitry. This has typically involved manipulating MEF2 activity in select brain regions and observing behavioral changes correlated to changes in dendritic spine density, which are neuronal structures that correlate with the presence of excitatory synapses.

One of the first examples was a study that demonstrated that chronic cocaine use in mice inhibits MEF2A and MEF2D in the nucleus accumbens. This inhibition leads to an increase in dendritic spines that may suppress sensitized drug responses. Perturbing this response by overexpressing a constitutively active MEF2-VP16 protein represses the increase in dendritic spines and increases behavioral sensitization to the drug (Pulipparacharuvil et al., 2008).

MEF2 family members have also been implicated in restricting memory formation by regulating spine development (Rashid et al., 2014). Through the use of dominant negative or constitutively active MEF2 factors as well as loss of function experiments, general principles have emerged for how MEF2 plays a role in memory. Memory formation leads to inhibitory phosphorylation of MEF2A and MEF2D at S408/S444, which allows for the increases in spine formation normally associated with memory formation (Cole et al., 2012). Increasing MEF2 activity by expressing MEF2-VP16 blocks this increase in spines and consequently new memory formation. This pathway has been implicated in memory and spine formation in the anterior cingulate cortex, hippocampus and amygdala (Cole et al., 2012; Vetere et al., 2011). Furthermore, recent work has suggested that much of this MEF2 dependent spine regulation is dependent on MEF2's regulation of its previously identified target gene *arc* (Cole et al., 2012; Flavell et al., 2008).

Given the effects on memory demonstrated throughout regions of the brain, it might be expected that MEF2 conditional knockout mice would have memory defects as well. However, MEF2A/MEF2D brain-specific deletions had no deficits in memory formation (Akhtar et al., 2012). MEF2C brain-specific knockout mice had limited defects in fear memory formation, having a deficit in contextual but not cued fear memory formation (Barbosa et al., 2008). The lack of significant memory defects may reflect compensation by remaining MEF2 family members. It might also reflect differences between the acute

manipulations employed to disrupt MEF2 in initial studies versus the effects of chronic loss of MEF2 early in neuronal development. Finally, it may also reflect complications in interpreting the phenotypes in these knockout mice, which still express large truncated MEF2 family members instead of full loss of function mutants (Akhtar et al., 2012; Barbosa et al., 2008).

MEF2s in the retina

Several studies have indirectly implicated MEF2 transcription factors as being possibly involved in photoreceptor function and disease. The MRE was found to be slightly enriched in regions bound by transcription factors important in photoreceptor biology (Hao et al., 2012). Additionally, *Mef2c* RNA expression levels are decreased in adult knockout mouse models of retinal degeneration, including CRX and NRL KO mice (Hsiao et al., 2007; Yoshida et al., 2004). *Mef2c* levels are also reduced in *Rpe65* knockout mice, another mouse model of retinal degeneration, however with the caveat that this photoreceptor abnormality is secondary to a defect intrinsic to retinal pigment epithelial cells (Escher et al., 2011). Finally, limited work has suggested MEF2C is important in the mature retina. One study found that NRL, a key photoreceptor transcription factor, could promote the transcription of *Mef2c* from a retina-specific promoter (Hao et al., 2011). Furthermore, MEF2C was important for the expression of a rhodopsin promoter reporter in retinal photoreceptors *in vivo*. Taken together, these studies have suggested that MEF2 factors, particularly MEF2C, may have a role in mature photoreceptors. Direct evidence of MEF2 factor regulation of photoreceptor biology, however, has thus far remained elusive.

MEFs in neurological disease

MEF2 family members have been implicated in several human neurological diseases. The most direct association is that haploinsufficiency of MEF2C leads to a neurological disorder characterized by epilepsy, mental retardation, absence of speech and other neurodevelopmental symptoms, many of which overlap with Rett syndrome (Bienvenu et al., 2013; Novara et al., 2010; Zweier et al., 2010; Zweier and Rauch, 2012). Other studies have also indirectly linked MEF2 to autism and neurodevelopmental disorders. Many neuronal genes that have been found to be MEF2 target genes are also possible disease genes associated with autism spectrum disorder (Flavell et al., 2008; Morrow et al., 2008), suggesting MEF2 or its targets may play an important role in regulating synaptic plasticity and misregulation of MEF2 or any of these target genes may lead to neurological disease. Furthermore, MEF2 has been proposed to work with FMRP to regulate excitatory synapse and dendritic spine number. FMRP is mutated in patients with fragile X syndrome, which is characterized by autism and mental retardation, as well as an excess of dendritic spines (Irwin et al., 2001). Mouse neurons missing FMRP do not undergo MEF2-mediated synapse restriction as WT neurons do (Pfeiffer et al., 2010). Together, these observations suggest that MEF2-mediated mechanisms to reduce spine number may be defective in these patients.

MEF2 has also been suggested to play a role in Parkinson's disease. In vitro experiments in a dopaminergic cell line suggested that inactive MEF2D is normally shuttled from nucleus to cytoplasm for degradation by chaperone-mediated autophagy, which is disrupted by alpha-synuclein, leading to neuronal death. As alpha-synuclein is elevated in patients with Parkinson's disease, this suggests a possible pathway of dopaminergic cell death in the disease. These results

are limited to cell culture experiments, although it was also noted that patients with Parkinson's disease have increased levels of MEF2D in their striata, suggesting some aspects of this mechanism may be related to human disease (Yang et al., 2009).

1.6 Gene regulation in photoreceptor development

Photoreceptors are the primary sensory neurons of the retina responsible for the initial processing of vision. When photons of light enter the eye, they travel through the eye until they reach the apical processes of the photoreceptors, known as the outersegments (**Figure 1.6A**). A single photon of light triggers the phototransduction cascade within the outersegment by isomerizing 11-cis-retinal into all-trans-retinal in visual pigments. This isomerization triggers a series of biochemical events that ultimately leads to the conversion of this photon of light into an electrical signal via the hyperpolarization of the photoreceptor. This hyperpolarization reduces excitatory synaptic activity from the photoreceptor axon terminal to its postsynaptic neurons, bipolar and horizontal cells (Luo et al., 2008). These neurons propagate this signal to amacrine and retinal ganglion cells, which ultimately transmit this information to the brain

Photoreceptors vastly outnumber other neuronal cell types in the retina, making up ~ 80% of neurons. Rod photoreceptors make up 97% of all photoreceptors, with the remaining 3% being cones (Jeon et al., 1998; Young, 1985). The retina is characterized by a stereotypical and well-defined anatomy (**Figure 1.6B**), and photoreceptors are tightly packed together, with nuclei in the outer nuclear layer (ONL) and synaptic contacts in the outer plexiform layer (OPL).

Retinal Photoreceptor Development

While there are ultimately ~55 distinct cell types in the mammalian retina, there are six broad categories of retinal neuron types: photoreceptors-rods and cones, bipolar cells, horizontal

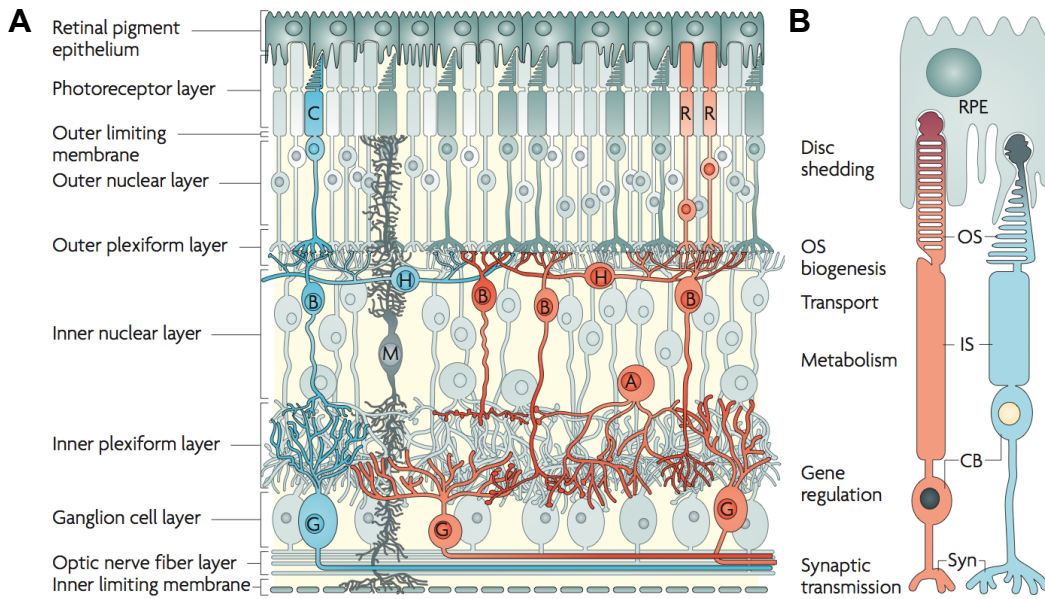


Figure 1.6. Structure of the retina and retinal photoreceptors.

(A) Overall structure of the retina. Light enters from the ganglion cell layer side and traverses the neural retina until arriving at the photoreceptor layer, where it activates the phototransduction system in either rod (R) or cone (C) photoreceptors. Rods and cones transmit this signal to horizontal cells (H) and bipolar cells (B) and then these signals are integrated with amacrine cells (A) until finally the signal reaches ganglion cells (G), which transmit the information to the brain. Also depicted are Muller glia which help support the neurons of the retina.

(B) Magnified structure of rod (on left) and cone (on right) photoreceptors demonstrates their unique morphology. The apical processes of photoreceptors are stacked membranous disks known as outer segments (OS) that contact the retinal pigment epithelium (RPE) for a continuous recycling process. The inner segment (IS) has metabolic machinery; the cell bodies (CB) contain the nuclei and are located in the retinal outer nuclear layer. Images adapted from (Swaroop et al., 2010).

cells, amacrine cells and retinal ganglion cells (Masland, 2001). These different categories of neurons have some distinct features, which include their localization in the retina, their morphologies, and their birth order in the development of the retina. All retinal neurons as well as Mueller glia originate from a common retinal progenitor cell. The developmental time point at which they are born, combined with intrinsic and extrinsic cues helps determine their fate (Cepko et al., 1996). For example, cone photoreceptors are among the earliest cells born in retinal development in mice, and are born from embryonic day 10 (E10) to E18, peaking at ~ E14 (Carter-Dawson and LaVail, 1979), whereas rod photoreceptors are born over a broader time period between E13 and postnatal day 7 (P7), peaking at P0-P1 (Carter-Dawson and LaVail, 1979)(**Figure 1.7**).

After each neuron type is specified from retinal progenitor cells, these newborn neurons differentiate into the unique morphologies necessary for the distinct functions of that particular cell type. At about P6, photoreceptors begin to make synapses with their postsynaptic neurons as well as elaborate their outersegments (Olney, 1968). Outersegment growth in mice continues rapidly until P21 and by ~P28 the mouse retina is mature (Olney, 1968). Early in this development, multiple important photoreceptor specific genes begin to be expressed, for example rhodopsin which begins to be expressed at about P2 (Swaroop et al., 2010). Precise control of gene expression from photoreceptor birth through maturation is critical for normal photoreceptor development.

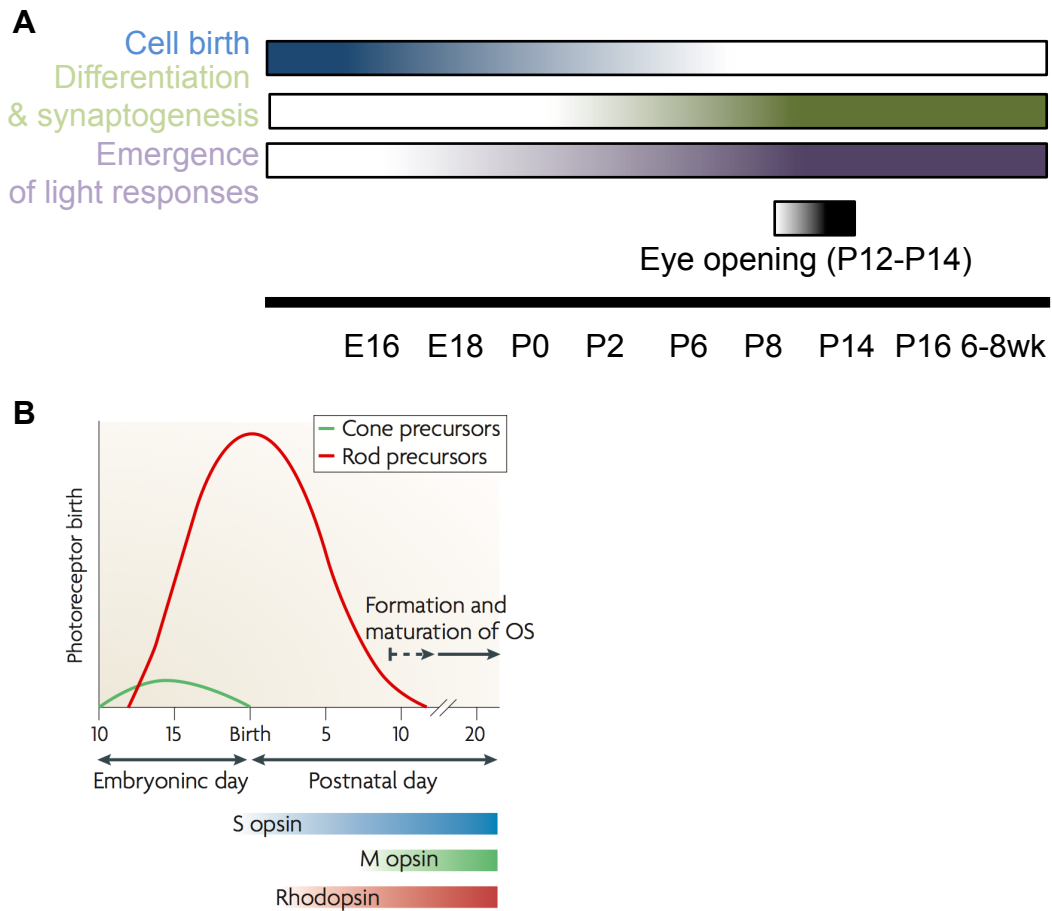


Figure 1.7. Timeline of retinal development.

(A) Overview of retinal development. Neuronal cell birth begins embryonically and continues until it begins to taper off in the first postnatal week. Synaptogenesis and differentiation begin to increase in the first postnatal week, especially for photoreceptors. Retinal light responses emerge prior to eye opening, which is generally at P12-P14.

(B) Timing of photoreceptor birth in mice. Cone photoreceptors are born early, prior to mouse birth. Rods have a wider time range of birth but peak perinatally. In the first week after birth, rod photoreceptor cell birth decreases and photoreceptor maturation begins, including formation of OS and expression of key phototransduction molecules such as the opsins. Image adapted from (Swaroop et al., 2010).

Transcriptional networks that regulate photoreceptor development

The regulatory networks that mediate retinal neuron development have been most extensively studied in the case of photoreceptors. One of the first transcriptional regulators demonstrated to be critical for photoreceptor fate determination and further differentiation of photoreceptors is the homeobox factor *Otx2*. Mice missing *Otx2* have a defect in producing photoreceptors, whereas misexpressing *Otx2* leads to a cell fate bias toward rods versus other retinal neurons (Nishida et al., 2003). *Blimp1* and bHLH factors have also been implicated in photoreceptor cell fate determination and bHLH factors have been shown to be important in rod survival as well as in other critical functions in retinal development (Brzezinski et al., 2010; Hatakeyama et al., 2001; Katoh et al., 2010; Morrow et al., 1999).

Once photoreceptor cell fate is specified, another transcriptional network becomes important in promoting photoreceptor differentiation and specific gene expression. *Crx* is a homeobox factor closely related to *Otx2* that is expressed very early after photoreceptor cell fate is determined (Chen et al., 1997; Furukawa et al., 1997). *Otx2* and *CRX* are expressed in both rods and cones and play critical roles in gene expression in both cell types, including promoting the expression of downstream TFs. TFs specific to cone photoreceptors include Thyroid hormone receptor beta, specific to green cones in mice (Ng et al., 2001), as well as *Nr2b3/RXR γ* , which is critical for blue cones (Roberts et al., 2005). *Nrl* expression is required for rod differentiation and *NRL* induces the expression of *Nr2e3*, which reinforces the rod differentiation phenotype primarily by repressing cone genes (Chen et al., 2005; Mears et al., 2001).

The TFs NRL, CRX and NR2E3 are particularly important for establishing the photoreceptor transcriptional network (Hsiao et al., 2007), and loss of any of these 3 proteins severely disrupts photoreceptor development and leads to human retinal disease (Bessant et al., 1999; Coppieters et al., 2007; Gerber et al., 2000; Haider et al., 2000; Nishiguchi et al., 2004; Swain et al., 1997). This underscores the necessity of proper gene regulation and activation of regulatory elements for normal photoreceptor development.

The molecular mechanisms by which NRL, CRX and NR2E3 cooperate to activate gene expression are now beginning to be elucidated. CRX and NRL co-bind genome-wide and NRL, CRX and NR2E3 activate key photoreceptor regulatory elements as seen by increases in histone acetylation and DNA looping (Corbo et al., 2010; Hao et al., 2012; Rao et al., 2011). CRX has also been found to bind the histone acetyltransferase (HAT) P300, suggesting that these factors recruit co-activators to promote photoreceptor gene expression (Peng and Chen, 2007; Yanagi et al., 2000).

Cis-regulatory logic of photoreceptor differentiation as a model for neural development

Mouse retinal development is an excellent system for systems biology research of gene regulatory networks, primarily due to the extensive research on retinal cell fate determination and cell differentiation of retinal neurons (Zhang et al., 2011). Furthermore, the retina is easily accessible for genetic manipulation using for example DNA electroporations or viral infections (Cepko et al., 1998; Matsuda and Cepko, 2004), particularly when compared to the rest of the CNS. Another significant difficulty in studying gene regulation in the CNS arises from its diversity of cell types and heterogeneity of neurons throughout the brain. A key advantage of rod photoreceptors is that they make up about 80% of neurons and 75% of all retinal cells (Jeon et

al., 1998; Young, 1985). This facilitates analyses focused on this single neuronal cell type without necessitating complex processing of tissues that might distort the endogenous biological mechanisms being studied.

The cis-regulatory logic controlling photoreceptor development has been particularly well studied and serves as an excellent example of how a cell type specific program of gene expression is coordinated in the nervous system (Hsiau et al., 2007; Swaroop et al., 2010). Transcription factors important for photoreceptor development as well as their target genes have also been found to be mutated in human disease, suggesting that a better understanding of the gene regulatory networks underlying the biology of photoreceptor development will provide critical insight for future medical therapies (Swaroop et al., 2010). Taken together, these advantages suggest that photoreceptors are an excellent model for studying *in vivo* gene regulation in the CNS.

1.7 Summary of the dissertation

The highly conserved MEF2 family of transcription factors plays important roles in many aspects of neuronal development and function. However, the mechanisms by which MEF2 comes to regulate neuronal-specific genes is poorly understood, and no co-factors for MEF2 in the nervous system have been reliably identified. At the outset of this dissertation we sought to elucidate the molecular mechanisms by which MEF2 regulates gene expression in the nervous system.

In Chapter 2, we discover that MEF2D is the unique MEF2 family member expressed in developing retinal photoreceptors, and generate MEF2D knockout mice to evaluate the role of MEF2D in these neurons. We find that MEF2D is important for normal retinal photoreceptor development and that MEF2D knockout mice are blind. Retinal photoreceptor development is an excellent model for exploring gene regulatory networks in the CNS, and so we chose to use this model to study MEF2-mediated gene expression. Using genome-wide analyses, we found that MEF2D directly regulates a cohort of photoreceptor-specific and retinal disease-associated genes. MEF2D co-regulates these genes with the retina-specific co-factor CRX, and these factors have similar defects in photoreceptor development as well. The mechanism of co-regulation is two-fold. First, CRX recruits MEF2D to retina-specific enhancers that have a weak MRE, at the expense of other MEF2D binding sites that have a strong MRE. Next, CRX and MEF2D co-activate regulatory elements to co-regulate target genes. These analyses demonstrated that the broadly expressed TF MEF2D acquires tissue-specific functions in the nervous system by co-binding and co-activation of tissue-specific enhancers with the tissue-specific TF CRX.

In Chapter 3, we use the behavior of MEF2D in developing photoreceptors as a system to investigate a fundamental feature of transcriptional biology: that transcription factors bind the genome extensively, but regulate a relatively small number of target genes. This has often been observed in genome-wide studies but has yet to be carefully examined. To investigate the causes of this discrepancy, we evaluate in an unbiased manner the activity of all MEF2D-bound enhancers as determined by levels of H3K27 acetylation and eRNA production. We determine that the majority of our MEF2D-bound enhancers are inactive, and so not directly regulating gene expression at the time we evaluate changes in gene expression. Of those that are active, about half are not dependent on MEF2D for that activity, suggesting significant redundancy among bound TFs exists within an enhancer. This demonstrates that TF binding significantly overestimates how many TF-bound regulatory elements are directly engaged in regulating gene expression, and suggests that functional analyses of enhancer activity are essential for delineating the specific function of a TF in regulating gene expression.

Taken together, the work in this dissertation describes a novel role for MEF2D in regulation of photoreceptor development, and provides an in depth analysis of the mechanisms MEF2D uses to perform this function, including how it acquires a highly tissue-specific role. We show that MEF2D selectively activates a cohort of its bound enhancers and cooperates with the tissue-specific factor CRX for both regulatory element binding and activation. This provides a model of how MEF2D functions in neuronal development and how it might function in other cell types *in vivo* as well.

Chapter 2

MEF2 regulates retinal photoreceptor development through synergistic binding and selective activation of tissue-specific enhancers

2.1 Abstract

Development of the central nervous system requires the precise coordination of intrinsic genetic programs to instruct cell fate, synaptic connectivity and function. The MEF2 family of transcription factors plays many essential roles in neuronal development, however the mechanism by which this broadly expressed TF contributes to the great diversity of cell types in the brain remains unclear. We find that one MEF2 family member in particular, MEF2D, is an essential regulator of retinal photoreceptor development and function. Despite being expressed broadly across many tissues, in the retina MEF2D binds to retina-specific enhancers and regulates photoreceptor-specific transcripts including critical retinal disease genes. Functional genome-wide analyses demonstrate that MEF2D achieves tissue-specific binding and action through cooperation with a retina-specific transcription factor, CRX. CRX recruits MEF2D away from canonical MEF2 binding sites by promoting MEF2D binding to retina-specific enhancers that lack a strong consensus MEF2 binding sequence. Once bound to retinal specific enhancers, MEF2D and CRX work together to regulate a cohort of genes critical for normal photoreceptor development. These findings demonstrate that MEF2D, a broadly expressed transcription factor, contributes to retina-specific gene expression in photoreceptor development by binding to and selectively activating tissue-specific enhancers cooperatively with CRX, a tissue-specific co-factor. Thus, broadly expressed transcription factors may achieve tissue specificity through competitive recruitment to enhancers by tissue-specific transcription factors and selective activation of these enhancers to regulate tissue-specific target genes.

2.2 Background and Significance

A remarkable feature of the development of complex multicellular organisms is that this extraordinary process is controlled by a relatively limited number of transcription factors (TFs). TFs determine the exquisite patterns of gene expression that define the tissues and cell types of an organism. The diversity of TF function is especially evident in the brain, where a vast array of different cell types gives rise to our ability to extract information from the external environment and respond appropriately. While a number of TFs with tissue-specific expression have been identified, most TFs somehow function in a wide range of cell types, yet in a given cell type can contribute to cell type specific gene expression. The best evidence that broadly expressed TFs contribute to cell type specific functions is that mutations in broadly expressed TFs often result in tissue-specific disease phenotypes (Amiel et al., 2007; Amir et al., 1999; Novara et al., 2010). Nevertheless, it is not yet well understood how the function of widely expressed TFs is tailored to achieve cell type specificity. Elucidating the mechanisms that specify the function of a broadly expressed TF within a given tissue is critical for understanding how genes are differentially regulated to achieve the diversity of cell types throughout the organism.

The highly conserved MEF2 family of transcription factors (MEF2A-D) is expressed in virtually all cells of multi-cellular organisms yet plays specific and critical roles in development of the brain, muscle, bone and hematopoietic lineages (reviewed in (Potthoff and Olson, 2007)). In the mammalian nervous system MEF2s regulate neural-progenitor differentiation, neurotrophin and activity-dependent neuronal survival, the activity-dependent restriction of excitatory synapse number as well as synaptic plasticity and behavior (Akhtar et al., 2012; Barbosa et al., 2008; Chen et al., 2012; Cole et al., 2012; Flavell et al., 2006; Li et al., 2008a;

Pulipparacharuvi et al., 2008; Shalizi et al., 2006) In humans, mutations in MEF2C can lead to severe intellectual disability, epilepsy and an absence of speech. (Bienvenu et al., 2013; Novara et al., 2010) Despite their clear importance in the nervous system and many other tissues, relatively little is known about how these globally expressed TFs regulate distinct steps in the development of the nervous system and a wide range of other tissues.

The effect of MEF2 on gene expression in a given cell type is determined at least in part by where MEF2 binds across the genome. MEF2 family members are known to recognize and bind to a common consensus DNA motif (YTAWWWTAR) termed the MEF2 responsive element (MRE) (Flavell et al., 2008; Potthoff and Olson, 2007). In vitro experiments indicate that DNA sequences that conform to this consensus site bind MEF2 with high affinity, while sequences that differ from the consensus MRE bind MEF2 with lower affinity (Pollock and Treisman, 1991). These findings have led to the suggestion that MEF2 binding in a cell might be inferred from the presence of good consensus MREs within the promoters of genes whose expression is altered when MEF2 function is inhibited.

One clue as to how MEF2 family members achieve their tissue specific functions has been provided by characterization of MEF2 target genes in distinct tissues. This has been accomplished using chromatin immunoprecipitation assays to identify genomic regions that bind MEF2, and gene disruption experiments to determine if the expression of MEF2-bound genes is altered by the inhibition of MEF2 function. Using these approaches in neurons, MEF2 has been shown to control the transcription of synaptic regulatory proteins such as *Arc* and *Syngap1*, and in myocytes and hematopoietic cells to regulate *Myog* and *Il2* respectively (Andres et al., 1995; Flavell et al., 2008; Pan et al., 2004; Potthoff and Olson, 2007; Sebastian et al., 2013). While to date no experiments have directly compared MEF2 target genes across different tissues, this

work suggests that MEF2 functions at least in part by regulating distinct target genes in different cell types. However, it is not known if MEF2 achieves cell type specificity by differential binding to promoters or by binding to the same regulatory elements across tissues but differentially activating target genes in these distinct cell types.

The recent identification of enhancers as important mediators of tissue-specific gene expression (Spitz and Furlong, 2012) raises the possibility that MEF2 achieves at least some of its tissue-specific function by binding to and regulating tissue-specific enhancers. Alternatively, MEF2 could bind to the same enhancers in all tissues, but function at just a subset of these sites in a specific tissue. Significant innovations in high-throughput sequencing technology now make it possible to identify sites of TF binding genome-wide and to assess the activity of each bound region (Creyghton et al., 2010; Johnson et al., 2007; Kim et al., 2010; Rada-Iglesias et al., 2011), however these approaches have not yet been used to determine whether or how MEF2 selectively regulates enhancers or promoters in a tissue-specific manner.

Once bound to an MRE that is present in an enhancer or target gene promoter, MEF2 is believed to either repress or activate nearby target genes, largely through interactions with co-factors such as histone deacetylases and acetylases (Potthoff and Olson, 2007). In addition, it has been suggested that in myocytes MEF2 family members work together with muscle specific bHLH factors to regulate gene expression. Several models for the possible functions of this interaction have been proposed, ranging from cooperative binding to cooperative activation (Black and Olson, 1998; Molkenin et al., 1995). However, whether MEF2's interaction with co-factors actually contributes to MEF2-dependent gene expression *in vivo*, and if MEF2s employ similar mechanisms to regulate gene expression in the central nervous system (CNS) have not been examined.

To determine how a widely expressed TF such as MEF2 regulates tissue specific gene expression during key steps in CNS development, we identified a cell type in the CNS, the photoreceptor cells of the mouse retina, where a single MEF2 family member, MEF2D, is predominantly expressed. A newly generated loss-of-function allele for MEF2D revealed a critical role for MEF2D in mouse retinal photoreceptor development and in the regulation of cell type-specific gene expression, including genes that are mutated in human retinal diseases. *In vivo* genomic and phenotypic analyses demonstrated that MEF2D regulates cell type-specific gene expression in photoreceptors by binding tissue-specific enhancers together with the retina-specific TF CRX. Analysis of MEF2D binding and enhancer activation in *Crx* KO retinæ revealed that CRX shapes MEF2D function by recruiting MEF2D to tissue specific enhancers that based on their sequence would have been expected to bind MEF2 only weakly, and once bound, co-activating a subset of the MEF2D-CRX bound elements. These findings suggest that broadly expressed TFs acquire their tissue-specific functions through competitive recruitment to enhancers by tissue-specific TFs and selective activation of these enhancers to regulate tissue-specific target genes.

2.3 Results

***Mef2d* is required cell-autonomously for photoreceptor development and function**

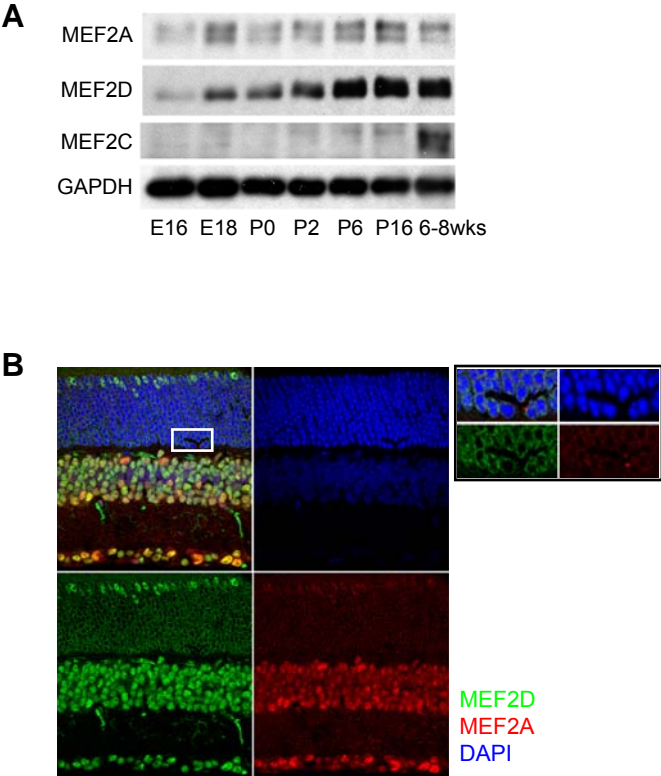
To address how the broadly expressed MEF2 transcription factor family achieves tissue-specific function in the CNS, we focused our studies on a single family member, *Mef2d*, that is widely expressed and has been implicated in critical aspects of neural development (Flavell et al., 2006; Flavell et al., 2008). We first sought to identify a region of the CNS where MEF2D is the predominant family member expressed and therefore is not likely to be functionally redundant with other MEF2 family members. We reasoned that such a region could serve as an experimental system for understanding the context-dependent role of MEF2D in neuronal development. An investigation of MEF2 expression in the cortex, hippocampus and cerebellum revealed that the major cell types of these regions co-express MEF2 family members (data not shown). We therefore turned to the retina, whose well-characterized and spatially separated cell types might allow us to identify a cell type that exclusively expresses MEF2D. We found that both MEF2A and MEF2D are expressed in the developing retina. In contrast MEF2C is only expressed after retinal development is complete (**Figure 2.1A**). While both MEF2A and D are co-expressed in many types of retinal neurons such as horizontal, bipolar, amacrine and retinal ganglion cells (**Figure 2.1B**), MEF2D is the dominant MEF2 family member expressed in maturing photoreceptor cells in the outer nuclear layer (ONL) (**Figure 2.1B**). Retinal photoreceptor cells are a specialized class of primary sensory neurons that detect the incidence of photons upon the retina and transduce this event into a neural signal for processing by downstream regions of the visual system. Given the importance of MEF2 family members in neuronal development we hypothesized that MEF2D may play a critical role in the development

Figure 2.1. Expression of MEF2 family members in the retina

(A) Western blot of MEF2 family member expression in mouse retina over development.

(B) Immunofluorescence (IF) of P25 WT retina for MEF2A (red) and MEF2D (green), DAPI (blue).

Figure 2.1. (Continued) Expression of MEF2 family members in the retina



of photoreceptor cells and that this role may yield important insights into the cell-type specific functions of MEF2 factors.

To explore the role of MEF2D in photoreceptors we generated a *Mef2d* knockout allele in which the first five protein-coding exons of *Mef2d*, including the entirety of the highly conserved MADS and MEF2 DNA-binding and dimerization domains, were removed (**Figure 2.2**). This allele differs from a previously generated mutant allele of *Mef2d*, in which only the second coding exon of *Mef2d* was removed (Kim et al., 2008). This previously generated allele results in a highly expressed truncated protein product with a partial DNA binding domain. The presence of this residual protein product could potentially complicate the interpretation of phenotypes in these mice. This potential problem is eliminated in the new line of conditional *Mef2d* knock out mice, termed *Mef2d*^{A2-6} (**Figure 2.2**). These mice were used for all subsequent analyses and are referred to below as *Mef2d* KO mice.

Mef2d KO mice are born in Mendelian ratios and are fertile but exhibit a slightly decreased body weight compared to WT littermates ($p=1.35e-6$; **Figure 2.2H**). While MEF2D is expressed throughout the CNS, the brains of *Mef2D* KO mice appear normal, most likely due to compensation by other MEF2 family members. By contrast, the retinæ of *Mef2d* KO mice display a significant defect in the maturation of rod and cone photoreceptors. At postnatal day 11 (p11) *Mef2d* KO retinæ are grossly normal and contain all major cell types. However, by p21, *Mef2d* KO photoreceptor cells differ strikingly from WT photoreceptors in that they lack the outer segment structures that are necessary for vision (**Figure 2.3**). Photoreceptor outer segments are an apical organelle of stacked membranous discs in which phototransduction

Figure 2.2. Generation and validation of new *Mef2d* knockout and conditional mice

(A) **Schematic of the *Mef2d* gene targeting strategy.** Top, WT allele schematic, aligned with the corresponding part of the targeting construct. The *Mef2d* allele was targeted by flanking exons 2 through 6 of the *Mef2d* genomic locus with loxP sequences (red triangles). Exons 2 and 3 include the highly conserved MEF2 and MADS domains critical for DNA-binding and MEF2 dimerization. A neomycin positive selection cassette (N) was inserted with a 3rd loxP site at the 3' end of the targeted region and Diphtheria toxin A (DTA) served as a negative selection marker. Targeted ES cells were selected by resistance to G418 (and survival, and therefore lack, of DTA) and analyzed by Southern analysis. Purple and blue boxes represent relative positions external to the targeted region of 5' and 3' southern probes, respectively, and southern digest sites are denoted in corresponding colors as (T) and (AI) again for 5' and 3' southern analysis of ES cells. Distances between endogenous Tth111I or ApaI restriction sites for southern analysis in either the WT locus or targeted allele are illustrated. Successfully targeted ES cells were then injected into pseudopregnant females, and subsequent progeny were assessed for successful germline transmission of the targeted allele. Mice carrying the targeted allele were crossed to the EIIA-Cre deleter line to generate *Mef2d* KO mice, where the entire region between the most 5' and 3' loxP sites was deleted, and *Mef2d*^{fl/fl} conditional mice, where only the neomycin cassette was removed by Cre but two loxP sites remained in a now otherwise WT locus. Green and yellow arrows denote relative positions of PCR genotyping primers.

Figure 2.2. (Continued) Generation and validation of new *Mef2d* knockout and conditional mice

(B) Southern analysis of ES cells. Southern blot analysis of Tth111I (top) or ApaI (bottom)-digested genomic DNA from targeted ES cells using 5' or 3' probes (purple and blue boxes in Figure 2.2A, respectively) indicates correct targeting of the *Mef2d* genomic locus. Expected genomic DNA fragment lengths are illustrated in Figure 2.2A above. Southern analysis shown was performed prior to Cre-mediated removal of the neomycin cassette.

(C) Southern analysis of targeted mice. Southern blot performed as described above using ApaI-digested genomic DNA from mouse liver and the same 3' probe. Genomic fragment lengths indicate correct targeting of the *Mef2d* genomic locus. Southern analysis shown was performed prior to Cre-mediated removal of the neomycin cassette.

(D) PCRs used for routine genotyping of *Mef2d* floxed mice. Genotyping of the *Mef2d* conditional allele. Genotyping was performed by PCR using primer pairs 5'F (5'-gggttcagtccccagtgtaa-3') and 5'R (5'-cccctagtcagagcttg-3') as well as 3'F (5'-tgaggtaacctgtgcttg-3') and 3'R (5'-aaggcctggagagaaggtg-3'), which span the 5' and 3' loxP sites introduced in introns I and VI, respectively.

Figure 2.2. (Continued) Generation and validation of new *Mef2d* knockout and conditional mice

(E) PCRs used for routine genotyping of *Mef2d* knockout mice. Genotyping of the *Mef2d* null allele. Genotyping was performed by PCR using primers as described above in the following pairs: 5'F and 5'R, or 5'F and 3'R, to test for the presence of a WT or null allele, respectively. 5'F and 3'R are significantly far away on the WT allele and so a productive PCR reaction is only observed with a null allele.

(F) Absence of full-length MEF2D protein in *Mef2d* KO mice. Western blot of MEF2D in whole brain lysates in *Mef2d* KO mice and littermates heterozygous or WT for *Mef2d*. An antibody that recognizes part of the protein C-terminal to the exons deleted in the *Mef2d* targeting strategy demonstrates complete loss of the full-length protein in the KO mice. A small truncated product appears in *Mef2d* KO lysates with very low levels of expression (asterisk).

(G) Effective removal of conditional *Mef2d* allele. Western blot of MEF2D in whole brain lysates of a *Mef2d*^{fl/fl} mouse with nestin-cre and a littermate *Mef2d*^{fl/fl} mouse with no Cre. Actin was used as a loading control.

(H) *Mef2d* KO mice have reduced body weight. *Mef2d* KO mice were weighed at p11 along with a paired WT littermate. N=24 pairs. Graph demonstrates mean +/- SEM. *p=1.35e-6.

Figure 2.2 (Continued). Generation and validation of new MEF2D knockout and conditional mice

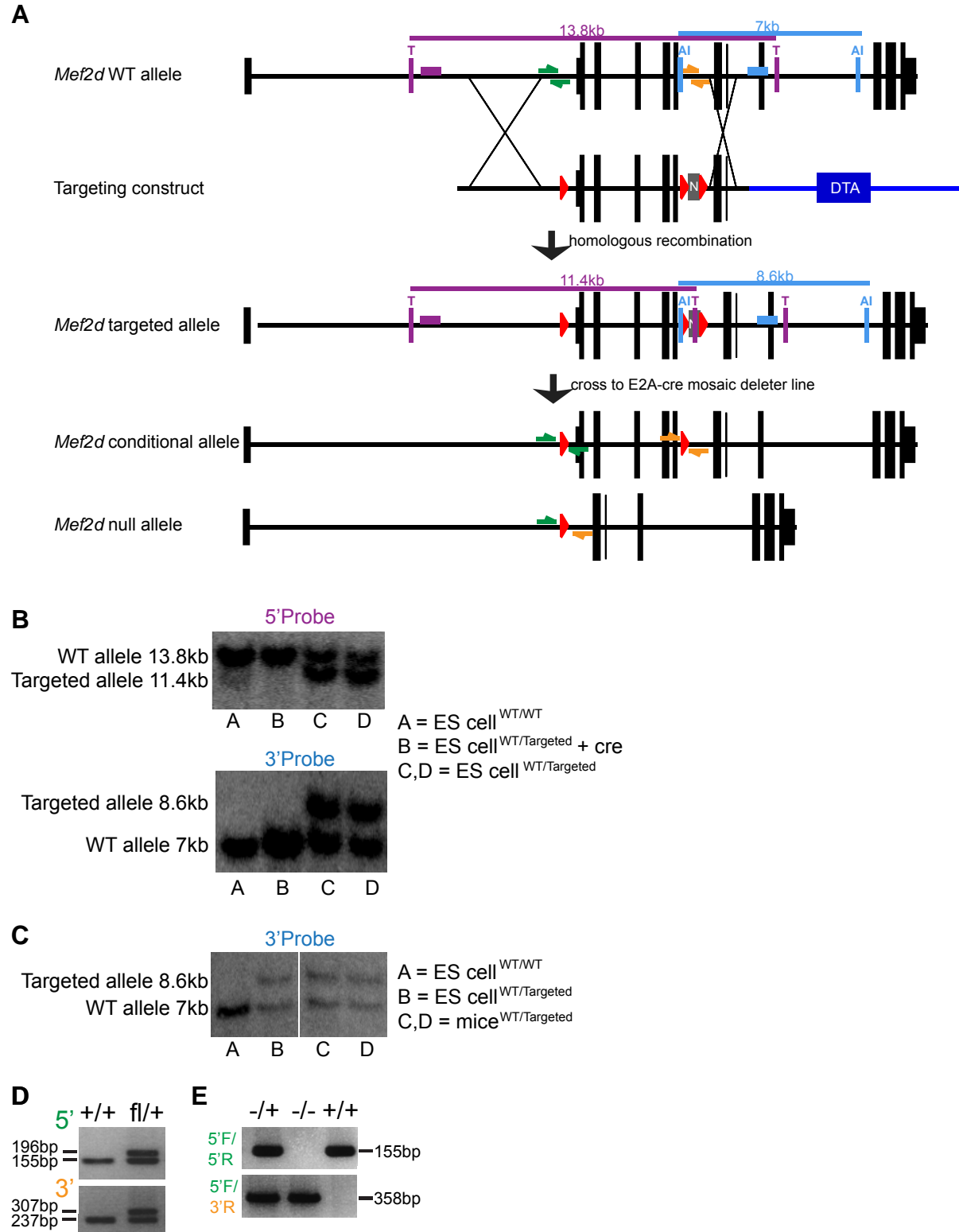


Figure 2.2 (Continued). Generation and validation of new MEF2D knockout and conditional mice

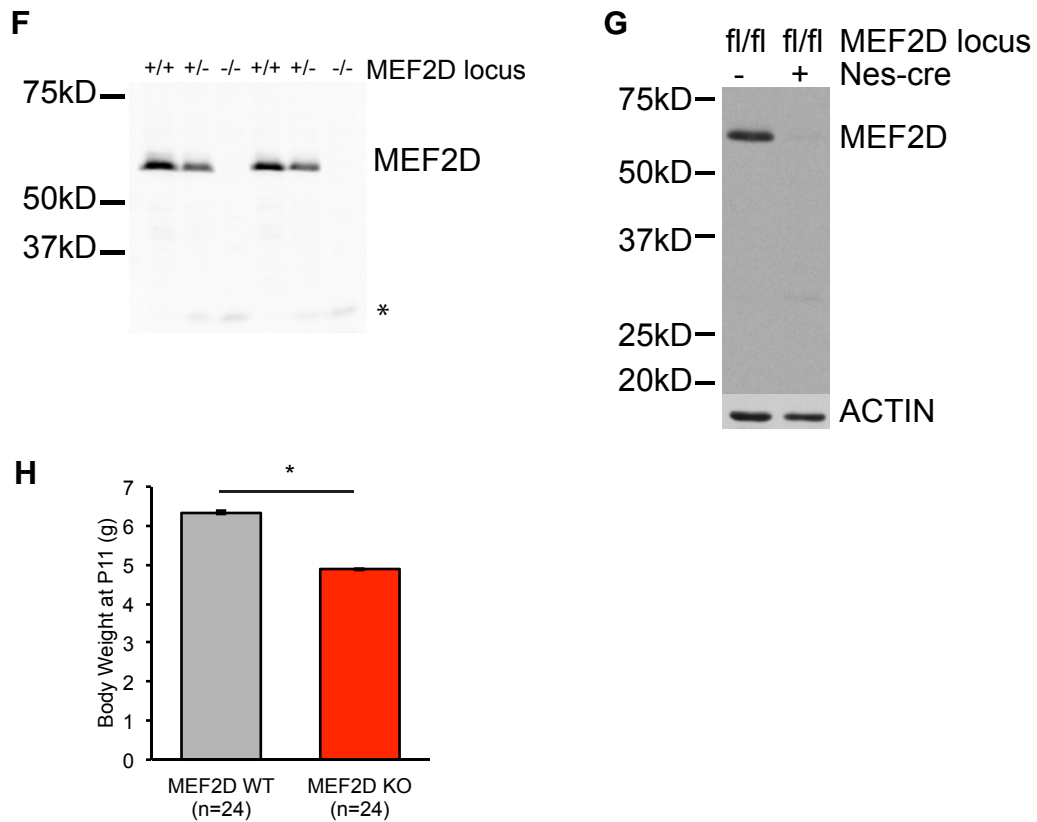
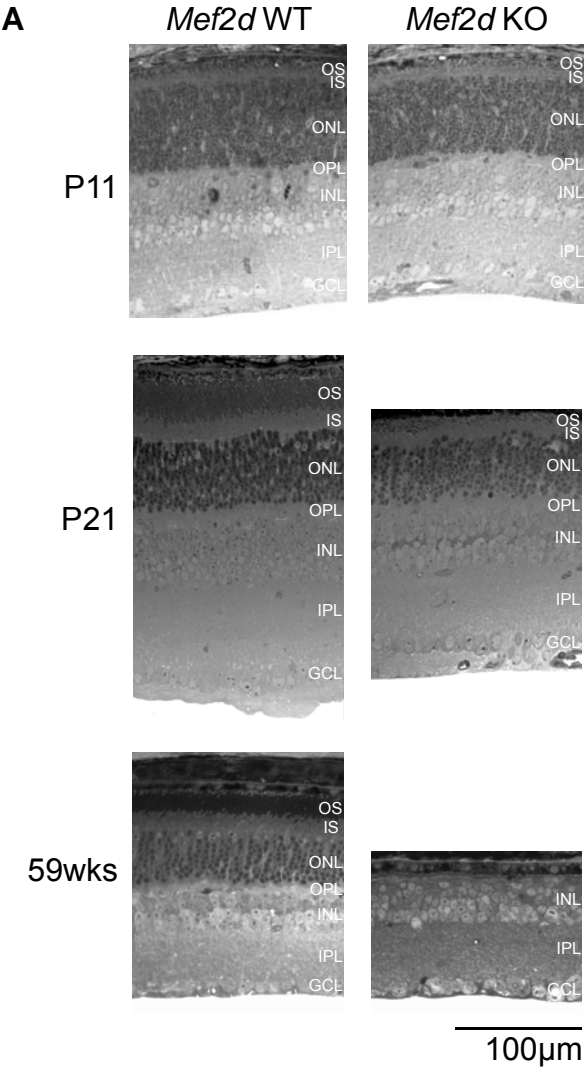


Figure 2.3. *Mef2d* KO mice have defects in retinal photoreceptor development

(A) Time course of toluidine blue-stained 1 μ m cross-sections of MEF2D KO and WT littermate retinas.

Figure 2.3. (Continued) *Mef2d* KO mice have defects in retinal photoreceptor development



occurs and where the cascade of neuronal signaling that underlies the visual response to light begins. The development of these structures normally occurs between p11 and p28, which corresponds to the functional maturation of photoreceptors. The failure of outer segment development in *Mef2d* KO retinae should lead to a deficit in photoreceptor function. Correspondingly, *in vivo* electroretinograms (ERGs) performed at p21 revealed that visual responses are almost completely absent in *Mef2d* KO mice compared to WT littermates in both dark and light-adapted conditions (**Figure 2.4**). This indicates that both rod and cone photoreceptors are non-functional in *Mef2d* KO mice, and that the failure of rods and cones to elaborate outer segments in the absence of MEF2D renders *Mef2d* KO mice blind. Very few apoptotic cells are present in *Mef2d* KO retinae at p21, however the failure of *Mef2d* KO photoreceptors to develop normally eventually leads to a slow retinal degeneration (**Figure 2.3**). Taken together these findings indicate that MEF2D is required for photoreceptor development, long-term survival and vision.

Since MEF2D is expressed in retinal photoreceptors, the developmental failure of photoreceptors to form outer segments in *Mef2d* KO retinae seems likely to be due to a cell-intrinsic requirement for *Mef2d*. However, to rule out the possibility that a MEF2D-dependent alteration in the extracellular environment during photoreceptor development is responsible for the deficits observed (Thompson et al., 2000), we selectively removed *Mef2d* from individual developing photoreceptors by sparsely introducing Cre recombinase into *Mef2d^{fl/fl}* photoreceptors using *in vivo* electroporation. We found that at p21, photoreceptors in which the expression of MEF2D is disrupted have highly abnormal outer segments when compared to photoreceptors still expressing MEF2D (**Figure 2.5**). The abnormal morphology was also recapitulated in

Figure 2.4. *Mef2d* KO mice are functionally blind

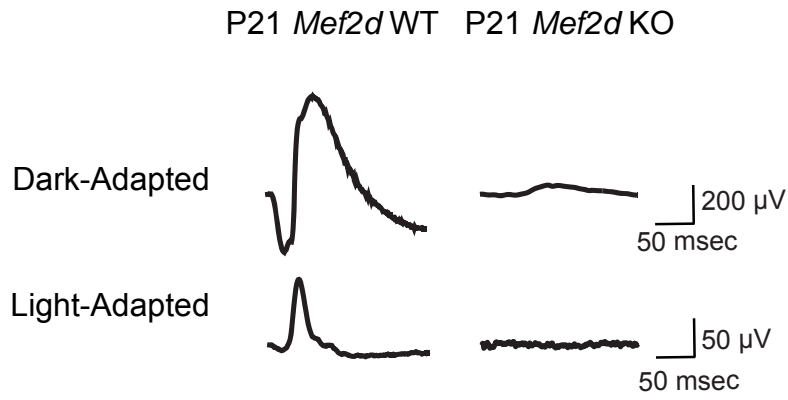
(A) Representative electroretinograms (ERGs) from a P21 MEF2D KO mouse and WT littermate in both dark-adapted (DA) and light-adapted (LA) conditions.

(B) Quantification of A and B wave amplitudes from individual mice for ERGs shown in (A).

N=3 each MEF2D WT and KO littermates. ND= not detected.

Figure 2.4. (Continued) Mef2d KO mice are functionally blind

A



B

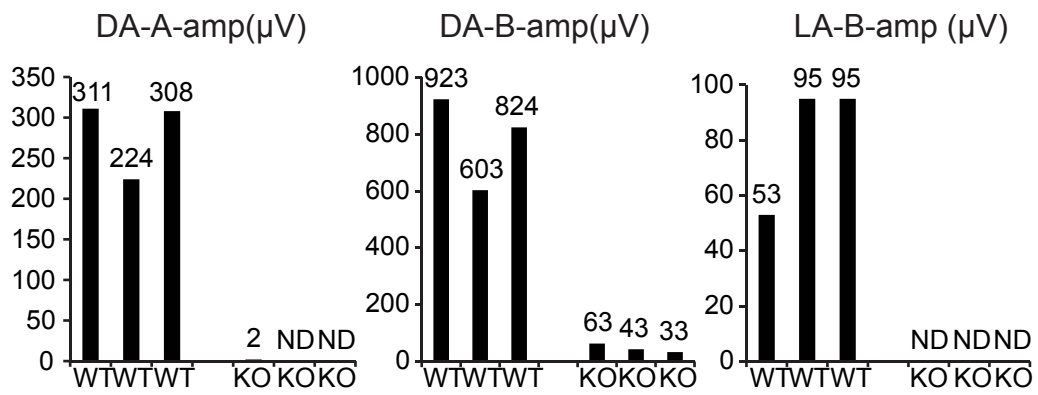


Figure 2.5. *Mef2d* is required cell autonomously for photoreceptor development

(A) Representative image of MEF2D immunofluorescence of photoreceptor nuclei in ONL of P21 retina electroporated at P0 for sparse expression of CRE recombinase and GFP in a *Mef2d*^{fl/fl} mouse. Asterisks indicate example GFP+ cells expected to be expressing CRE and to have removed MEF2D.

(B) Schematic of quantification of disruption of OS in sparse electroporations. ABCA4 immunostaining identified outer segments (OS) and the area between ABCA4 and DAPI staining was considered inner segments (IS). Mean GFP intensity in the OS was normalized to mean GFP intensity in the IS.

(C) Representative immunofluorescence images of morphology of P21 retinal photoreceptor cells electroporated at P0 for sparse expression of Cre recombinase and GFP in either *Mef2d*^{fl/fl} or *Mef2d*^{fl/+} mice.

(D) Quantification of OS from GFP-positive photoreceptors as shown in (C). Mean GFP intensity in the ABCA4-positive region (OS GFP) was normalized to mean GFP intensity in the inner segments (IS GFP) as a control for electroporation density (*Mef2d*^{fl/+}, N=6; *Mef2d*^{fl/fl}, N=3 retinas). Error bars represent S.E.M.

(E) Representative image of MEF2D IHC of photoreceptor nuclei in ONL of P21 retina electroporated at P0 with GFP and MEF2D shRNA in an otherwise WT mouse. Asterisks indicate example GFP+ cells expected to be expressing MEF2D shRNA.

Figure 2.5. (Continued) *Mef2d* is required cell autonomously for photoreceptor development

(F) Left, representative images of IHC of photoreceptors of P21 WT retinas electroporated at P0 for sparse expression with pCAG-GFP and either a scrambled shRNA control (scrm shRNA), or MEF2D shRNA. Right, Quantification of OS disruption from GFP-positive photoreceptors as shown at left. Error bars represent S.E.M.

(G) Left, representative images of IHC of photoreceptors of P21 WT retinas electroporated at P0 for sparse expression with pCAG-GFP and either MEF2D shRNA or MEF2D shRNA with an shRNA-resistant form of MEF2D (MEF2D RiR). Right, Quantification of OS disruption from GFP-positive photoreceptors as shown at left. Error bars represent S.E.M.

Figure 2.5. (Continued) Mef2d is required cell autonomously for photoreceptor development

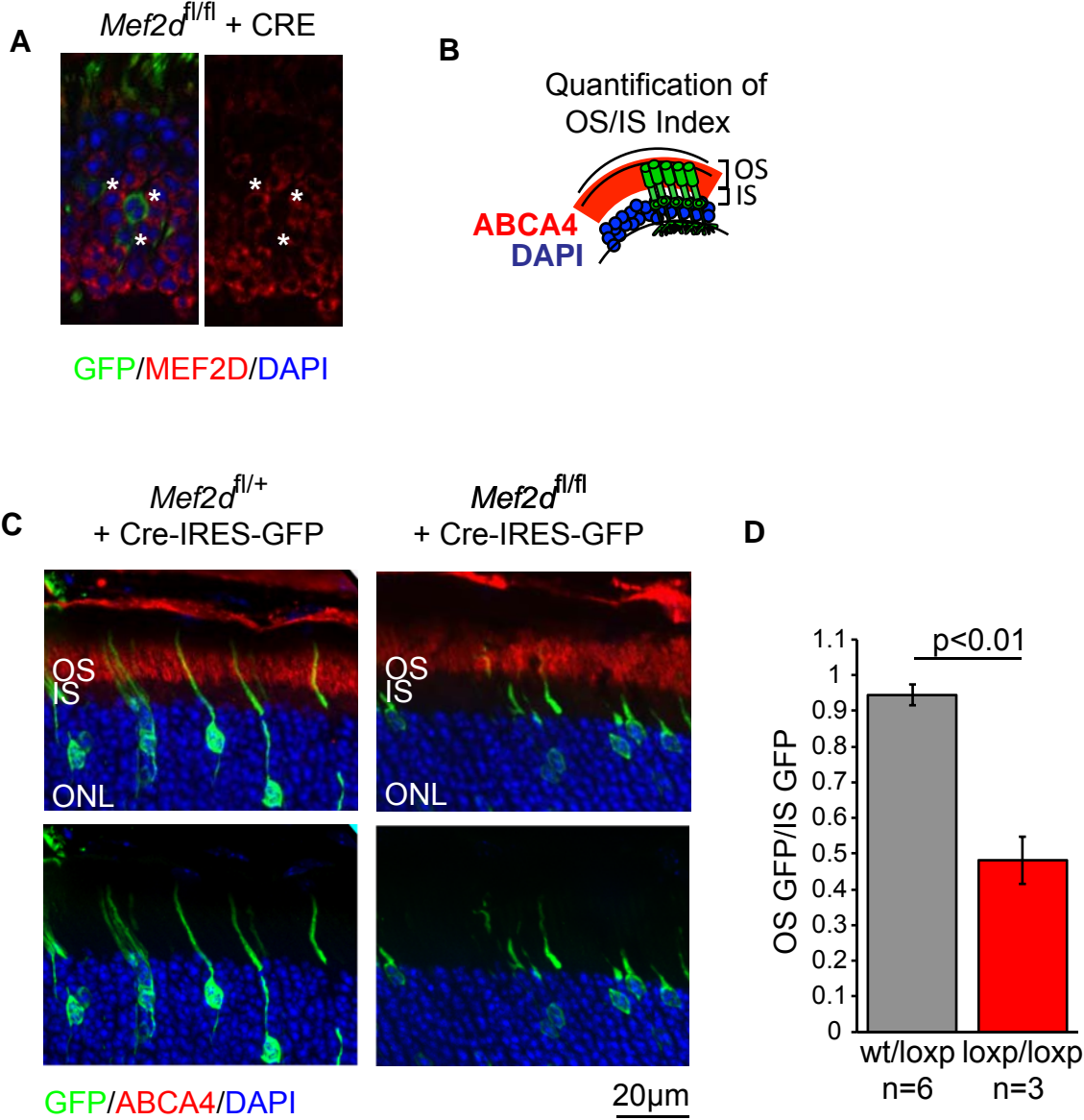
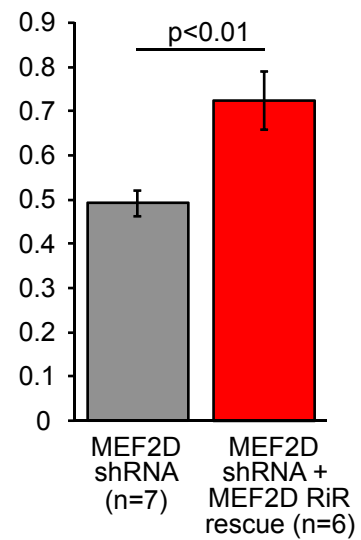
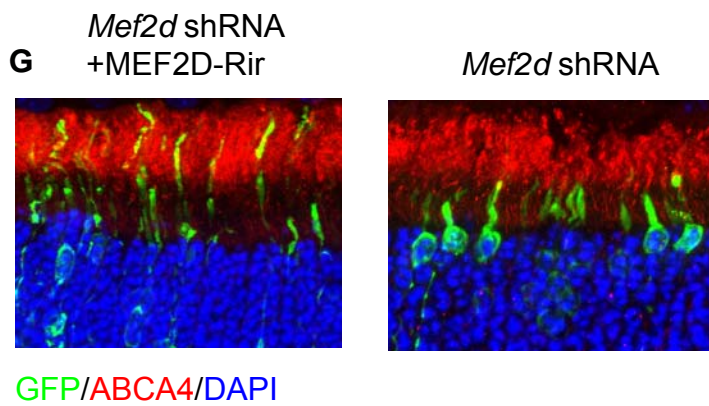
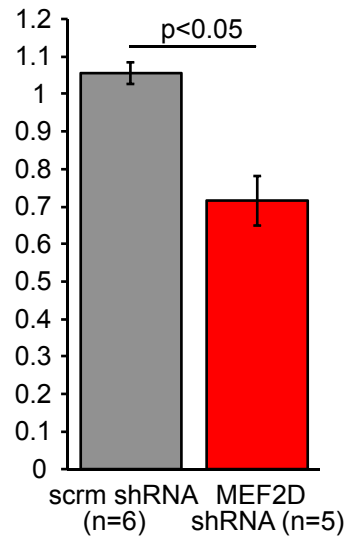
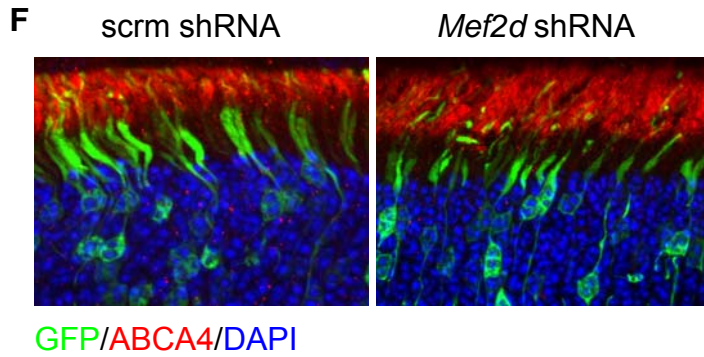
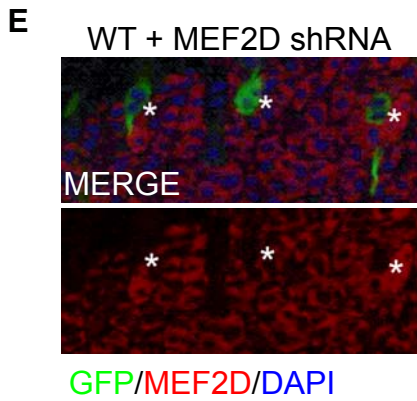


Figure 2.5 . (Continued) Mef2d is required cell autonomously for photoreceptor development



photoreceptors where MEF2D shRNA was selectively introduced in an otherwise WT retina. Finally, the disruption of photoreceptor development was reversed when the MEF2D shRNA was co-expressed with an shRNA-resistant form of MEF2D (**Figure 2.5**). Taken together these findings suggest that MEF2D functions cell-intrinsically to promote photoreceptor development, and that in the absence of MEF2D, photoreceptors fail to mature and ultimately die.

MEF2D regulates critical cell-type specific targets and disease genes in the retina

Given that MEF2D is a TF it is likely that the gene targets of MEF2D regulate aspects of photoreceptor development and function. One possibility is that MEF2D regulates photoreceptor-specific target genes that encode proteins necessary for photoreceptor development. Alternatively, because MEF2 family members are expressed in a multitude of different tissues, it could be that MEF2D controls photoreceptor differentiation by regulating a core set of target genes that are shared across cell types. To distinguish between these possibilities and to identify candidate target genes of MEF2D we performed high-throughput RNA sequencing (RNA-seq) of total RNA from WT and *Mef2d* KO retinæ at p11. At p11, MEF2D is strongly expressed but WT and *Mef2d* KO retinæ are morphologically indistinguishable. Thus, differences in gene expression between WT and *Mef2d* KO retinæ at p11 should be primarily due to the disruption of MEF2D-dependent transcriptional programs rather than due to cell attrition or the secondary effects of disrupted retinal development.

We find that the expression of most genes is unchanged when WT and *Mef2d* KO p11 retinæ are compared (Spearman's correlation coefficient $r = 0.988355$) (**Figure 2.6**). However, a

Figure 2.6. MEF2D regulates critical cell-type specific targets and disease genes in the retina

(A) RNA-seq average exon density for individual genes in P11 WT and MEF2D KO retinæ are displayed in gray (n=2 per genotype). Genes were considered upregulated (green dots) or downregulated (red dots) if average KO exon density was 2x or more reduced with respect to average WT exon density. The black line indicates unity.

(B) qPCR validation of RNA-seq results for example MEF2D target genes; n=3 for each data point. Error bars represent S.E.M.

(C,D) IHC of P11 MEF2D KO and WT littermate retinæ for MEF2D target genes (C) GUCA1B AND (D) ARR3.

(E) Western blot for ARR3 expression in P11 MEF2D KO and WT littermate retinas.

(F) Examples of MEF2D target genes relevant to photoreceptor cell biology. Genes implicated in retinal disease are in blue.

Figure 2.6. (Continued) Mef2d regulates critical cell-type specific targets and disease genes in the retina

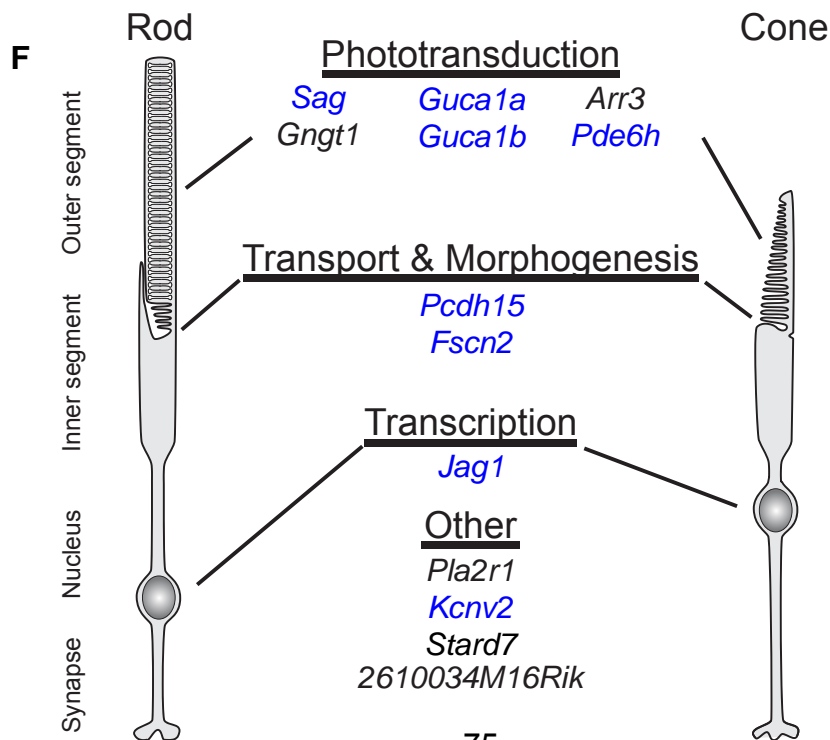
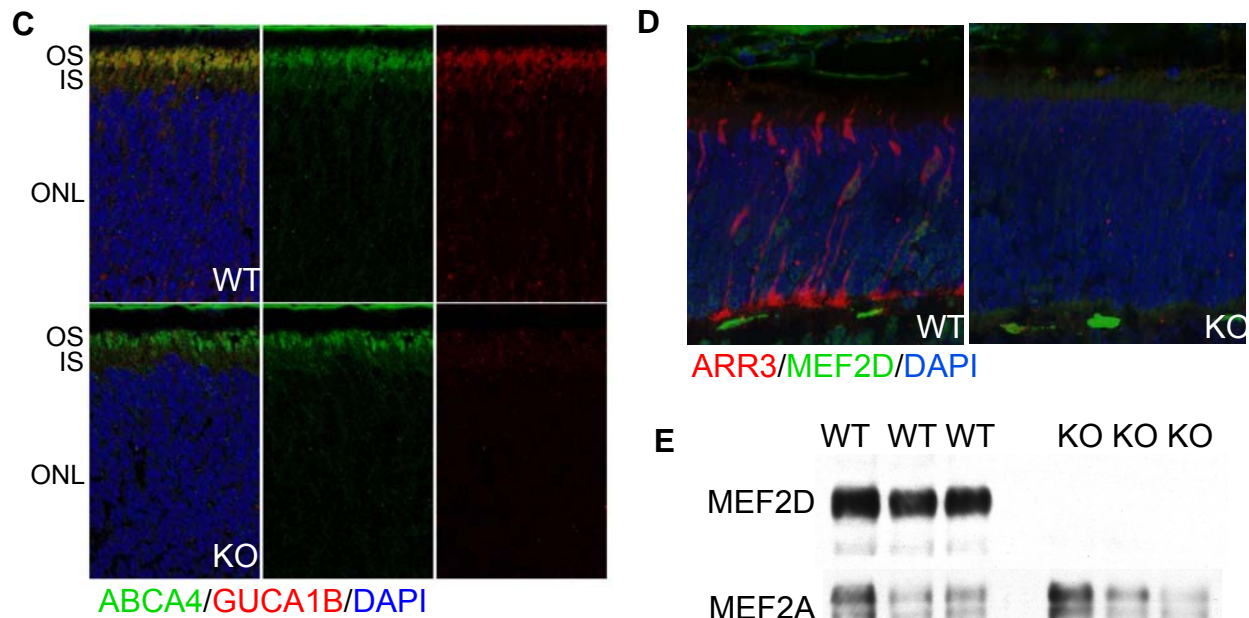


Table 2.1. Significantly misregulated genes in MEF2D KO versus WT retinae

Gene	GeneID	RefSeqs	Avg WT exon density	Avg KO exon density	KO/WT exon density
Ahrr	11624	NM_009644.2	0.202	0.030	0.146
Apobec2	11811	NM_009694.2	3.617	0.474	0.131
Arg2	11847	NM_009705.1	2.299	1.042	0.453
Atp10a	11982	NM_009728.1	0.122	0.042	0.342
Pcdh15	11994	NM_023115.2	4.611	0.606	0.131
Zfp3612	12193	NM_001001806.2	1.960	0.558	0.285
Cacnal1s	12292	NM_001081023.1	0.137	0.023	0.168
Cdc25c	12532	NM_009860.2	0.153	0.052	0.338
Cdr2	12585	NM_007672.1	8.160	3.417	0.419
Cr2	12902	NM_007758.2	0.053	0.203	3.830
Cst7	13011	NM_009977.2	0.040	0.126	3.152
Drd4	13491	NM_007878.2	10.252	3.078	0.300
Egr1	13653	NM_007913.5	0.177	0.581	3.293
Gngt1	14699	NM_010314.2	236.598	115.056	0.486
Lrp2	14725	NM_001081088.1	0.955	0.295	0.309
Gpr56	14766	NM_018882.2	0.103	0.211	2.047
Guca1a	14913	NM_008189.2	11.870	5.147	0.434
Hk2	15277	NM_013820.2	1.424	0.190	0.133
Igj	16069	NM_152839.1	1.036	0.026	0.025
Cd74	16149	NM_001042605.1 NM_010545.3	0.046	0.238	5.234
Jag1	16449	NM_013822.3	4.285	1.855	0.433
Mesp1	17292	NM_008588.1	0.215	0.585	2.729
Mod1	17436	NM_008615.1	3.134	1.456	0.465
Myom1	17929	NM_010867.1	0.308	0.113	0.368
Nppb	18158	NM_008726.3	0.047	0.116	2.495
Pax7	18509	NM_011039.2	0.085	0.298	3.496
Pcolce	18542	NM_008788.2	0.206	0.457	2.219
Prkcm	18760	NM_008858.2	2.843	1.342	0.472
Pla2r1	18779	NM_008867.1	6.804	0.267	0.039
Ppp1r1b	19049	NM_144828.1	0.184	0.416	2.266
Prss12	19142	NM_008939.1	0.070	0.193	2.767
Prtn3	19152	NM_011178.2	0.108	0.053	0.492
Pygm	19309	NM_011224.1	2.681	0.854	0.319
Rps3a	20091	NM_016959.3	23.658	0.356	0.015
Sag	20215	NM_009118.2	516.187	205.101	0.397
Six1	20471	NM_009189.2	0.038	0.193	5.013
Slc31a2	20530	NM_025286.2	3.711	0.791	0.213
Slc6a2	20538	NM_009209.2	0.113	0.010	0.088
Tnfaip3	21929	NM_009397.2	4.588	1.654	0.361
Tnfsf12	21944	NM_011614.1	3.048	1.316	0.432
Tnnt1	21955	NM_011618.1	1.142	0.501	0.439
Tph1	21990	NM_009414.2	0.318	0.710	2.234
Vtn	22370	NM_011707.1	23.612	4.136	0.175
Clca3	23844	NM_017474.1	0.615	0.262	0.426
Slc27a2	26458	NM_011978.2	0.250	0.570	2.283
Rnu32	27209	NR_000002.8	0.659	1.337	2.027
Mapk12	29857	NM_013871.2	0.378	0.139	0.367

Table 2.1. (Continued) Significantly misregulated genes in MEF2D KO versus WT retinae

Gene	GeneID	RefSeqs	Avg WT exon density	Avg KO exon density	KO/WT exon density
Chst3	53374	NM_016803.2	0.328	0.158	0.482
Col5a3	53867	NM_016919.2	0.421	1.101	2.617
Srpk3	56504	NM_019684.1	0.167	0.019	0.114
Ankrd2	56642	NM_020033.1	0.392	0.884	2.252
Rabgef1	56715	NM_019983.2	9.874	3.114	0.315
Rgs20	58175	NM_021374.3	0.673	0.100	0.148
Rab37	58222	NM_021411.3	0.146	0.401	2.742
Fcamr	64435	NM_144960.1	0.236	0.018	0.076
1110032A04Rik	66183	NM_133675.1	0.322	0.713	2.212
2310007A19Rik	66353	NM_025506.2	3.096	1.185	0.383
Pep4l1	66425	XM_484933.5	5.257	2.561	0.487
Asrgl1	66514	NM_025610.3	6.175	2.413	0.391
Grtp1	66790	NM_025768.2	5.386	1.986	0.369
D16Ert472e	67102	NM_025967.2	2.817	1.097	0.389
Ube2t	67196	NM_026024.2	0.219	0.679	3.101
2810055F11Rik	67217	NM_026038.2	0.618	1.255	2.031
Lass4	67260	NM_026058.3	11.140	4.316	0.387
Hapln3	67666	NM_178255.3	0.287	0.133	0.462
Wfdc2	67701	NM_026323.2	0.069	0.171	2.478
Tmem86a	67893	NM_026436.2	2.501	5.102	2.040
Rpl34	68436	NM_001005859.2 NM_026724.1	12.895	0.582	0.045
1110012N22Rik	68515	XM_126634.6	0.372	0.132	0.355
Uckl1	68556	NM_026765.3	10.491	4.285	0.408
1110020G09Rik	68646	NM_001040395.2	26.976	11.732	0.435
Fndc1	68655	NM_001081416.1	0.168	0.081	0.482
Mybphl	68753	NM_026831.1	0.125	0.021	0.169
2610034M16Rik	69239	NM_027001.1	5.578	0.008	0.001
Tnfsf13	69583	NM_023517.2	6.526	2.420	0.371
2610528A11Rik	70045	XM_980662.1	0.078	0.177	2.270
Dpf3	70127	NM_058212.1	6.821	2.902	0.425
2510049J12Rik	70291	XM_132808.3	0.376	0.765	2.033
Lrfrn2	70530	NM_027452.2	0.859	0.325	0.378
Glb1l3	70893	XM_983469.1	0.121	0.015	0.127
4921537P18Rik	70952	NM_026256.2	0.114	0.027	0.234
5430419D17Rik	71395	NM_175166.3	0.450	0.002	0.003
Bbs7	71492	NM_027810.2	27.336	13.118	0.480
Ppm1j	71887	NM_027982.2	0.999	0.363	0.363
Slc39a4	72027	NM_028064.2	0.080	0.256	3.187
Tnfrsf13c	72049	NM_028075.2	0.090	0.493	5.472
Rrp1b	72462	NM_028244.1	6.624	2.801	0.423
2810030E01Rik	72668	NM_028317.1	4.211	1.616	0.384
Rbm20	73713	XM_001002314.2	1.077	2.236	2.076
Psd	73728	NM_028627.2	4.247	1.566	0.369
Arsg	74008	NM_028710.2	1.353	0.601	0.444
2310042D19Rik	74183	NM_172417.2	0.079	0.184	2.323
1700092M07Rik	74307	XM_897786.2	0.088	0.226	2.566
4833403I15Rik	74574	XM_988298.1	0.030	0.141	4.712

Table 2.1. (Continued) Significantly misregulated genes in MEF2D KO versus WT retinae

Gene	GeneID	RefSeqs	Avg WT exon density	Avg KO exon density	KO/WT exon density
Rab3i1	74760	NM_144538.2	0.671	1.605	2.390
Calml4	75600	NM_138304.2	0.769	3.222	4.188
Dock8	76088	NM_028785.3	0.200	0.463	2.311
Gpsm2	76123	NM_029522.1	5.163	2.560	0.496
Slc38a3	76257	NM_023805.2	12.139	4.815	0.397
D230044M03Rik	76743	XM_354583.3	0.399	1.346	3.374
C030048H21Rik	77481	XM_975397.2	0.590	1.183	2.005
A930004D18Rik	77940	XR_035303.1	0.624	0.283	0.454
A930023M06Rik	77958	XM_001478569.1	0.456	0.072	0.158
D730039F16Rik	77996	NM_030021.2	0.644	1.395	2.168
Pde6h	78600	NM_023898.4	20.224	2.878	0.142
Cstad	78617	NM_030137.2	0.308	0.154	0.498
Il23a	83430	NM_031252.2	0.066	0.172	2.613
Lin28	83557	NM_145833.1	0.151	0.474	3.136
Kcnn1	84036	NM_032397.1	1.714	3.866	2.256
Igsf9	93842	NM_033608.2	1.196	0.426	0.356
Ehd4	98878	NM_133838.3	2.555	0.855	0.335
Stard7	99138	NM_139308.1	12.281	5.639	0.459
Olfml3	99543	NM_133859.2	0.973	0.297	0.305
AW011738	100382	XM_001478065.1	0.458	1.023	2.234
Cd276	102657	NM_133983.3	1.044	0.306	0.293
Sncb	104069	NM_033610.2	8.279	3.870	0.467
Nxph4	104080	NM_183297.2	0.301	0.631	2.097
Slc16a6	104681	NM_001029842.1 NM_134038.2	7.231	1.344	0.186
Gucal1b	107477	NM_146079.1	6.373	0.260	0.041
Hist1h1t	107970	NM_010377.2	0.074	0.164	2.205
Chrna5	110835	NM_176844.3	1.370	0.599	0.437
Emid2	140709	NM_024474.2	0.602	2.598	4.317
P2ry14	140795	NM_001008497.1 NM_133200.3	0.204	0.080	0.394
Arr3	170735	NM_133205.2	7.210	0.023	0.003
Glmn	170823	NM_133248.1	11.118	3.420	0.308
Accn3	171209	NM_183000.1	0.729	1.554	2.131
Cnksr1	194231	NM_001081047.1	0.472	0.179	0.379
4831426I19Rik	212073	NM_001042699.1 NM_172500.2	0.313	1.207	3.856
6330514A18Rik	216166	NM_183152.2	3.498	8.922	2.550
Atad4	217138	NM_146026.1	0.038	0.148	3.854
Tmc6	217353	NM_145439.1 NM_181321.3	0.127	0.290	2.290
BC048943	217874	XM_127170.7 XM_902085.2	29.618	13.858	0.468
BC027072	225004	NM_146082.3	11.219	4.303	0.383
5430407P10Rik	227545	NM_144883.3	1.759	4.459	2.534
1700019L03Rik	227736	NM_025619.1	0.141	0.067	0.474
Bpil3	228796	NM_199303.1	0.200	0.021	0.105
Adamts14	229595	NM_144899.2	0.089	0.209	2.339

Table 2.1. (Continued) Significantly misregulated genes in MEF2D KO versus WT retinae

Gene	GeneID	RefSeqs	Avg WT exon density	Avg KO exon density	KO/WT exon density
Ddefl1	230837	NM_001008232.1	0.548	1.143	2.084
Xylt1	233781	NM_175645.3	1.034	0.484	0.468
Dnahc9	237806	XM_110968.7	0.652	0.275	0.421
Fscn2	238021	NM_172802.2	5.271	0.516	0.098
Kcnv2	240595	NM_183179.1	36.929	16.085	0.436
Kcng1	241794	NM_001081134.1	0.052	0.130	2.491
BC029684	242707	XM_205950.7	1.474	3.066	2.081
Padi6	242726	NM_153106.2	0.047	0.194	4.142
Srd5a2l2	243078	NM_153801.2	0.291	0.034	0.117
Hspb6	243912	NM_001012401.2	1.459	0.238	0.163
Wdr17	244484	NM_028220.2	25.765	7.561	0.293
BC038479	244757	NM_153803.1	5.651	1.541	0.273
Kcne2	246133	NM_134110.2	6.383	2.810	0.440
Sntg2	268534	NM_172951.2	0.746	0.084	0.112
Scube3	268935	NM_001004366.1	1.054	2.814	2.670
Hist2h2ac	319176	NM_175662.1	15.087	4.005	0.265
Lrtm1	319476	NM_176920.3	5.236	2.281	0.436
Tmem26	327766	NM_177794.2	0.850	0.240	0.283
9130227L01Rik	329159	XM_488894.3	0.067	0.152	2.268
Pla2g4e	329502	NM_177845.4	0.136	0.066	0.488
Catsper4	329954	NM_177866.3	0.245	0.065	0.263
Adamts3	330119	NM_001081401.1	2.106	0.409	0.194
Ccdc63	330188	NM_183307.2	0.205	0.094	0.461
Gal3st4	330217	NM_001033416.2	0.469	1.962	4.181
Mapk15	332110	NM_177922.2	0.097	0.355	3.642
Col27a1	373864	NM_025685.3	0.126	0.451	3.583
EG381438	381438	NM_198657.2	0.338	0.001	0.003
Gm1698	382003	NM_001033467.1	0.199	0.025	0.127
Adcyl1	432530	NM_009622.1	8.049	2.454	0.305
LOC434166	434166	XM_001478477.1	2.646	1.258	0.476
1700120B06Rik	436062	NM_001033980.1	0.089	0.298	3.330
EG545987	545987	XM_899834.2	0.845	1.952	2.311
LOC546006	546006	XM_620573.4	0.341	0.002	0.005
EG546164	546164	XM_620794.4	0.201	0.072	0.360
OTTMUSG0000006683	550619	NM_001017362.2	0.193	0.602	3.123
Tnfrsf12-tnfrsf13	619441	NM_001034097.1 NM_001034098.1	4.582	1.779	0.388
EG624121	624121	XR_035463.1	0.249	0.589	2.367
EG639545	639545	XM_974340.2	0.101	0.419	4.163
EG667728	667728	XR_035232.1	0.086	23.528	274.058
LOC100039504	100039504	XM_001473019.1	0.347	0.745	2.147
LOC100039605	100039605	XM_001473183.1	1.445	0.602	0.416
LOC100040711	100040711	XM_001474867.1	0.114	0.044	0.384
LOC100042271	100042271	XM_001477849.1	0.357	0.867	2.430
LOC100042588	100042588	XM_001478609.1	0.266	0.008	0.032
LOC100043173	100043173	XM_001479673.1	0.137	0.002	0.017
LOC100043305	100043305	XM_001480125.1	0.004	0.352	80.805
LOC100043412	100043412	XM_001479664.1	1.592	0.191	0.120
LOC100043600	100043600	XM_001480969.1	0.193	0.073	0.379

subset of 185 genes are strongly misregulated in *Mef2d* KO retinae (**Figure 2.6, Table 2.1**). This set of misregulated genes is significantly enriched for retina-specific genes ($p=5e-9$) using the DAVID web tool (Dennis et al., 2003; Huang da et al., 2009a, b). Furthermore, gene ontology (GO) analysis found that these misregulated genes are most enriched for genes involved in processes such as visual perception and sensory perception of a light stimulus. This analysis suggests that MEF2D promotes photoreceptor development by regulating a network of genes essential for photoreceptor function rather than a common set of core target genes shared across cell types and tissues.

The most highly misregulated candidate MEF2D target genes have critical roles in photoreceptor function (**Figure 2.6**). For example, *Sag*, *Gngt1*, *Arr3*, *Pde6h*, *Gucal1a* and *Gucal1b* are key components of the phototransduction cascade. Misregulation of these transcripts in combination would be expected to severely disrupt phototransduction and is likely to be the primary cause of the abnormal photoresponses in *Mef2d* KO mice. Indeed human mutations in *Sag*, *Pde6h*, *Gucal1a* and *Gucal1b* are all associated with visual disorders (Downes et al., 2001; Fuchs et al., 1995; Kohl et al., 2012; Nakazawa et al., 1998; Payne et al., 1998; Piri et al., 2005; Sato et al., 2005). Other photoreceptor-specific target genes which are not directly part of the phototransduction cascade may contribute to the structural defects in outer segment formation observed in *Mef2d* KO retinae. For example, *Fscn2*, a photoreceptor specific actin-bundling protein, is mutated in human forms of retinitis pigmentosa and has been demonstrated to be necessary for outer segment elongation (Wada et al., 2003; Wada et al., 2001; Yokokura et al., 2005). Similarly, *Pcdh15*, a cadherin superfamily member, has been implicated in vesicular trafficking between the inner and outer segments and is mutated in a form of Usher Syndrome (USH1F) characterized by visual impairment and hearing loss (Cosgrove and Zallocchi, 2014;

Daiger et al., 2013). In contrast, MEF2 targets that have been identified in other neuronal cell types such as *Nur77*, *Arc* and *Syngap1* (Flavell et al., 2008) are not strongly expressed in the developing retina under normal conditions. These analyses suggest that the primary function of MEF2D in the retina is to regulate the expression of genes that are critical for specific photoreceptor functions rather than genes with common functions across cell types.

MEF2D binds tissue-specific enhancers with the retina-specific co-factor CRX

We next sought to understand the mechanism by which MEF2D achieves photoreceptor specific regulation of its targets. Elucidating this mechanism is of interest because many MEF2D targets are essential for photoreceptor function and are mutated in human diseases of the retina. The simplest and most prevalent model of MEF2 function is that MEF2 binds to MEF2 consensus binding sites (MREs) in the promoters or enhancers of its target genes and thereby controls their expression (Edmondson et al., 1992; Sandmann et al., 2006; Yee and Rigby, 1993). Given the photoreceptor-specific expression of many MEF2D target genes, in this model the binding of MEF2D would be expected at MREs that are accessible in photoreceptors but not other neuronal cell types. The ability of MEF2D to recognize and bind to these photoreceptor specific MREs would somehow be specified during CNS development, for example through changes in DNA accessibility or through interaction with tissue-specific co-factors. A second possibility is that MEF2D binds to a common set of MREs accessible in all tissues and that these bound elements are selectively activated in a tissue-specific manner. To begin to distinguish between these possibilities we analyzed MEF2D binding across the retinal genome by ChIP-Seq and compared MEF2D binding in the retina to that observed in cortex and muscle.

To determine the sites of MEF2D binding in the retina with high confidence we performed two bioreplicates of MEF2D ChIP-Seq using p11 wild type retinæ, and also performed MEF2D ChIP-Seq in *Mef2d* KO retinæ as a control for specificity. Because ~80% of cells in the mouse retina are photoreceptors, it is likely that the vast majority of identified MEF2D binding sites represent MEF2D binding in photoreceptors instead of other retinal cell types (Jeon et al., 1998). Each MEF2D ChIP-Seq replicate alone yielded ~12,000 unique MEF2D-binding sites with an overlap of ~4,000 reproducible binding sites between the two replicates, suggesting that a high degree of biological or technical noise is inherent to these experiments. The number of high-confidence MEF2D binding sites was further decreased to 2403 when we considered only those peaks that are specifically reduced in the *Mef2d* knockout (**Figure 2.7A,B**). As an independent check for specificity, we determined that the MEF2 response element (MRE) is the top significantly enriched motif under the MEF2D peaks in the genome using a hypergeometric test ($p=1e-1255$; 1261/2403 peaks) (**Figure 2.7C**) (Heinz et al., 2010). Strikingly, 2403 is a large number of MEF2D binding sites compared to 185 highly misregulated target genes, suggesting that only a small number of the MEF2D bound sites are likely to be essential for normal gene expression. We next asked whether these MEF2D binding sites were proximal to target genes. MEF2D was found to bind to 18 promoter regions and 75 enhancers near genes that are highly misregulated in *Mef2d* KO retinæ including many genes that are photoreceptor-specific and associated with retinal diseases (**Figure 2.7D; Table 2.2**). Thus, MEF2D appears to regulate many of its photoreceptor-specific targets by binding to proximal regulatory elements, suggesting this binding may be unique to the retina and help define the function of MEF2D in regulating retinal gene expression.

Figure 2.7. MEF2D binds broadly throughout the retinal genome

(A) *Gucal1b* genomic locus with MEF2D ChIP-seq data from both WT and KO retinae; arrow denotes *Gucal1b* transcriptional start site (TSS). Horizontal rows display the numbers of normalized ChIP-Seq reads across the locus, for both Input and MEF2D antibody. A light gray vertical bar highlights the identified MEF2D peak. Mammalian conservation is also displayed.

(B) Binding profile of MEF2D ChIP-seq signal at MEF2D peaks in P11 retinae. 2 WT and 1 MEF2D KO experiment are shown. Each MEF2D peak is represented as a single line centered on the peak summit. Intensity of color correlates with ChIP-seq peak size. MEF2D peaks are ordered according to peak size.

(C) Top, Position weighted matrix (PWM) of top motif enriched in MEF2D-bound genomic regions in retina obtained with *de novo* motif discovery using Homer. Bottom, top ranking JASPAR matrix corresponding to most enriched PWM. Matrix was identified in JASPAR as MEF2.

(D) Distribution of MEF2D ChIP-Seq peaks with respect to MEF2D target genes (n=71 with a proximal MEF2D peak). Each line represents a gene locus. MEF2D peaks (purple triangles) are shown with respect to the gene TSS (black line) and gene body (gray bar). TSS's were aligned and peaks were ordered according to their proximity to the TSS.

Figure 2.7. (Continued) MEF2D binds broadly throughout the retinal genome

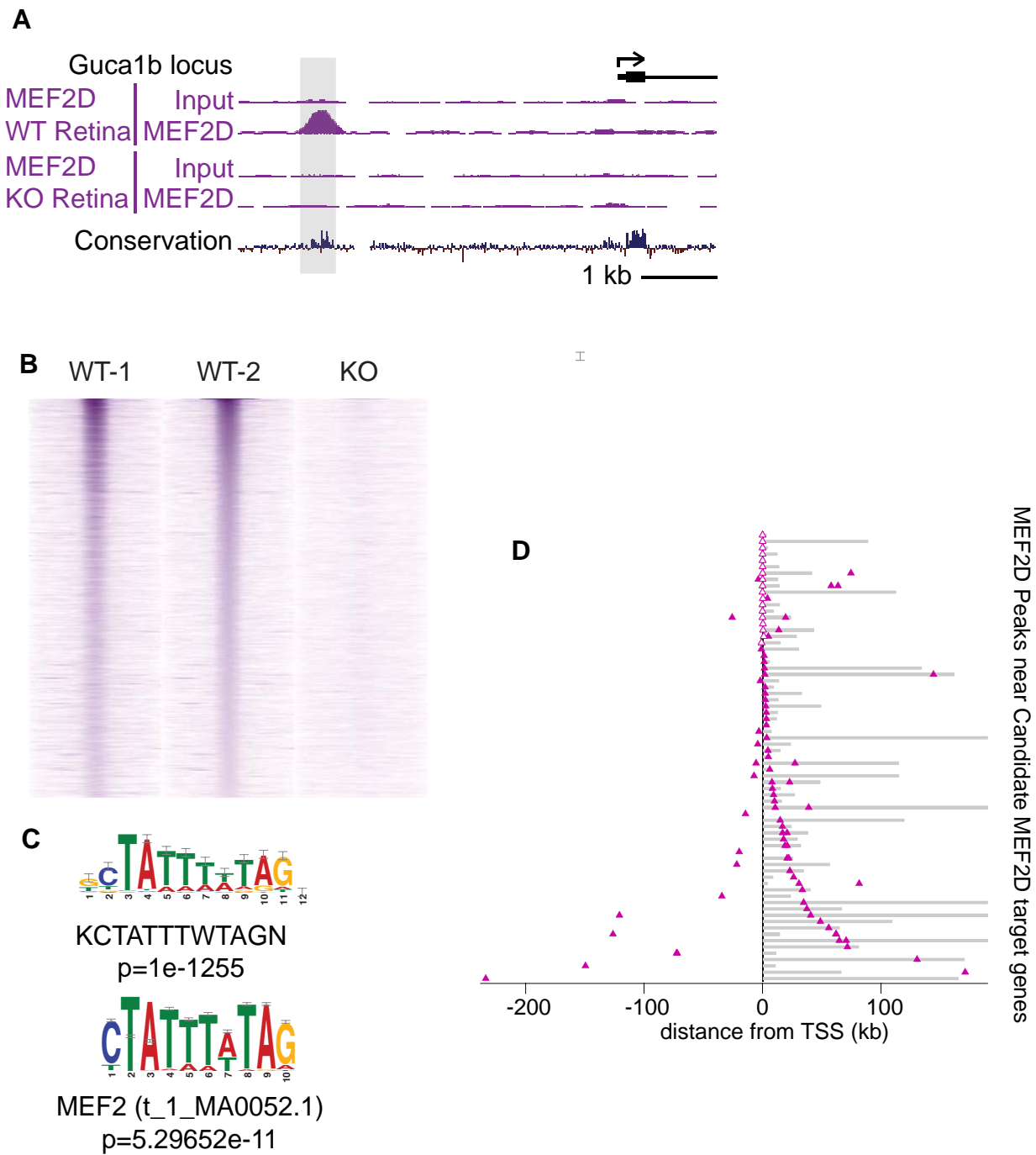


Table 2.2. Direct MEF2D target genes and associated MEF2D-bound regulatory elements

Chr	Summit Location	Distance to closest TSS	Closest Gene to Peak	GeneID	RefSeqs	Avg WT exon density	Avg KO exon density	KO/WT exon dens.	CRX co-bound
chr1	4960826	-48634	Rgs20	58175	NM_021374.3	0.673	0.100	0.148	YES
chr1	55945098	72655	913022 7L01Rik	329159	XM_488894.3	0.067	0.152	2.268	NO
chr1	55945661	72092	913022 7L01Rik	329159	XM_488894.3	0.067	0.152	2.268	YES
chr1	89700137	118	Sag	20215	NM_009118.2	516.187	205.101	0.397	YES
chr1	89774674	-74419	Sag	20215	NM_009118.2	516.187	205.101	0.397	NO
chr1	132695454	2025	Fcamr	64435	NM_144960.1	0.236	0.018	0.076	NO
chr1	137986723	-37245	Cacnals	12292	NM_001081023.1	0.137	0.023	0.168	NO
chr1	173131342	4176	Pcp4l1	66425	XM_484933.5	5.257	2.561	0.487	NO
chr10	18673126	-62047	Tnfaip3	21929	NM_009397.2	4.588	1.654	0.361	NO
chr10	18673550	-61623	Tnfaip3	21929	NM_009397.2	4.588	1.654	0.361	YES
chr10	18861494	12632 1	Tnfaip3	21929	NM_009397.2	4.588	1.654	0.361	YES
chr10	68164696	21820	Tmem26	327766	NM_177794.2	0.850	0.240	0.283	NO
chr10	73163753	12087 8	Pcdh15	11994	NM_023115.2	4.611	0.606	0.131	YES
chr10	73325126	-40495	Pcdh15	11994	NM_023115.2	4.611	0.606	0.131	YES
chr11	6956206	7286	Adcy1	432530	NM_009622.1	8.049	2.454	0.305	YES
chr11	69507194	-2062	Tnfsf12	21944	NM_011614.1	3.048	1.316	0.432	YES
chr11	120227626	-4778	Fscn2	238021	NM_172802.2	5.271	0.516	0.098	YES
chr11	120509487	-164	111001 2N22Rik	68515	XM_126634.6	0.372	0.132	0.355	NO
chr12	31054807	-3386	Sntg2	268534	NM_172951.2	0.746	0.084	0.112	YES
chr12	51715529	-34556	Prkcm	18760	NM_008858.2	2.843	1.342	0.472	YES
chr12	113215518	-4010	BC048943	217874	XM_127170.7 X M_902085.2	29.618	13.858	0.468	NO
chr12	113219396	-132	BC048943	217874	XM_127170.7 X M_902085.2	29.618	13.858	0.468	NO
chr13	54861823	-5978	Sncb	104069	NM_033610.2	8.279	3.870	0.467	YES
chr13	74358316	-71441	Ahrr	11624	NM_009644.2	0.202	0.030	0.146	YES
chr15	9018188	-16758	111002 0G09Rik	68646	NM_001040395.2	26.976	11.732	0.435	YES
chr15	9022022	-20592	111002 0G09Rik	68646	NM_001040395.2	26.976	11.732	0.435	YES
chr15	102488755	-1197	LOC10043600	100043600	XM_001480969.1	0.193	0.073	0.379	NO
chr16	78574823	-2069	D16Ert d472e	67102	NM_025967.2	2.817	1.097	0.389	YES

Table 2.2. (Continued) Direct MEF2D target genes and associated MEF2D-bound regulatory elements

Chr	Summit Location	Distance to closest TSS	Closest Gene to Peak	GeneID	RefSeqs	Avg WT exon density	Avg KO exon density	KO/WT exon dens.	CRX co-bound
chr16	92295723	-3089	Kcne2	246133	NM_134110.2	6.383	2.810	0.440	YES
chr17	7827041	-170798	Fndc1	68655	NM_001081416.1	0.168	0.081	0.482	YES
chr17	32189809	-16702	Rrp1b	72462	NM_028244.1	6.624	2.801	0.423	YES
chr17	47519110	3232	Gucal1b	107477	NM_146079.1	6.373	0.260	0.041	YES
chr17	47536237	-1296	Gucal1a	14913	NM_008189.2	11.870	5.147	0.434	YES
chr17	48569850	-2203	Apobec2	11811	NM_009694.2	3.617	0.474	0.131	NO
chr17	48838040	233664	Lrfr2	70530	NM_027452.2	0.859	0.325	0.378	YES
chr17	59130930	132	2610034M16Rik	69239	NM_027001.1	5.578	0.008	0.001	YES
chr17	72102375	150	BC027072	225004	NM_146082.3	11.219	4.303	0.383	YES
chr17	84505867	-81420	Zfp3612	12193	NM_001001806.2	1.960	0.558	0.285	YES
chr17	84556701	-30586	Zfp3612	12193	NM_001001806.2	1.960	0.558	0.285	YES
chr19	6384312	117	Pygm	19309	NM_011224.1	2.681	0.854	0.319	NO
chr19	9244543	34487	Asrg11	66514	NM_025610.3	6.175	2.413	0.391	YES
chr19	27351339	14524	LOC10042588	100042588	XM_001478609.1	0.266	0.008	0.032	YES
chr19	27396961	148	Kcnv2	240595	NM_183179.1	36.929	16.085	0.436	YES
chr19	46397242	-4404	Psd	73728	NM_028627.2	4.247	1.566	0.369	YES
chr2	17959449	85	A930004D18Rik	77940	XR_035303.1	0.624	0.283	0.454	YES
chr2	30450437	127	Cstad	78617	NM_030137.2	0.308	0.154	0.498	NO
chr2	30508276	-57712	Cstad	78617	NM_030137.2	0.308	0.154	0.498	NO
chr2	30514109	-63545	Cstad	78617	NM_030137.2	0.308	0.154	0.498	NO
chr2	60389890	-1428	Pla2r1	18779	NM_008867.1	6.804	0.267	0.039	YES
chr2	69280084	-144400	Lrp2	14725	NM_001081088.1	0.955	0.295	0.309	YES
chr2	69422315	-1809	Lrp2	14725	NM_001081088.1	0.955	0.295	0.309	YES
chr2	119924608	-55703	Ehd4	98878	NM_133838.3	2.555	0.855	0.335	YES
chr2	127096882	-907	Stard7	99138	NM_139308.1	12.281	5.639	0.459	NO
chr2	127100727	-4752	Stard7	99138	NM_139308.1	12.281	5.639	0.459	YES
chr2	136919208	-22859	Jag1	16449	NM_013822.3	4.285	1.855	0.433	YES
chr2	181313708	-2970	Uck11	68556	NM_026765.3	10.491	4.285	0.408	YES
chr3	108166843	986	Mybphl	68753	NM_026831.1	0.125	0.021	0.169	YES
chr4	61950500	-3021	Slc31a2	20530	NM_025286.2	3.711	0.791	0.213	YES
chr4	62891121	-14675	Col27a1	373864	NM_025685.3	0.126	0.451	3.583	NO
chr4	133775111	-8172	Catsper4	329954	NM_177866.3	0.245	0.065	0.263	YES

Table 2.2. (Continued) Direct MEF2D target genes and associated MEF2D-bound regulatory elements

Chr	Summit Location	Distance to closest TSS	Closest Gene to Peak	GeneID	RefSeqs	Avg WT exon density	Avg KO exon density	KO/WT exon dens.	CRX co-bound
chr5	90273665	-38766	Adamts3	330119	NM_001081401.1	2.106	0.409	0.194	YES
chr5	90301852	-10579	Adamts3	330119	NM_001081401.1	2.106	0.409	0.194	YES
chr5	108003857	-22737	Glmn	170823	NM_133248.1	11.118	3.420	0.308	YES
chr5	108018804	-7790	Glmn	170823	NM_133248.1	11.118	3.420	0.308	YES
chr5	130672259	-9209	Rabgef1	56715	NM_019983.2	9.874	3.114	0.315	YES
chr6	3943960	52	Gngt1	14699	NM_010314.2	236.598	115.056	0.486	YES
chr6	82722022	-2431	Hk2	15277	NM_013820.2	1.424	0.190	0.133	YES
chr6	136929110	-26066	Pde6h	78600	NM_023898.4	20.224	2.878	0.142	NO
chr7	31338226	95	Hspb6	243912	NM_001012401.2	1.459	0.238	0.163	YES
chr7	66043947	-130245	Atp10a	11982	NM_009728.1	0.122	0.042	0.342	NO
chr7	124589155	-64662	Xylt1	233781	NM_175645.3	1.034	0.484	0.468	YES
chr7	124594924	-70431	Xylt1	233781	NM_175645.3	1.034	0.484	0.468	YES
chr7	128103838	-21960	Cdr2	12585	NM_007672.1	8.160	3.417	0.419	YES
chr7	128105256	-20542	Cdr2	12585	NM_007672.1	8.160	3.417	0.419	YES
chr8	4512335	-18831	Lass4	67260	NM_026058.3	11.140	4.316	0.387	YES
chr8	4514133	-20629	Lass4	67260	NM_026058.3	11.140	4.316	0.387	NO
chr8	13181321	-19303	Grtp1	66790	NM_025768.2	5.386	1.986	0.369	YES
chr8	13200780	156	Grtp1	66790	NM_025768.2	5.386	1.986	0.369	NO
chr8	13226390	25766	Grtp1	66790	NM_025768.2	5.386	1.986	0.369	YES
chr8	55804091	60	Wdr17	244484	NM_028220.2	25.765	7.561	0.293	YES
chr8	95518521	-33392	Slc6a2	20538	NM_009209.2	0.113	0.010	0.088	NO
chr8	97526145	-17642	Gpr56	14766	NM_018882.2	0.103	0.211	2.047	NO
chr8	122850933	149564	1700120B06Rik	436062	NM_001033980.1	0.089	0.298	3.330	YES
chr9	26600449	-13553	BC038479	244757	NM_153803.1	5.651	1.541	0.273	YES
chr9	26613638	-364	BC038479	244757	NM_153803.1	5.651	1.541	0.273	NO
chr9	58404017	1177	Cd276	102657	NM_133983.3	1.044	0.306	0.293	YES
chr9	86562592	-27238	Mod1	17436	NM_008615.1	3.134	1.456	0.465	YES
chr9	86595423	5593	Mod1	17436	NM_008615.1	3.134	1.456	0.465	YES
chr9	107559721	-9984	Slc38a3	76257	NM_023805.2	12.139	4.815	0.397	YES
chr9	115367584	19858	EG546164	546164	XM_620794.4	0.201	0.072	0.360	NO
chrX	71019690	71	Srpk3	56504	NM_019684.1	0.167	0.019	0.114	NO
chrX	97797141	3754	Arr3	170735	NM_133205.2	7.210	0.023	0.003	NO
chrX	97800771	124	Arr3	170735	NM_133205.2	7.210	0.023	0.003	NO

To explore the possibility that MEF2 regulates cell-type specific gene transcription by binding the genome in a cell-type specific manner, we compared MEF2D binding in the retina to MEF2D binding in two distinct cell types where MEF2 factors have been shown to be functionally important, cortical neurons and myocytes. We performed ChIP-Seq for MEF2D in DIV7 cultured cortical neurons and analyzed MEF2D ChIP-Seq data in C2C12 myocytes from a previously published dataset (Sebastian et al., 2013). A comparison of MEF2D binding in each of the three tissues showed that MEF2D binding to the enhancers and promoters that are necessary for retinal gene expression is highly tissue-specific (~82%, 76/93) (**Figure 2.8A**). Furthermore, the majority of MEF2D binding genome-wide in each tissue is tissue-specific (**Figure 2.8B,C**). This finding suggests that tissue-specific binding of MEF2D is an important mechanism governing the specific function of MEF2D in the retina.

We next investigated the mechanism by which MEF2D achieves tissue-specific binding to promoters and enhancers in the retina. Several previous studies have suggested that MEF2 family members can interact with tissue specific TFs and that this interaction imparts specificity to MEF2 binding. However, the functional importance of these TF interactions has not been examined in an *in vivo* genome-wide context (Black et al., 1996; Molkenin et al., 1995). We hypothesized that MEF2D interacts with a retinal-specific TF that recruits MEF2D to tissue-specific regulatory sites. To begin to identify such co-factors in an unbiased manner, we searched the MEF2D binding sites for common DNA sequence features using a *de novo* DNA motif search program (Heinz et al., 2010). This analysis revealed that after the MRE, the most abundant motif sequence present within retina-specific MEF2D-bound regions is the sequence TAATCNBNTT ($p=1e-85$) (**Figure 2.8D**). This sequence motif matches the binding site for the CRX homeodomain factor ($p=3.59e-6$). In contrast, no single recognizable motif was

Figure 2.8. MEF2D binds tissue-specific enhancers

(A) Fraction of MEF2D functional regulatory elements that are specifically bound in retina or are also sites of MEF2D binding in DIV7 cultured cortical neurons or myotubes.

(B) Overlap of all MEF2D-bound genomic regions from ChIP-seq performed in retina and DIV7 cultured cortical neurons, as well as mapped regions from published MEF2D ChIP-Seq data for myotubes.

(C) MEF2D ChIP-Seq tracks at the *Esrrb* locus (top) or *Nr4a1* locus (bottom) to demonstrate retina-specific or shared MEF2D binding, respectively. MEF2D ChIP-Seq reads from three different tissues are shown.

(D, E) PWMs of enriched motifs in (D) retina-specific peaks or (E) myotube-specific peaks. Below each is a high-ranking JASPAR matrix corresponding to the PWM.

Figure 2.8. (Continued) MEF2D binds tissue-specific enhancers

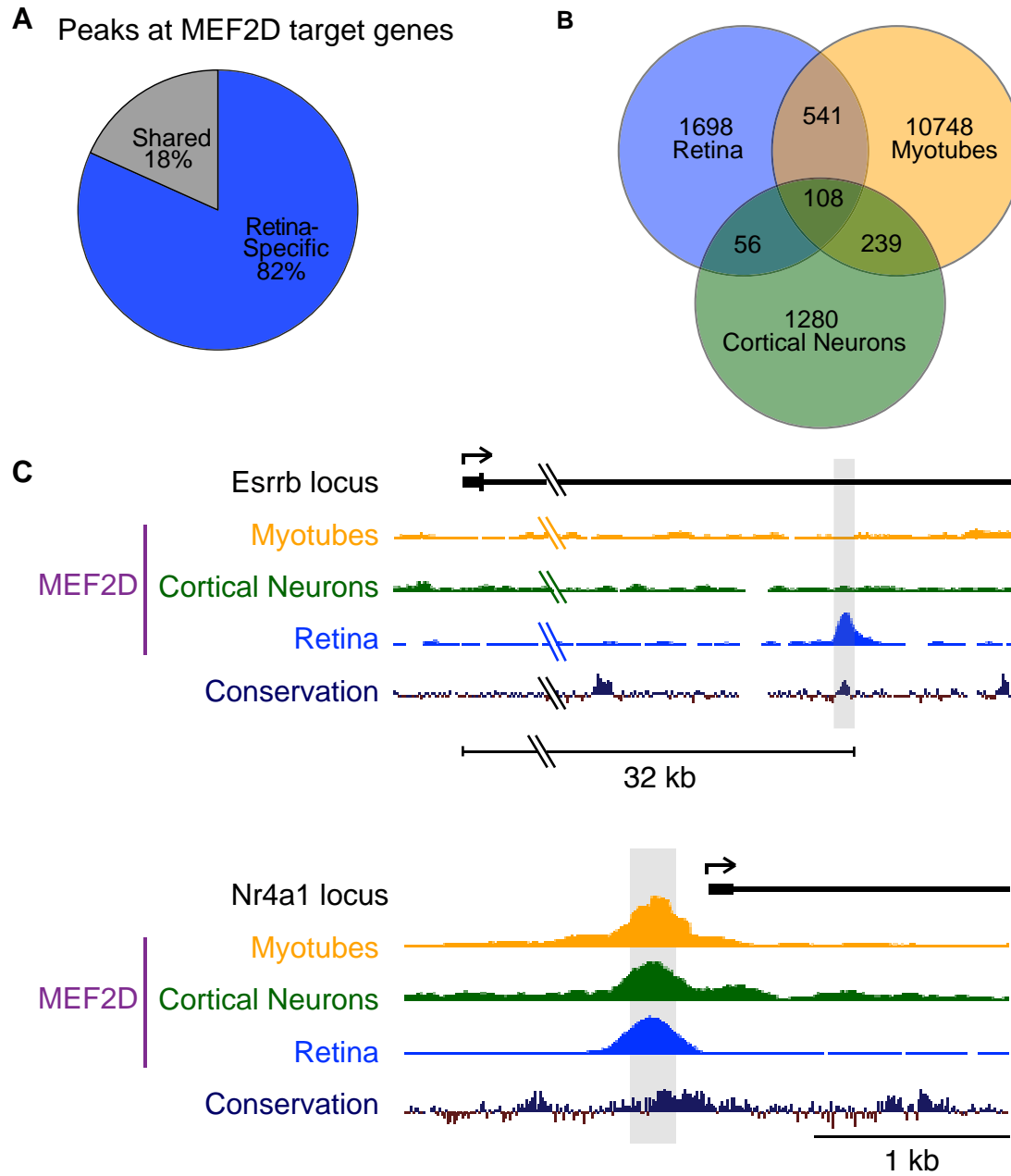
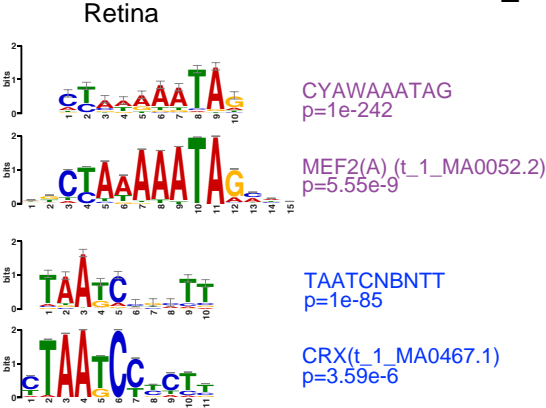
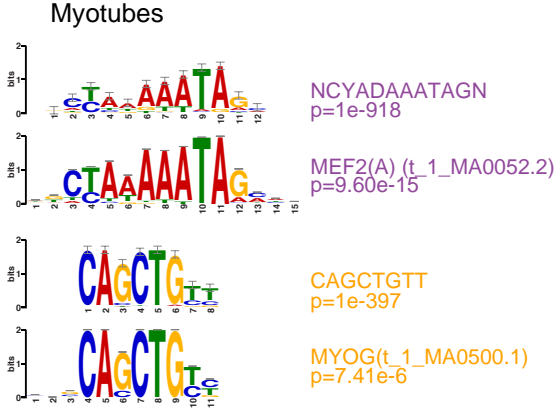


Figure 2.8. (Continued) MEF2D binds tissue-specific enhancers

D



E



significantly enriched at MEF2D binding sites in cortical neurons, apart from the MRE, likely due to the extreme heterogeneity of these cells. However, when we performed a *de novo* motif search of MEF2D-bound regions identified in myocytes the most prevalent sequence, besides the MRE, was CAGCTGTT ($p=1e-397$), which is the consensus site for binding myogenic basic helix-loop-helix (bHLH) proteins, such as MYOD ($p=7.41e-6$; **(Figure 2.8E)** (Molkentin et al., 1995). These findings raise the possibility that the specificity of MEF2 binding in different tissues (e.g. photoreceptors versus muscle) is determined by the presence of the binding site for a tissue specific TF adjacent to the MEF2 binding site. In particular, the enrichment of the CRX consensus motif at retina-specific MEF2D-binding sites suggests that in photoreceptors CRX influences the binding of MEF2D to the promoters and enhancers of photoreceptor specific genes.

CRX mediates a genome-wide competition for MEF2D binding to retina-specific sites

CRX is a retina-specific transcription factor that is mutated in human congenital blindness. Much like MEF2D, CRX is necessary for photoreceptor outer segment development and photoreceptor function (Chen et al., 1997; Freund et al., 1997; Furukawa et al., 1997; Furukawa et al., 1999; Swain et al., 1997). The enrichment of the CRX motif at MEF2D-bound sites suggested that CRX protein might be co-bound to these regulatory elements. However, recent work has demonstrated that CRX binds only a small fraction of its consensus motifs in the genome indicating that the presence of the CRX binding motif is not sufficient to conclude that CRX is bound to a given MEF2 binding site (White et al., 2013). We therefore analyzed CRX ChIP-Seq data (Corbo et al., 2010) to determine if CRX protein binds to MEF2D-bound sites in

Figure 2.9. CRX mediates a genome-wide competition for MEF2D binding to retina-specific sites

(A) Top, MEF2D and CRX ChIP-seq data tracks at the *Pla2r1* genomic locus. Arrow denotes transcriptional start site (TSS). A light gray vertical bar highlights the identified MEF2D peak.

(B) Distribution of MEF2D ChIP-Seq peaks with respect to MEF2D target genes as described in Figure 2.7D. Places of MEF2D and CRX co-binding (blue triangles) as well as places where MEF2D binds without CRX (purple triangles) are shown for MEF2D target genes.

(C) MEF2D ChIP-Seq signal in WT versus CRX KO retinæ at individual MEF2D-bound regions. Read density was calculated for the 400bp window around the summit of each MEF2D-bound region. Data from CRX KO retinæ was compared to the data from 3 different WT retinæ experiments. Peaks highlighted are at least 2x reduced (red) or 2x increased (green) in CRX KO retinæ as compared to the average ChIP-Seq read value of the 3 WT samples. To be considered changed, CRX KO versus the 3 WT values for MEF2D ChIP-seq density had to have $p < 0.01$ significance. Black line indicates unity.

(D) Aggregate plots of MEF2D ChIP-Seq signal in CRX WT and KO retinæ for 5.6kb region centered on summits of the different categories of MEF2D-bound regions.

(E) *Gngt1* (right) and *Stard7* (left) genomic loci with MEF2D ChIP-Seq tracks from CRX WT (representative 1 of 3 bioreplicates) and CRX KO retinæ.

Figure 2.9. (Continued) CRX mediates a genome-wide competition for MEF2D binding to retina-specific sites

(F) Aggregate plots of DNA binding motif occurrence for the MEF2 motif in a 2kb window centered on summits of MEF2D-bound regions. Motif enrichments at MEF2D peaks that are increased, unchanged, or decreased in CRX KO retinæ are shown.

(G) Cumulative distribution of MRE strength (p-value describing similarity to canonical MRE) for all MREs with $p < 1e-3$ found in 200bp regions centered on MEF2D peak summits. Peak sets include those where MEF2D peak size goes up greater than 2X (green), does not change (black), or goes down greater than 2X in CRX KO retinæ (red).

Figure 2.9. (Continued) CRX mediates a genome-wide competition for MEF2D binding to retina-specific sites

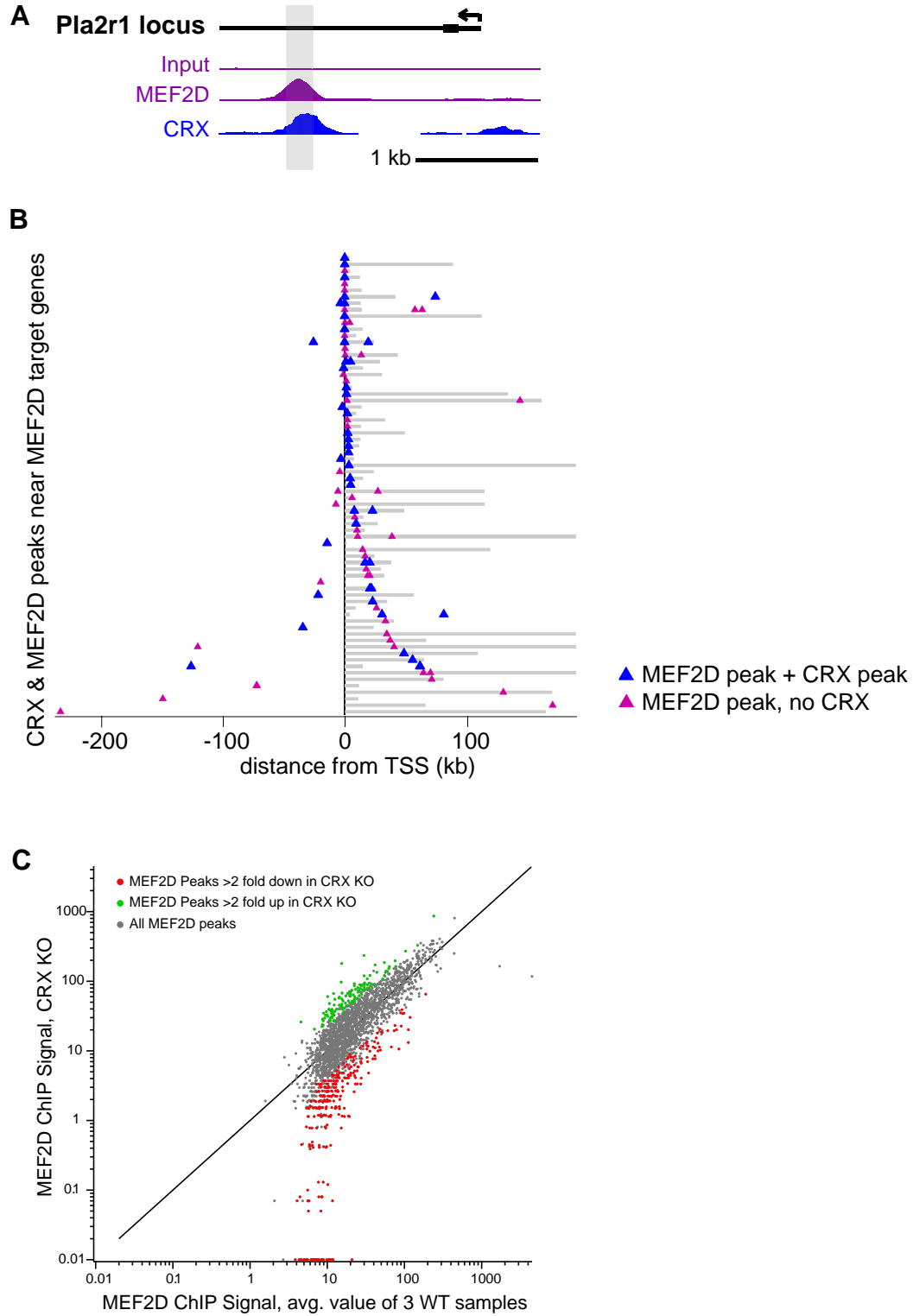
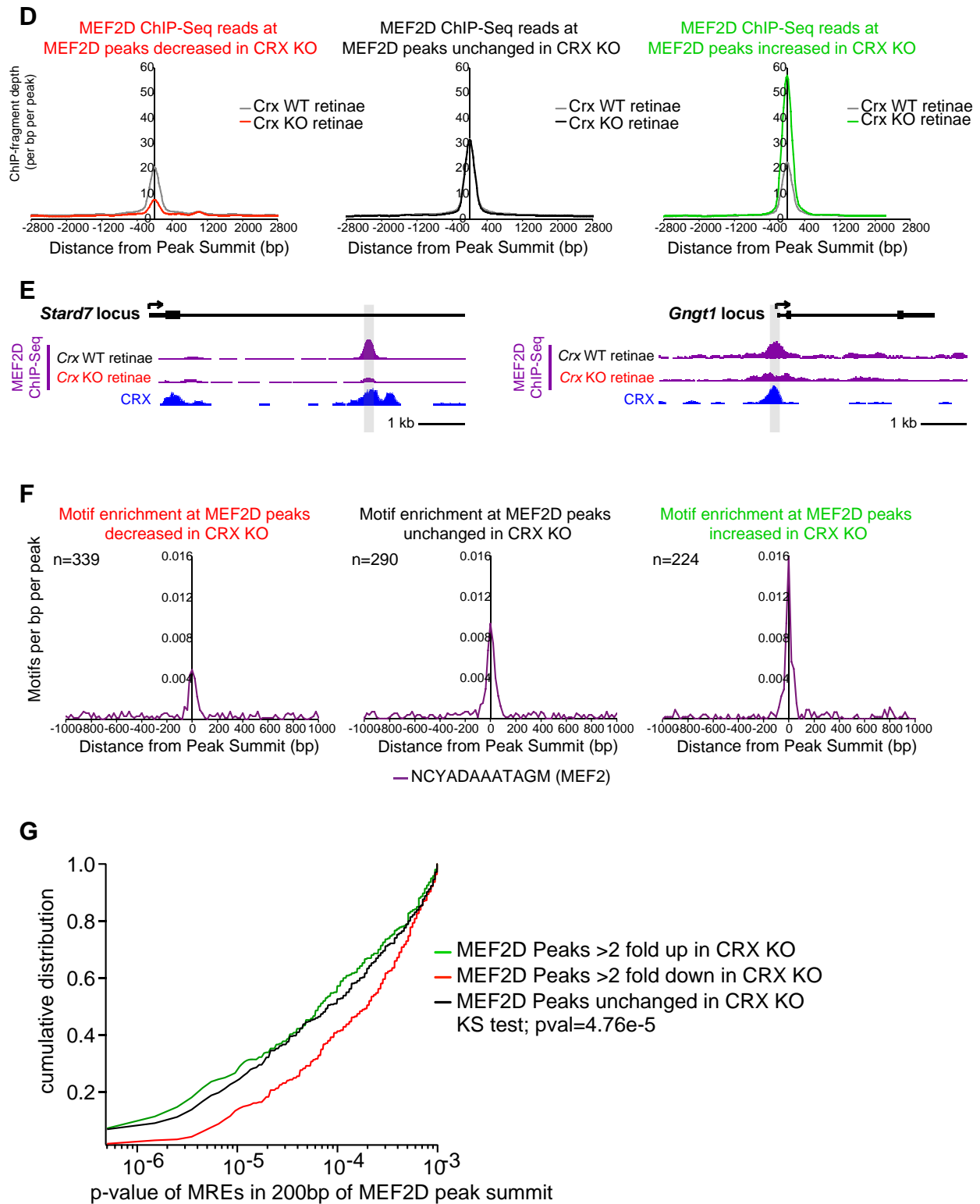


Figure 2.9. (Continued) CRX mediates a genome-wide competition for MEF2D binding to retina-specific sites



the retina. Strikingly, we found that in the retina ~70% of functional MEF2D regulatory elements are co-bound by CRX (**Figure 2.9A,B; Table 2.2**). This finding suggests that MEF2D may functionally interact with CRX to achieve tissue-specific binding to the promoters and enhancers of photoreceptor genes.

To test if CRX is required for retina-specific MEF2D binding we performed MEF2D ChIP-Seq in *Crx* KO retinæ and compared the pattern of MEF2D binding to that of WT retinæ. By ChIP-Seq we found that MEF2D binding is reduced >2x in *Crx* KO retinæ at 339 MEF2D binding sites including many MEF2D regulatory elements near MEF2D target genes (**Figure 2.9C,D**). For example, retina-specific MEF2D binding is particularly dependent on CRX near the MEF2D target genes *Gngt1*, a key component of the phototransduction cascade, and *Stard7*, which has been shown to be critical for photoreceptor development (Hao et al., 2012) (**Figure 2.9E**). *Mef2d* is not however a transcriptional target of CRX and therefore this decrease in MEF2D ChIP-Seq signal is not due to decreased expression of MEF2D in *Crx* KO retinæ (Hsiau et al., 2007). A possible explanation for why only a subset of MEF2D binding sites requires CRX is that MEF2D may only require CRX to stabilize binding at regulatory elements with weak MREs. In support of this idea, we find that the consensus MEF2D binding site is substantially de-enriched in regions where MEF2D binding is CRX-dependent ((**Figure 2.9F**). Surprisingly, we also found that MEF2D binding is actually significantly increased >2x in *Crx* KO retinæ at 224 MEF2D-binding sites genome-wide (**Figure 2.9C,D**). Notably, these regions are enriched for strong consensus MREs relative to MEF2D binding sites where the level of MEF2D binding decreases in the absence of CRX (KS test, $p=4.76e-5$) ((**Figure 2.9F,G**). Taken together, these data strongly suggest that MEF2D is recruited to a subset of retina-specific binding sites by cooperation with CRX, a retina-specific transcription factor, and that CRX

competes MEF2D away from other available binding sites. This genome-wide competition for MEF2D binding exists between sites with strong consensus MREs and sites that have weak MREs but are co-bound by CRX. This appears to be an important mechanism for conferring tissue-specific binding of MEF2D so that it may regulate photoreceptor-specific target genes.

MEF2D regulates retinal gene expression by selective activation of enhancers

As described above, tissue-specific MEF2D binding in the retina likely plays a critical role in specifying the function of MEF2D in photoreceptors. However, fewer than 4% of MEF2D-bound sites are located near target genes, suggesting that additional mechanisms exist to specify the function of MEF2D at tissue-specific regulatory sites. This broad binding of MEF2D but selective regulation of target genes is consistent with previous genome-wide analyses that demonstrate that only a small fraction of transcription factor occupancy relates to the expression of neighboring genes (Spitz and Furlong, 2012). We hypothesized that additional mechanisms are necessary to determine the action of MEF2D in photoreceptors beyond the regulation of binding, and that MEF2D may exclusively regulate expression of its target genes through selective activation of enhancers.

To test if MEF2D-bound regulatory sites are differentially active, we analyzed two features of enhancer activity, acetylation of histone 3 at lysine 27 (H3K27ac) and transcription of bidirectional enhancer RNAs (eRNAs), at MEF2D-bound enhancers proximal to target genes and compared these enhancers to a control set of MEF2D-bound sites that are not associated with changes in nearby gene expression. H3K27ac and eRNAs are hallmarks of enhancers that are

Figure 2.10. MEF2D regulates retinal gene expression by selective activation of enhancers

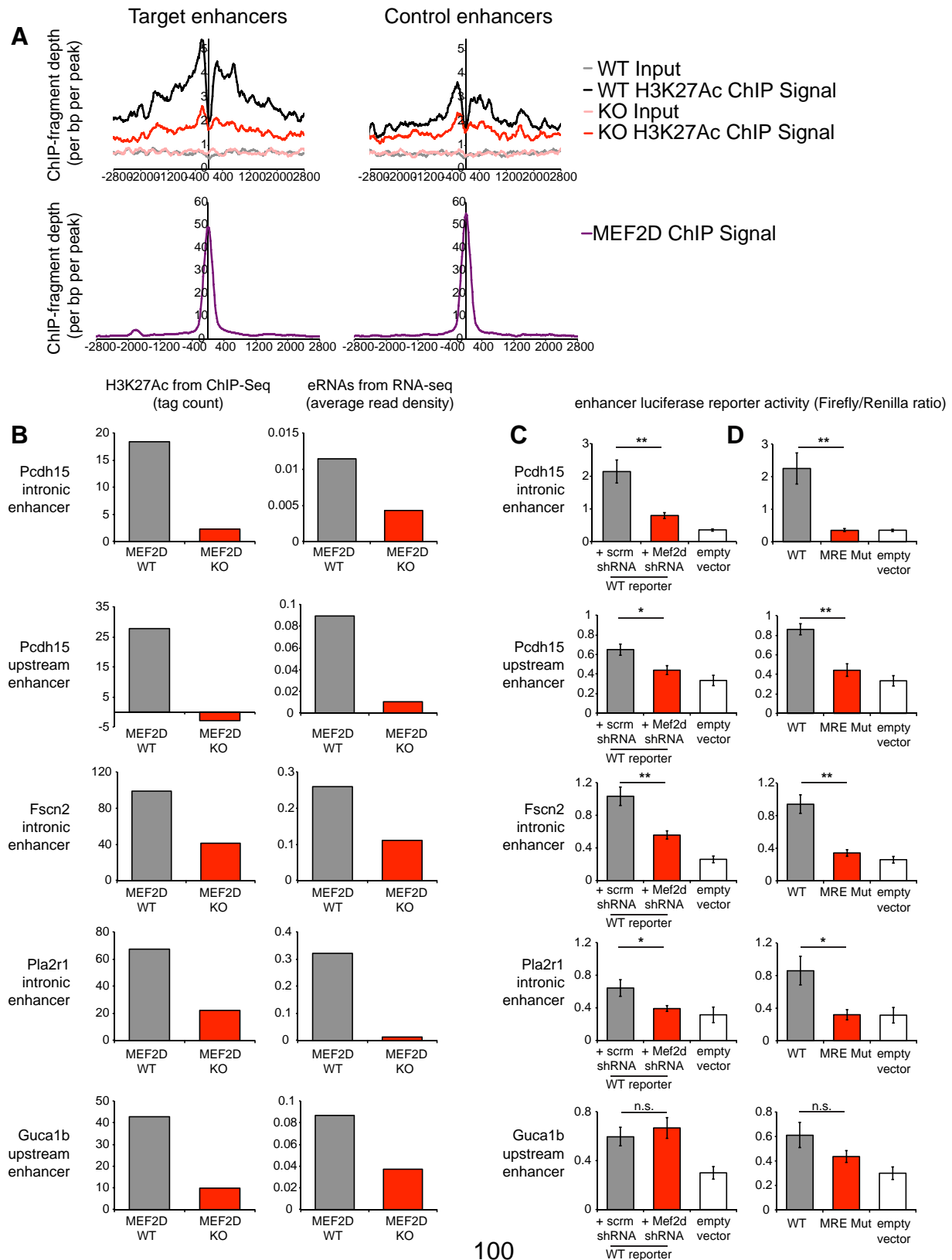
(A) Top, aggregate plots of H3K27Ac ChIP-Seq signal in MEF2D WT (black) or MEF2D KO (red) retinae. Plots are centered on summits of MEF2D-bound regions that are either proximal to MEF2D target genes (Target enhancers, left), or summits of MEF2D-bound regions proximal to genes that do not change in MEF2D KO retinae (Control enhancers, right). Bottom, aggregate plots of MEF2D ChIP signal for same regions, demonstrating normalization of data analysis to MEF2D peak size.

(B) H3K27Ac ChIP-seq read density (left) and eRNA read density (right) calculated +/- 1 kb from the center of the WT MEF2D peak for 5 MEF2D-dependent enhancers.

(C) MEF2D-bound enhancer regions (same as in (B)) were cloned into a luciferase reporter construct with a minimal promoter and electroporated into retinal explants at P0. DIV11 luciferase activity was measured from native reporter constructs (WT) together with control (scrm) or MEF2D shRNAs. * $p < 0.05$ ** $p < 0.005$

(D) WT reporter construct luciferase activity was compared to MEF2 responsive element (MRE) -mutated enhancers (MRE Mut). Signal normalized to renilla luciferase control. Error bars represent S.E.M., $n = 12-18$ retinae per experimental condition. * $p < 0.05$ ** $p < 0.005$.

Figure 2.10. (Continued) MEF2D regulates retinal gene expression by selective activation of enhancers



actively engaged in gene expression (Creyghton et al., 2010; Kim et al., 2010; Li et al., 2013; Rada-Iglesias et al., 2011; Wang et al., 2011). We found that MEF2D-bound enhancers near target genes were more active than other MEF2D binding sites ($p=0.0002$) (**Figure 2.10A**). Furthermore, the levels of H3K27ac were significantly decreased in MEF2D KO retinae as compared to WT retinae at enhancers proximal to MEF2D target genes, suggesting that MEF2D plays a key role in the activation of these enhancers to regulate nearby gene expression (**Figure 2.10A,B**). To support these results we isolated a subset of MEF2D-bound enhancers near target genes and tested their ability to regulate reporter gene expression in the intact retina in a MEF2D-dependent manner (**Figure 2.10C,D**). All 5 tested enhancers were sufficient to drive reporter gene expression in photoreceptors (**data not shown; Figure 2.10C**). Additionally, the activity of 4/5 of these reporters was significantly reduced in the presence of MEF2D shRNA or when the MRE was mutated, demonstrating that direct MEF2D binding to these elements is required to drive gene expression (**Figure 2.10C,D**). Together these results show that MEF2D regulates target gene expression by selectively activating only a subset of the sites to which it is bound. This reveals an additional level of control in how MEF2D regulates gene expression in photoreceptors, and helps explain why the number of MEF2D-bound enhancers greatly outnumber the number of MEF2D target genes.

CRX determines the selective activation of MEF2D-bound retinal enhancers

To determine the mechanism of selective MEF2D enhancer activation we considered the possibility that CRX could serve as a co-activator at MEF2D-bound enhancers, at sites where CRX is required for MEF2D binding but also at sites where MEF2D binding is independent of

CRX. To test this hypothesis, we first asked if CRX binding correlated with enhancer activity at MEF2D-bound sites. Genome-wide, the subset of MEF2D-bound enhancers co-bound by CRX was significantly more active than the subset of MEF2D-bound elements where CRX does not bind, even when the amount of MEF2D binding was similar (**Figure 2.11A**). This strongly suggested that the presence of CRX together with MEF2D might be required for the maximal activation of MEF2D-bound enhancers.

To determine if CRX co-binding was required for activation of MEF2D-bound regulatory elements, we performed RNA-Seq in WT and *Crx* KO retinae at p11 and quantified the levels of eRNAs at MEF2D-bound enhancers (**Figure 2.11B,C**). In addition, we performed ChIP for H3K27Ac at select CRX-bound enhancers in WT and *Crx* KO retinae to confirm that eRNAs and H3K27Ac correlated in reflecting loss of activity (**Figure 2.11D**). As expected we found that CRX was required for the majority of eRNA expression at active sites where MEF2D binding is dependent upon CRX (**Figure 2.11E**). CRX was also required for eRNA expression at an additional 38% of MEF2D-bound enhancers that are active in WT retinae, but do not require CRX for binding. These sites included enhancers of clinically relevant MEF2D target genes such as *Pcdh15*, *Gucal1a* and *Gucal1b*. These results indicate that CRX is required for the selective activation of MEF2D-bound regulatory elements not only by recruiting MEF2D, but also by directly activating these promoters and enhancers.

MEF2D and CRX coordinate gene expression through enhancer co-binding and co-activation

Figure 2.11. CRX determines the selective activation of MEF2D-bound enhancers

(A) Three sets of aggregate plots centered on summits of MEF2D-bound regions that are either co-bound by CRX (left) or do not have a CRX peak (right). Top, aggregate plots of H3K27Ac ChIP-Seq signal in MEF2D WT retinæ. Middle, aggregate plots of MEF2D ChIP signal (purple) or CRX ChIP signal (blue), demonstrating differential peak size of CRX and normalization of data analysis to MEF2D peak size. Bottom, aggregate plots of RNA-seq reads (coding reads removed) for forward (dark blue) and reverse (light blue) strands in *Mef2d* WT retinæ.

(B) MEF2D and CRX ChIP-Seq tracks at *Tnfrif3* example genomic locus. RNA-seq data from CRX WT (dark blue) and KO (yellow) retinæ is also shown. Arrow denotes transcriptional start site (TSS). A light gray vertical bar highlights the identified MEF2D peak.

(C) eRNA read density calculated from RNA-Seq in CRX WT and KO retinæ +/- 1 kb from the center of all MEF2D-bound enhancers where RNA-seq reads met minimum criteria for eRNAs (see methods). N=2 retinæ per genotype. Gray line indicates unity.

(D) Right, eRNA read density for 2 CRX-bound enhancers, 1 co-bound by MEF2D (*fscn2*) and one not (*rho*), in CRX WT and KO retinæ. Left, H3K27Ac ChIP-qPCR results from CRX WT and KO retinæ for same 2 CRX-bound enhancers. Error bars represent S.E.M.

Figure 2.11. (Continued) CRX determines the selective activation of MEF2D-bound enhancers

(E) Aggregate plots are shown centered on MEF2D enhancers whose MEF2D binding levels are unchanged or decreased in CRX KO retinæ. Top, aggregate plots of RNA-seq reads (coding reads removed) for forward (dark blue) and reverse (light blue) strands in *Crx* WT retinæ as well as forward (red) and reverse (pink) strands in *Crx* KO retinæ. Bottom, aggregate plots of MEF2D ChIP-Seq signal in CRX WT and KO retinæ for same groups of enhancers.

Figure 2.11. (Continued) CRX determines the selective activation of MEF2D-bound enhancers

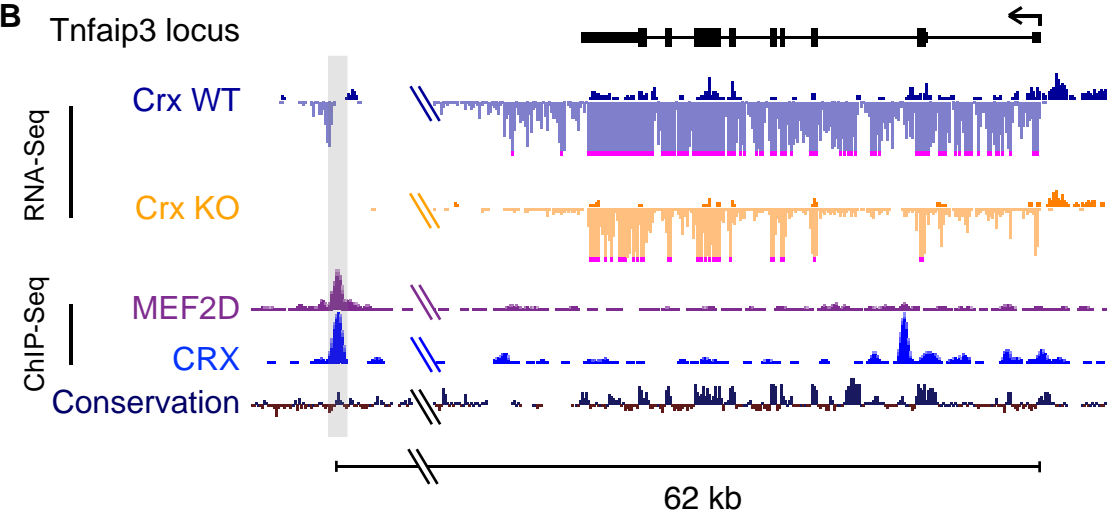
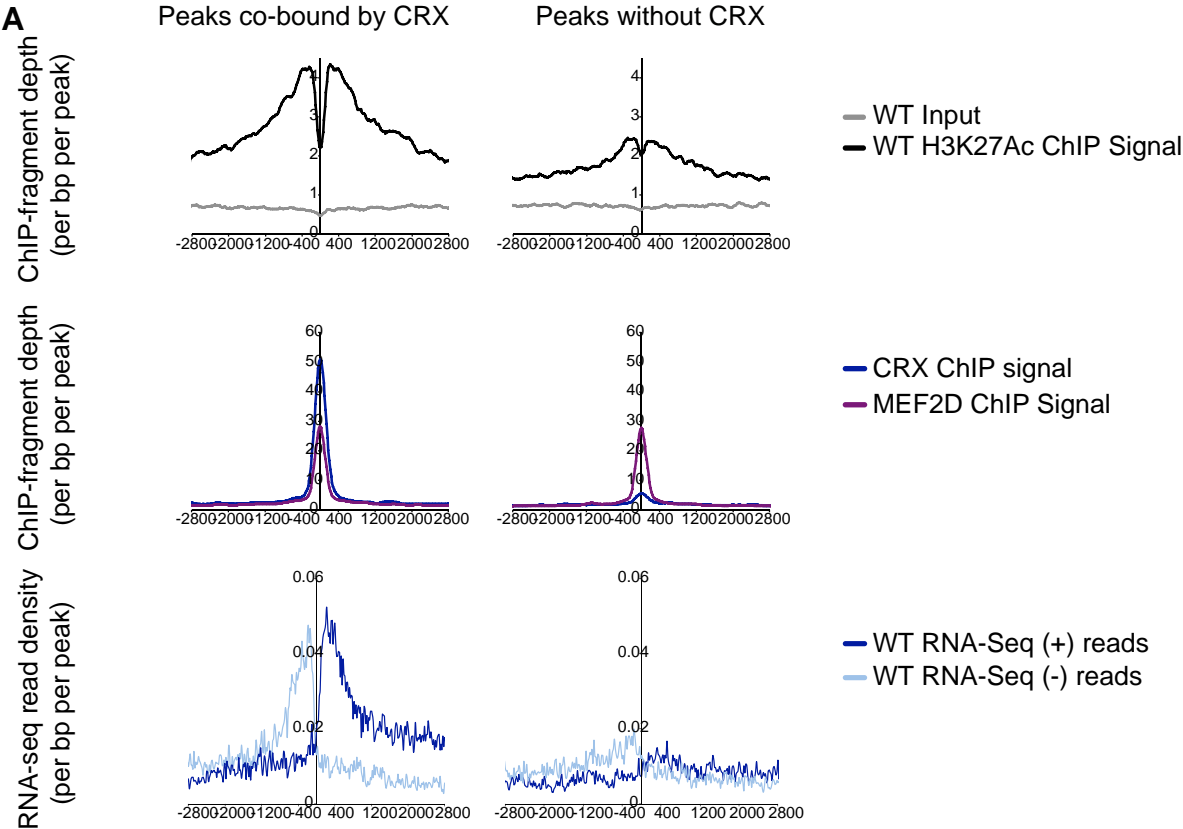
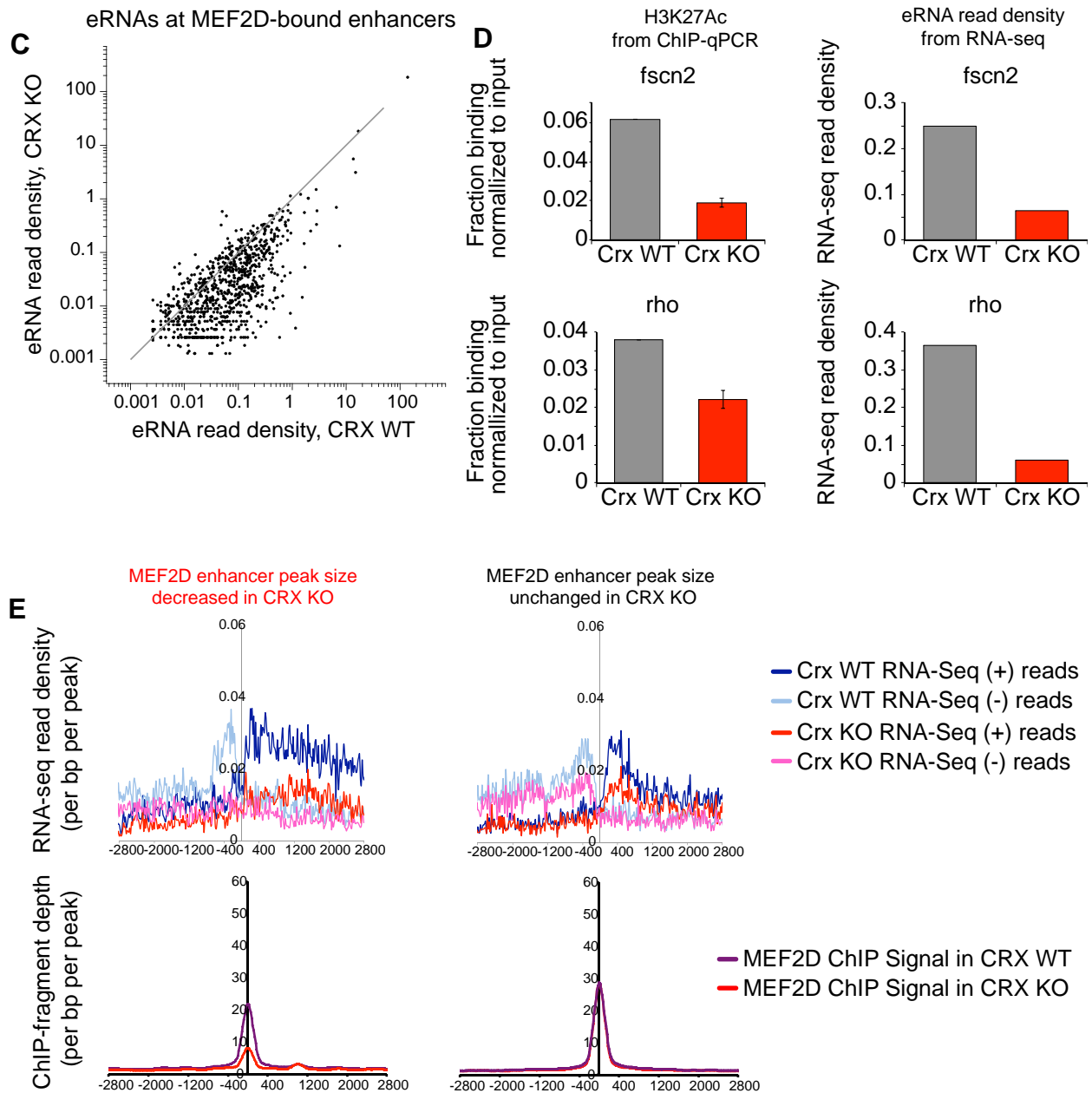


Figure 2.11. (Continued) CRX determines the selective activation of MEF2D-bound enhancers



Ultimately, the interactions of TFs at enhancers and promoters are read out through target gene expression. Given the interactions of MEF2D and CRX at critical retinal enhancers it is expected that MEF2D and CRX would share specific target genes. Furthermore, the shared loss of function phenotype for these two factors predicts that target genes shared between these TFs would be critical for photoreceptor development and function. To identify shared MEF2D and CRX target genes we compared the previously described RNA-Seq results from WT, *Mef2d* KO and *Crx* KO retinæ at p11 and found that ~51% of MEF2D direct target genes are also highly regulated by CRX (36/71 genes) (**Figure 2.12A,B**). These shared target genes included *Sag*, *Guca1a*, *Guca1b* and *Fscn2*, genes that together are essential for photoreceptor development and function. We found that ~92% of shared target genes have MEF2D and CRX co-bound at nearby enhancers or promoters, demonstrating that CRX and MEF2D are largely working at the same regulatory elements to direct expression of these genes. Of these regulatory sites, ~31% require CRX for MEF2D binding and activation (**Figure 2.12C**). The majority of remaining sites do not have significant changes in MEF2D binding but lose activity in the *Crx* KO (**Figure 2.12D**). Taken together, these data suggest two mechanistically distinct consequences of the interaction of MEF2D with CRX (**Figure 2.13**). First, CRX recruits MEF2D away from consensus binding sites toward retina-specific enhancers and stabilizes MEF2D binding at those enhancers where the MRE is particularly weak. Second, CRX contributes to activation of MEF2D-bound enhancers as determined by increased H3K27Ac levels and eRNA production. It is through these mechanisms that MEF2D achieves tissue-specific function in the development of the mouse retina. Disruption of these mechanisms leads to misregulated expression of critical cell type-specific genetic programs and abnormal photoreceptor development.

Figure 2.12. MEF2D and CRX coordinate gene expression through enhancer co-binding and co-activation

(A) Average gene expression levels as quantified by exon density of MEF2D direct target genes in either MEF2D WT compared to MEF2D KO retinae (left) or in CRX WT retinae compared to CRX KO retinae (right). N=2 mice per condition. Black line indicates unity. Red lines indicate a two-fold change from unity.

(B) MEF2D and CRX ChIP-Seq tracks at *Tnfrsf10b* example genomic locus. RNA-seq data from CRX WT (dark blue) and KO (yellow) retinae as well as MEF2D WT (black) and KO (red) retinae is also shown. Arrow denotes transcriptional start site (TSS). A light gray vertical bar highlights the identified MEF2D peak.

(C) MEF2D ChIP-Seq signal in WT versus CRX KO retinae at MEF2D-bound regulatory regions that are near MEF2D-CRX co-regulated genes. Gray line indicates unity. Red lines indicate cutoffs for a two-fold change.

(D) eRNA read densities at MEF2D-bound enhancers near MEF2D-CRX co-regulated genes. N=2 mice/genotype. eRNA Read densities are shown for (left) MEF2D WT versus MEF2D KO retinae and (right) CRX WT versus CRX KO retinae. Gray line indicates unity. Red lines indicate cutoffs for a two-fold change.

Figure 2.12. (Continued) MEF2D and CRX coordinate gene expression through enhancer co-binding and co-activation

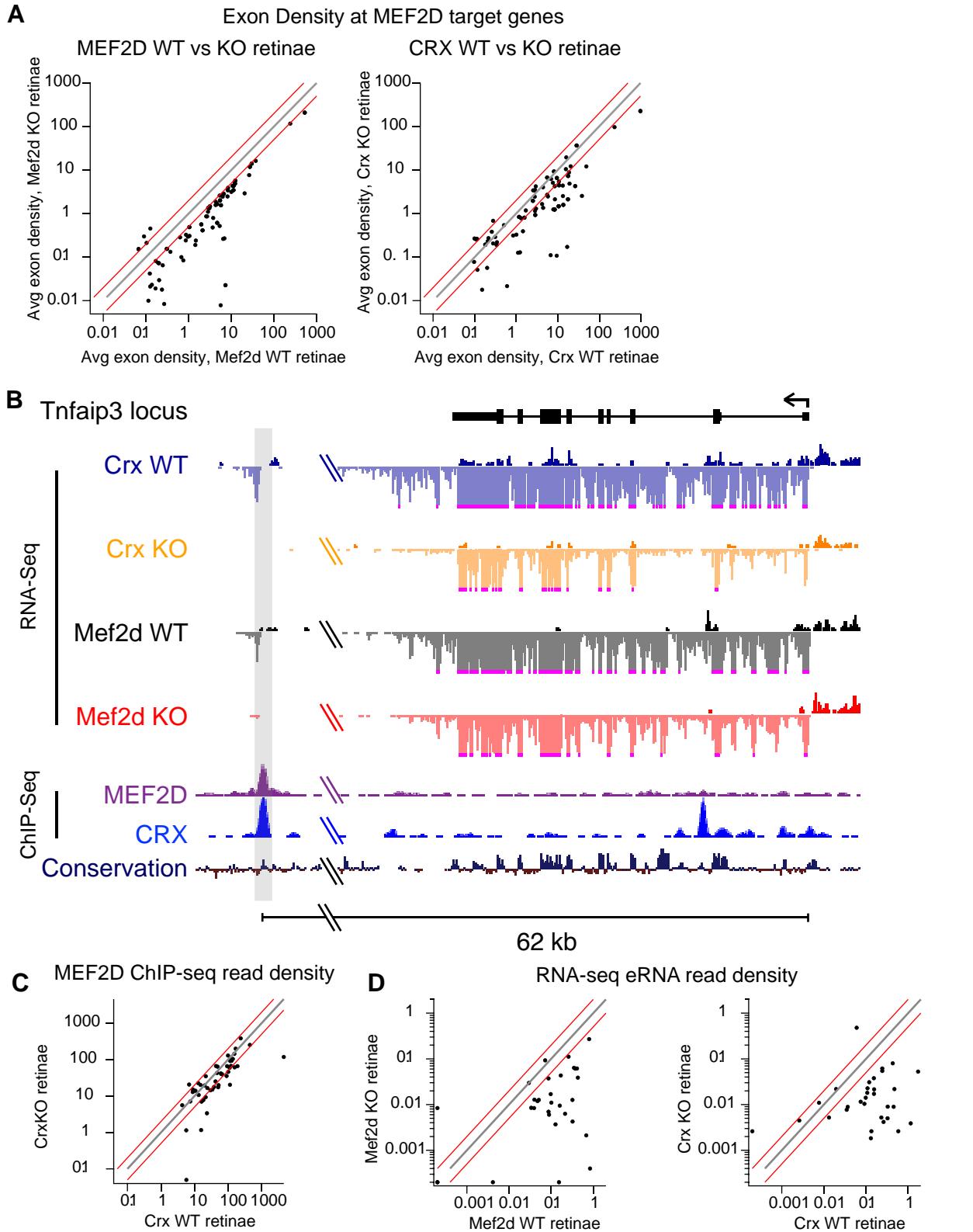


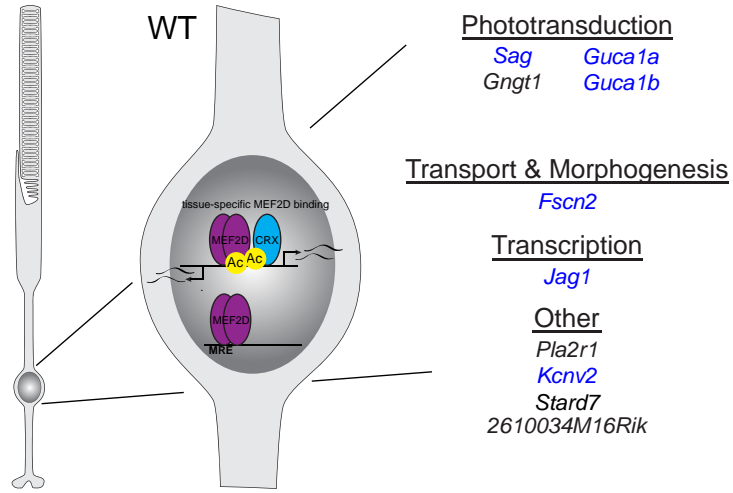
Figure 2.13. Model of MEF2D-CRX co-regulation of photoreceptor target genes

(A) Schematic demonstrating that MEF2D and CRX co-bound regulatory elements are more active, and that CRX and MEF2D co-bind near shared target genes (examples on right). As in Figure 2.6F, diagram on right demonstrates example genes that are common targets of MEF2D and CRX and important in photoreceptor cell biology. Genes implicated in retinal disease are in blue.

(B) Model of contributions of MEF2D and CRX to cooperative regulation of enhancers or promoters in the retinal genome. As shown in (A), CRX-MEF2D co-binding correlates with higher enhancer activity. *Left*, from top to bottom: in the absence of MEF2D, some, but not all MEF2D-CRX co-bound regulatory regions lose marks of activity such as acetyl and eRNAs. A smaller fraction of sites bound without CRX are active in WT retinae, and also a smaller fraction lose marks of activity in *Mef2d* KO retinae. It is not yet known if CRX binding is ever dependent on MEF2D. *Right*, from top to bottom: in the absence of CRX, a subset of CRX-MEF2D co-bound regulatory elements lose both MEF2D binding as well as marks of activity. Some sites remain bound but lose activity, and a relatively small subset of sites normally co-bound with CRX and MEF2D retain both MEF2D binding and activation in *Crx* KO retinae. Finally some sites with MREs where MEF2D is generally bound without CRX in WT retinae see an increase in MEF2D binding, and how this affects activity has not yet been elucidated.

Figure 2.13. (Continued) Model of MEF2D-CRX co-regulation of photoreceptor target genes

A



B



2.4 Discussion

MEF2 TFs have many well-established roles in the development and function of the nervous system and have been implicated in neurological disorders including Alzheimer's and Parkinson's disease, autism and intellectual disability (Rashid et al., 2014). Despite their importance in neuronal biology the mechanisms of how MEF2 regulates neuronal gene expression are still poorly understood. The development of genome-wide methods for the analysis of gene expression, TF binding and enhancer activity allows new insights to be gained by revisiting longstanding questions of gene regulation. However, using these techniques to dissect TF function in the CNS has remained difficult given the heterogeneity of cell types. Evaluating MEF2 function in the CNS has proven still more challenging, as multiple MEF2 factors often overlap in expression and function. Previous efforts therefore have been limited to studying MEF2 regulation of neuronal gene expression through reporter assays and *in vitro* analyses (Black et al., 1996; Flavell et al., 2008).

Here, we identify retinal photoreceptors as a neuronal cell type in the CNS that predominantly expresses a single MEF2 family member, MEF2D, during development and that requires MEF2D cell-autonomously for functional differentiation *in vivo* (**Figures 2.1-2.5**). MEF2 TFs have been previously proposed to play a role in photoreceptors (Escher et al., 2011; Hao et al., 2011), but attempts to identify this role have been unsuccessful because they focused on MEF2C, which is not expressed until retinal development is complete, when it is likely redundant (**Figure 2.1**). Instead our analyses demonstrate that MEF2D plays a unique role in retinal development by binding to and activating photoreceptor specific enhancers and thereby regulating critical photoreceptor-specific genes including genes mutated in human forms of

retinal disease. Within the CNS, retinal photoreceptors are notable because they are a homogeneous and functionally well-characterized cell type that makes up the vast majority of cells (~80%) in the retina. This made it possible to perform genomic and epigenetic analyses *in vivo* to functionally dissect the mechanisms of how MEF2D regulates photoreceptor development, illustrating that photoreceptors are an effective model for genomic studies of transcriptional regulation in the CNS.

Although broadly expressed across many tissues, we find that MEF2D regulates key photoreceptor-specific and retinal disease genes by binding to and activating retina-specific enhancers synergistically with the retina-specific homeodomain TF CRX and that interaction with CRX is critical for the tissue-specific function of MEF2D. Our experiments demonstrate that the function of MEF2D-CRX interactions is two-fold. First, CRX recruits MEF2D to certain photoreceptor-specific enhancers that lack a consensus MRE (**Figure 2.9**). This suggests that CRX actively stabilizes MEF2D binding rather than functioning solely as a pioneer factor by opening up chromatin to reveal MREs. Second, CRX interacts with MEF2D to co-activate MEF2D-bound enhancers as determined by increased H3K27Ac levels and eRNA production where MEF2D and CRX co-bind. These functional interactions may be significant for other cell types, as CRX is closely related to two other homeobox factors OTX1 and OTX2 that have critical roles in development of the CNS as well as in many non-neuronal cell types (Boncinelli et al., 1994; Boyl et al., 2001). Discovery of these dual mechanisms of interaction demonstrates how a broadly expressed TF such as MEF2D achieves tissue-specific functions in the retina by working with a tissue-specific co-factor to regulate photoreceptor development and function.

These observations provide *in vivo* and genome-wide validation of early studies of MEF2-cofactor interactions, while bringing novel insight into the functional nature and biological consequences of these interactions in the nervous system. *In vitro*, MEF2 has been shown to interact with myogenic bHLH heterodimers during myocyte differentiation (Molkentin et al., 1995). In this system, MEF2 and bHLH heterodimers can activate heterologous reporters in the absence of an MRE as long as the bHLH recognition element (E-box) is present, suggesting that MEF2 can be recruited to these reporters in a sequence independent manner (Molkentin et al., 1995). In contrast, others have demonstrated that each factor must bind to its recognition element for reporter activation (Naidu et al., 1995). Parallel roles for MEF2-bHLH cooperativity have been proposed in neurons however a functional understanding of these interactions has remained elusive (Black et al., 1996; Mao and Nadal-Ginard, 1996). Together these experiments suggest multiple models of MEF2-bHLH interactions. However, given the heterologous nature of these reporter studies, it is unclear how each of these mechanisms contributes to endogenous gene expression. Our results demonstrate that in the nervous system, MEF2 interacts with a homeodomain-containing TF, CRX, with two distinct consequences at endogenous sites at the level of cooperative binding and enhancer activation to co-regulate photoreceptor gene expression and development *in vivo*.

While MEF2D binding is lost in CRX KO retinæ at many sites without consensus MREs, we unexpectedly observed a significant increase in MEF2D binding in the CRX KO at distinct sites that are enriched for consensus MREs (**Figure 2.9**). This finding is noteworthy as it demonstrates that CRX mediates a genome-wide competition for MEF2D binding between these two populations of enhancers. Previous work has demonstrated a competition between functional DNA binding sites and non-functional binding sites located in satellite regions and repetitive

DNA, which are thought to limit free TF concentration in the nucleus (Liu et al., 2007). Our results suggest that CRX biases the genome-wide competition for MEF2D binding toward regulatory sites that are relevant to photoreceptor gene expression. However sites where MEF2D binding increases in CRX KO retinae are not merely sponges for TF binding, but may in fact have critical biological roles as they are highly conserved (data not shown). Furthermore, MEF2D-bound regions that are shared across tissues are overrepresented among the sites of MEF2D binding that go up in CRX KO retinae, suggesting that these sites may be active in other tissues, when paired with other co-factors, or that these sites may be active in many tissue types in a stimulus-dependent manner. In support of this hypothesis, GREAT analysis of enhancers where MEF2D binding increases in CRX KO retinae reveals that nearby genes are most significantly associated with generic biological processes such as “response to endogenous stimulus” or “response to insulin stimulus” (McLean et al., 2010). Conversely, GREAT analysis of MEF2D peaks whose binding is CRX-dependent demonstrates that these peaks are proximal to genes associated with disease ontologies of retinitis pigmentosa and retinal degeneration, providing evidence for a more tissue-specific role for this cohort of regulatory regions. This suggests that MEF2 transcription factors might employ two different mechanisms to regulate distinct gene expression programs within the same cell. The first mechanism, shared among tissues, regulates broadly expressed genes through binding to regulatory sites with consensus MREs, and may function in a stimulus dependent manner. In competition, the second mechanism regulates tissue-specific gene expression with a tissue-specific co-factor, and is critical for programs of differentiation. How both mechanisms might function simultaneously, and whether these mechanisms determine dual functions of MEF2 across different cell types, remains to be explored.

Once bound to the genome, we find that additional mechanisms must regulate the action of MEF2 function because only a small subset of MEF2D binding sites are required for expression of nearby genes. We found that selective activation of a subset of MEF2D-bound enhancers plays a significant role in determining which genes require MEF2D for their expression, and that CRX contributes to this selective activation (**Figures 2.10,2.11**). In non-neural tissues, MEF2 co-factors have been suggested to help recruit co-activators such as histone acetyltransferases (HATs) (Sartorelli et al., 1997; Youn et al., 2000a). As CRX binds the HAT P300 (Yanagi et al., 2000), this raises the possibility that MEF2D and CRX cooperatively recruit HATs. Such a tripartite complex may also stabilize MEF2D binding, in which case a single mechanism would account for the contribution of CRX to MEF2D binding and selective activation of MEF2D-bound regulatory elements.

These findings join a significant body of work done to elucidate the network of TFs that are critical for photoreceptor development (Swaroop et al., 2010). The cooperative gene regulation by MEF2D and CRX, a key member of this network, suggests that MEF2D also plays an important role. MEF2D is a notable addition to this transcriptional network because while previously identified critical members such as CRX, NRL and NR2E3 are highly tissue specific, MEF2D is broadly expressed and likely achieves photoreceptor specificity only as part of this network. Furthermore, MEF2 family members have been characterized as stimulus-responsive TFs, and developing photoreceptors respond to several different stimuli, for example taurine, dopamine, and light among others (Cohen et al., 1992; Nir et al., 2002; Young and Cepko, 2004). We propose that MEF2D could contribute a stimulus-dependent component to the transcriptional regulation of photoreceptor development, though this remains to be explored.

Finally, the present study suggests that MEF2D has the potential to be a key player in human retinal disease or may be an as of yet unrecognized retinal disease gene itself. MEF2D co-regulates critical retinal disease genes with CRX, which itself is mutated in several retinal diseases characterized by photoreceptor degeneration (Sohocki et al., 1998). Importantly, the identification of active photoreceptor enhancers allows us to identify critical MEF2D-bound functional regulatory elements, which can be as much as 100kb away from the transcriptional start site of retinal disease genes. This is significant as these regulatory elements may correspond to sites of genetic variation in humans and may ultimately be found to harbor disease-causing mutations. For example, SNPs in these regulatory elements that affect the binding of MEF2D or CRX might disrupt enhancer activity and nearby gene expression, leading to retinal disease. Such situations would join a growing cohort of enhanceropathies that contribute to human disease (Smith and Shilatifard, 2014). Thus these genome-wide analyses provide a rich resource for considering how non-coding regulatory regions function in normal development of the retina and potentially in human disease.

2.5 Experimental Procedures

Generation of MEF2D knockout mice and in vivo phenotype analysis

The targeting construct used for homologous recombination (**Figure 2.2**) in ES cells was cloned using nested PCR amplification from mouse sv129 genomic DNA into a vector containing a floxed neomycin-resistance positive selection cassette (NEO) and a diphtheria toxin A negative-selection cassette (DTA). The final targeting construct inserted 1 loxP site into intron I and 2 loxP sites flanking a NEO cassette into intron VI. Care was taken to place loxP sites and the NEO cassette in non-conserved regions of the intron. The region between loxP sites flanked a 5.1kb region of the *Mef2d* locus that spanned exons 2-6. This included the first five coding exons of MEF2D including the translational start site and the conserved MADS and MEF2 domains, which include the critical DNA and protein binding residues of MEF2D. The arms used flanking the targeted region were 4.1kb 5' and 2kb 3' to the targeted regions.

All targeting constructs were confirmed by direct sequencing in their entirety prior to use in gene targeting. The constructs were linearized and electroporated into J1 ES cells. Genomic DNA isolated from G418-resistant ES cell clones was screened by Southern blot. 5' and 3' probes external to the genomic fragment contained within the targeting vector were used. For the 5' southern, ES cell DNA was digested with Tth111I and positive targeting was indicated by a 2.4 kb decrease in the digested fragment due to a new Tth111I digest site in the NEO cassette. The 3' side was analyzed by digesting ES cell DNA with ApaI and positive targeting was indicated by a 1.6 kb increase in the size of the digested product as compared to wild-type ES cell genomic DNA representing the presence of the NEO cassette in the *Mef2d* endogenous locus. ES cell clones positive for correct targeting of the *Mef2d* locus by Southern screening

were karyotyped and those with karyotypes > 95% were used to generate mice.

Two confirmed MEF2D targeted ES cell clones were injected into C57BL/6 blastocysts and subsequently implanted into pseudopregnant females. The resulting chimeric offspring were mated with C57BL/6 mice, and the agouti offspring were screened by PCR genotyping to confirm germline transmission of the mutant allele. Targeted mice were then crossed to E2A-CRE expressing mice (stock number 003724; The Jackson Laboratory) and offspring were analyzed for expression of the Cre allele and the state of the targeted MEF2D allele using PCR genotyping. Mice that expressed Cre and had either excised the neomycin cassette or the full targeted region were bred to wildtype C57BL/6 mice and offspring that no longer expressed Cre and had transmission of either the floxed allele or the null allele without neomycin were used to establish mouse lines.

Mice were analyzed for gross phenotypes by preservation in Bouin's Solution (Sigma) and histology using hematoxylin and eosin staining of tissues throughout the mouse. Results were reviewed with a pathologist.

Animal husbandry and colony management

For routine experimentation, animals were genotyped using a PCR-based strategy. CRX knockout mice were obtained from The Jackson Laboratories (stock number 007064) and genotyped according to their protocols. Animals harboring the *Mef2d* null allele were genotyped with a forward primer upstream of *Mef2d* exon 2 and a reverse primer either 155bp downstream (for the WT allele) or a reverse primer just downstream of exon 6 (for the null allele).

Conditional knockout animals were genotyped for the presence of the loxP site, which shifts the size of the PCR product. See Figure S1 for PCR product sizes and primer sequences. The use of animals was approved by the Animal Care and Use Committee of Harvard Medical School. All experiments described here were performed using animals derived from a sv129/C57BL/6 hybrid genetic background, with the mutation backcrossed in the C57BL/6 background (Charles River Laboratories) between 3 and 8 generations.

Semi-Thin microscopy of retinas

Retinae were dissected and eyecups were fixed with 2% formaldehyde and 2.5% glutaraldehyde in 0.15 M Sorenson's phosphate buffer (pH 7.4), followed by 1% OsO₄, 1.5% potassium ferrocyanide, and stained en bloc with 1% uranyl acetate. 0.5-1 μM thick sections of the eyecup were stained with toluidine blue and examined with a Nikon Eclipse E600 microscope.

Electroretinograms

Mice were dark-adapted overnight and anesthetized with sodium pentobarbital injected intraperitoneally prior to testing. Pupils of each animal were topically dilated with phenylephrine hydrochloride and cyclopentolate hydrochloride, and mice were then placed on a heated platform. Rod dominated responses were elicited in the dark with 10-μs flashes of white light (1.37×10^5 cd/m²) presented at intervals of 1 minute in a Ganzfeld dome. Light-adapted, cone

responses were elicited in the presence of a 41 cd/m² rod-desensitizing white background with the same flashes (1.37 x 10⁵ cd/m²) presented at intervals of 1 Hz. ERGs were monitored with a silver wire loop electrode in contact with the cornea topically anesthetized with proparacaine hydrochloride and wetted with Goniosol, with a cotton wick electrode in the mouth as the reference; an electrically-shielded chamber served as ground.

All responses were differentially amplified at a gain of 1,000 (-3db at 2 Hz and 300 Hz; AM502, Tektronix Instruments, Beaverton, OR), digitized at 16-bit resolution with an adjustable peak-to-peak input amplitude (PCI-6251, National Instruments, Austin, TX), and displayed on a personal computer using custom software (Labview, version 8.2, National Instruments). Independently for each eye, cone responses were conditioned by a 60 Hz notch filter and an adjustable artifact-reject window, summed (n=4-20), and then fitted to a cubic spline function with variable stiffness to improve signal:noise without affecting their temporal characteristics; in this way we could resolve cone b-wave responses as small as 2 μV.

Immunoblotting

Dissected retinæ were homogenized in RIPA buffer (50 mM Tris pH 8.0, 150 mM NaCl, 1% Triton-X-100, 0.5% sodium Deoxycholate, 0.1% SDS, 5 mM EDTA, 10 mM NaF, 1 mM sodium orthovanadate, complete protease inhibitor cocktail tablet (Roche)) and protein levels were measured using the Bradford method (BioRad). 15μg of each protein sample was used. Conventional western blotting used enhanced chemiluminescence and HRP-conjugated secondary antibodies. Commercial antibodies used include anti-ARR3 (1:5000, EMD Millipore

AB15282) anti-MEF2D (mouse 1:1000, BD Biosciences), anti-MEF2C (rabbit 1:1000, Abcam ab64644) and anti-GAPDH (rabbit 1:5000, Sigma). A MEF2A antibody was raised in rabbit against amino acids 272-484 of human MEF2A (1:1000).

Immunohistochemistry

For immunostaining experiments retinas or eyecups were cryopreserved and 20 μ m sections were generated on a Leica CM1950 cryostat and mounted on slides. Sections were incubated in block solution (10% goat serum and 0.25% Triton X-100 in 1XPBS) for 1 hour and then incubated with primary antibodies in block solution for 2 hours at room temperature or 4° C overnight. Alexa dye-conjugated secondary antibodies were used at 1:500 dilutions in block solution (Life Technologies). Primary antibodies were anti-ARR3 (rabbit, 1:5000, EMD Millipore AB15282), anti-MEF2D (mouse 1:1000, BD Biosciences 610775), anti-MEF2A (rabbit 1:1000, generated in the Greenberg lab as described above) and anti-GFP (chicken 1:1000, Aves Labs GFP-1020). The anti-GUCA1B antibody (rabbit, 1:2500) was a kind gift from Dr. A. Dizhoor (Salus University). Slides were mounted using Prolong Gold AntiFade reagent with 4',6-diamidino-2-phenylindole (DAPI) (Life Technologies).

Images were acquired on a Zeiss LSM5 Pascal confocal microscope at 1024x1024 pixel resolution or using a Zeiss Axio Imager microscope with a 63x objective with the use of an apotome.

Quantification of outer segment disruption

Immunohistochemistry was performed as described above. Primary antibodies used were anti-ABCA4 (mouse, 1:1000, Novus Biologicals NBP1-30032) and anti-GFP (chicken, 1:1000, Aves labs GFP-1020). For quantification, images were acquired using a Zeiss Axio Imager microscope with a 63x objective with the use of an apotome. Microscope settings were optimized for each image with settings selected such that no pixels were beyond the range of the detector. For each neuron, a Z-stack of 10 sections with a step size of 1 μ m was collected, and a maximal intensity projection was created and used for analysis. Retinae were analyzed blind to genotype or experimental condition. ImageJ was used for processing. Initial defining of areas for analysis was done blind to GFP-image, using ABCA4 and DAPI layers only. Regions of interest (ROI) were obtained for both outer segments (OS, ABCA4-positive) or inner segments as the control for electroporation efficiency and signal intensity (IS, between ABCA4+ and DAPI+ areas). Mean pixel intensity was quantified for GFP in the OS and IS ROI and an index of photoreceptor apical process growth was defined as mean GFP in OS/ mean GFP in IS. Mean values for an experimental condition were determined from at least 3 retinae imaged from at least 2 different sections. Mean index data from each retina was used to analyze significance by Student's T-test.

Plasmids

Previously characterized MEF2D shRNA and mutant shRNAs cloned into the pLL3.7 vector (Addgene Plasmid 11795) were used (Flavell et al., 2006; Lin et al., 2008). Mouse MEF2D cDNA was made resistant to MEF2D-specific shRNA by mutating the sequence 5'-AGCTCTCTGGTC-3'; to 5'-AGCTCACTAGTC-3' (mutations in bold) using site-directed mutagenesis (Agilent Technologies) The cDNA was then cloned into the pFUIGW vector (Zhou et al., 2006).

In vivo retinal electroporations

Adapted from (Cherry et al., 2011; Matsuda and Cepko, 2008) with the following modifications: approximately 0.75µl DNA for electroporation were injected into the subretinal space of p0 mice using a Nanoject II and pulled glass needles (Drummond Scientific, Broomall, PA).

Cortical neuron cell culture and Potassium Chloride-mediated depolarization of cultured neurons

To obtain cortical neurons, mouse cortices were dissected from E16.5 C57BL/6 mouse embryos in dissection medium (DM) (10mM MgCL₂, 10mM HEPES, 1mM kynurenic acid in 1X Hank's Balanced Salt Solution, pH 7.2) and then dissociated for 10 minutes in DM containing 20U/ml papain (Worthington Biochemicals) and 0.32 mg/ml L-cysteine (Sigma). Enzymatic dissociation was terminated by washing dissociated cells three times for two minutes

each in DM containing 1% ovomucoid (Worthington Biochemicals) and 1% bovine serum albumin (Life Technologies). Cells were then triturated using a glass Pasteur pipette to fully dissociate cells. After dissociation, neurons were kept on ice until plating. Dissociated neurons were plated and maintained in Neurobasal medium with B27 supplement (Life Technologies), 1 mM L- glutamine, and 100 U/mL penicillin/streptomycin for 7 days. For ChIP-Seq experiments, neurons were plated at an approximate density of 4×10^7 in 15 cm culture dishes pre-coated with a solution of 20 $\mu\text{g/ml}$ poly-D-lysine (Sigma) and 4 $\mu\text{g/ml}$ mouse laminin (Life Technologies) in water. For KCl-mediated depolarization of neurons, neuronal cultures were pre-treated with 1 μM tetrodotoxin (TTX, Fisher) and 100 μM DL-2-amino-5-phosphopentanoic acid (D-APV, Tocris Bioscience) overnight to reduce endogenous neuronal activity prior to stimulation (“silencing”). Neurons were membrane depolarized with 55 mM extracellular KCl by addition of prewarmed depolarization buffer (170 mM KCl, 2 mM CaCl₂, 1 mM MgCl₂, 10 mM HEPES pH7.5) to a final concentration of 31% in the neuronal culture medium in the plate. Neurons collected for ChIP were either only silenced or silenced with 2 hours of membrane depolarization.

Chromatin Immunoprecipitation

ChIP antibodies used were anti-MEF2D (Flavell et al., 2008), anti-H3K27Ac (Abcam AB4729). MEF2D ChIP from mouse cortical cultures was performed as described in (Kim et al., 2010). MEF2D ChIP from mouse retinae was performed as previously described for brain tissue (Hong et al., 2008) with the following modifications: p11 mouse retinae were dissected in ice-cold HBSS prior to homogenization and crosslinking. 4 μg of MEF2D antibody was pre-

bound to 15 μ l of Protein A dynabeads (Life Technologies) per IP from approximately 100 million retinal cells. Histone ChIP was performed as described above with the following modifications: 10 mM sodium butyrate was added to all solutions until post-IP washes with the exception of cross-linking buffer. Chromatin was fragmented for histone ChIP by MNase (New England Biolabs) digestion for 8 minutes at 37C to generate mononucleosomes. 0.25 μ g of anti-H3K27Ac was used per IP from 10 million retinal cells. After reverse crosslinking all samples were purified using phenol/chloroform/isoamyl alcohol followed by column clean up (Qiagen, QIAquick PCR Purification Kit).

ChIP-qPCR

Quantitative PCR analysis of ChIP samples was carried out using the StepOnePlus qPCR system and Power SYBR Green mix (Life Technologies, Beverly, MA). Fraction of input values were calculated by comparing the average threshold cycle of the ChIP DNA to a standard curve generated using serial dilutions of input DNA. Fold enrichment for each genomic region evaluated was calculated as its fraction of input divided by the average fraction of input value calculated for standard background regions at least 2 kb away. Amplicon primers were designed using Primer3Plus (Untergasser et al., 2007). Primer sequences available upon request.

ChIP-Seq Sequencing, Data Processing and Peak Characterization

ChIP samples were submitted to the Beijing Genomic Institute (BGI) for 50 base pair

single end sequencing on the Illumina HiSeq 2000 platform. For each sample, over 20 million clean reads were obtained.

Sequencing data was obtained from BGI in gzipped fastq file format. Sequencing reads were then aligned to the July 2007 assembly of the mouse genome (NCBI 37, mm9) using the Burrows- Wheeler Aligner (BWA) with settings `-q 0 -t 4 -n 5 -k 2 -l 32 -e -1 -o 0`. The resulting bwa files were then converted to sam files and uniquely mapped reads were extracted from the sam files. Sam files of the uniquely mapped reads were then converted to bam files and bed files. SAMTools and BEDTools-2.16.2 were used for the above conversions. Chromosome names were changed using a custom perl script. Bed files were then used for peak calling using Model-based Analysis of ChIP-Seq (MACS) 1.4.0 (Zhang et al., 2008) with the following parameters: default parameters ($p=1e-5$) except `-bw 200`, and for histone marks, default parameters ($p=1e-5$) except `--nomodel --shiftsize 73`. To visualize ChIP-Seq data on the UCSC genome browser, reads in ChIP-Seq bed files were extended to 200 bp for transcription factors or 146 bp for histone marks using a custom perl script. BEDTools was then used to convert this file to bedgraph, at which point each file was normalized to 10 million total reads, then converted to bigwig track format and displayed as the number of input normalized ChIP-Seq reads.

MEF2D peaks were considered high confidence peaks if they appeared in 2 WT bioreplicates and the MEF2D ChIP-Seq read density in the peak was $\geq 2.5X$ the read density in a MEF2D KO ChIP-Seq. Bioreplicate 1 had 13749 peaks called by MACS over input chromatin. Bioreplicate 2 had 11979 peaks. 3664 peaks appeared in both replicates, and 2403 of these peaks were down $\geq 2.5x$ in the MEF2D KO as compared to its wildtype littermate, Bioreplicate 2. We used this set of reproducible and specific MEF2D peaks for subsequent analysis.

MEF2D peaks were classified based on their location relative to genes in the NCBI Reference Sequence Database (RefSeq). MEF2D peaks were classified as being proximal if they were within 1kb of an annotated transcriptional start site (TSS). MEF2D peaks were classified as being distal if they were greater than 1kb from an annotated transcriptional start site (TSS). Distal MEF2D peaks were further classified as intragenic if they occurred within a RefSeq gene (but not within 1kb of the TSS), or as extragenic if they did not occur within a RefSeq gene (and were greater than 1kb away from a TSS). For chromatin modifications (e.g. H3K27ac), the number of input-normalized ChIP-Seq reads within a two kb window centered on each binding site was taken to be the ChIP-Seq signal at the binding site. For transcription factors (e.g. MEF2D), the number of input-normalized ChIP-Seq reads within a 400 bp window centered on each binding site was taken to be the ChIP-Seq signal at the binding site. The number of reads was calculated using HOMER (annotatepeaks.pl; (Heinz et al., 2010)) except in the case of the initial MEF2D peak ChIP-Seq analysis between MEF2D WT and KO, where read density was calculated using a custom perl script for comparison.

Raw read data, lists of called peaks, as well as raw data for peak enrichment analysis are available upon request.

Previously published ChIP-Seq data sets

In addition to ChIP-Sequencing data we generated, we used previously published data for MEF2D isoform $\alpha 1$ and MEF2D $\alpha 1$ -blocked control ChIP-seq in myocytes (GSE43223) (Sebastian et al., 2013). In addition, we used ChIP-Seq data for two bioreplicates of CRX as well

as an IgG control (GSE20012) (Corbo et al., 2010). Sequencing data was mapped and peaks were called as described above.

ChIP-Seq analysis (peak overlap, data plots and motif enrichment)

For determining overlap of called peaks, intersectbed from BEDTools-2.16.2 was used with default settings except the `-u` option was used to get a list of each unique original feature that overlapped from one of the two compared groups instead of overlap regions or other outputs. 1 bp was sufficient to determine overlap.

HOMER 4.1 (Heinz et al., 2010) was used for the majority of the analysis of ChIP-Seq data. The mm9 genome was used for mapping and fasta file generation. ChIP tag directories were created using bed files of unextended reads and Homer MakeTagdirectory with fragment length specified as 200 for sonicated samples (transcription factors and H3K27Ac in cortical culture), 146 for MNase digested samples (histone marks in retina).

For further analysis the following commands were used with the generated tag directories. Settings used were default unless specified otherwise.

Counts of reads, or “Tag counts” were generated using `annotatePeaks.pl` with default options and a size of 400 bp centered on the peak summit for DHS and transcription factors, or a size of 2000 bp centered on the peak summit for histone marks.

Fixed line plots were generated in R using data generated from Homer 4.1 using `annotatePeaks.pl`, with the following options: `-size 2000 -len 200 -noann -nogene -ghist -hist 20`.

Aggregate plots were generated using `annotatePeaks.pl` with options `-d -size 6000 -hist 20` for ChIP-seq data. Options for motif aggregate plots were `-m -hist 20 -size 400`.

De novo and known Motif Enrichment was performed using `findMotifsGenome.pl` with options `-len 6,8,10,12 -S 15 -h`. Regions used for Motif calculations were either 400bp (in the case of Figure 2.7C) or 200bp (for all other motif enrichments). Unless otherwise specified, background for motif enrichment for each peak was an equally sized genomic window at the edge of the peak, provided the background region did not overlap with another peak in the relevant dataset.

PWMs from top de novo motifs found were then put into TOMTOM from the MEME suite (Bailey et al., 2009) and evaluated for their similarity to motifs in the JASPAR Vertebrates and UniPROBE Mouse databases using a Pearson's correlation coefficient.

For a finer analysis of motif strength based on its similarity to a given PWM, FIMO from the MEME suite was used to identify motifs and their p-values based on provided PWMs and a p-value $\geq 1e-4$. Sequence FASTA files for input into FIMO were generated using Homer 4.1 `homertools extract -fa`. 200bp regions centered on the peak summit were used.

MEF2D-bound enhancers were classified into different categories based on the behavior of the eRNA read density (quantification described below) and quantified H3K27ac signal at each enhancer. Enhancers were classified as having H3K27ac if they had >10 normalized reads (tag count, per Homer) in a 2 kb window centered on the MEF2D peak summit. Enhancers with H3K27ac were classified as having a MEF2D-dependent decrease in H3K27ac if they exhibited a two fold or greater decrease in H3K27ac signal in MEF2D KO retinae.

MEF2D-bound promoters were analyzed for H3K27ac signal presence and MEF2D-dependence as described above for enhancers but eRNAs were not assessed.

RNA isolation, reverse transcription & qPCR

Total RNA was extracted with Trizol reagent (Life Technologies) followed by column purification using the RNeasy Micro kit (Qiagen) with on column DNase digest. RNA quality was assessed on a 2100 Bioanalyzer (Agilent). RNA was reverse transcribed with the High Capacity cDNA Reverse Transcription kit (Life Technologies). Real-time quantitative PCR analysis was carried out using the StepOnePlus qPCR system and Power SYBR Green mix (Life Technologies). Reactions were run in duplicates or triplicates and *Tuba1* levels were used as an endogenous control for normalization. Real-time PCR primers were selected from an existing database (Origene). Primer sequences available upon request.

RNA-Seq sequencing, data processing and eRNA quantification

RNA-Seq was performed to a depth of at least $\sim 8 \times 10^7$ clean reads per sample. Mapping of RNA-Seq reads and subsequent analysis of read-densities across all UCSC annotated genes was performed as described (Kim et al., 2010). Exon read density was calculated based on # of reads normalized to 10 million/exon length.

Misregulated genes were defined using the following criteria: To be considered, genes needed to be expressed at a read density level of >0.1 in either both WT datasets, or both KO

datasets. Genes were considered misregulated if KO/WT was >2 or <0.5 , and the log p-value of the KO versus WT datasets was <0.05 .

To evaluate which biological processes might be enriched in our misregulated genes, we used the DAVID Functional Annotation web tool (<http://david.abcc.ncifcrf.gov>), limiting our analysis to DAVID's GO biological process FAT category. DAVID was also used to determine tissue enrichment of the gene sets (Dennis et al., 2003; Huang da et al., 2009a, b).

To define eRNAs, a 2kb window centered on the summit of each enhancer was defined. For extragenic enhancers, only those enhancers with a summit >2 kb away from the end or TSS of a gene were considered. For intragenic enhancers, only those enhancers with a summit >1.2 kb downstream of the TSS and >2 kb away from the end of the gene or TSS of another gene were considered. Additionally, for intragenic enhancers the sense strand and its RNA-seq reads was removed from consideration. In order to be considered eRNAs, 3 reads were required within the 2kb window between the 2 WT samples combined. In addition, a z score of ≥ 1.645 was required for read# downstream of the peak summit versus upstream. This excluded enhancers with reads that were not sufficiently asymmetric on a given strand with respect to the enhancer summit, as eRNAs have been characterized as being located primarily downstream of enhancer peaks on each strand. For extragenic enhancers, a z score of ≥ 1.645 , indicating bias of RNA-seq reads downstream of the enhancer summit, was required on both strands. For intragenic enhancers, a z score of ≥ 1.645 was required on only the anti-sense strand and sense reads were ignored. For enhancers that met these criteria, eRNA read density was then calculated in the 1kb region downstream of the enhancer summit only, which represented 2 1kb windows for extragenic enhancers and 1 1kb window for intragenic enhancers. These eRNA read densities

were averaged using a geometric mean within a genotype (n=2 retinae per condition) and changes were compared.

For eRNA aggregate plots, HOMER 4.1 was used. Reads that were on the transcribed sense strand within genes were removed from the analysis using a custom script. As described for ChIP-Seq, a tag directory was generated using MakeTagDirectory.pl with a fragment length of 90 and Aggregate plots were generated using annotatepeaks.pl and options -d -size 6000 -hist 20.

Reporter cloning

Luciferase reporters were generated by amplifying MEF2D-bound promoter or enhancer sequences from genomic DNA isolated from C57Bl6/J mouse tissue and cloning promoter regions into the pGL4.10 vector (Promega) using SacI and XhoI sites and enhancer regions into the pGL4.23 vector using BamHI and SalI sites.

Primers used in cloning reporters

<u>MEF2D bound region</u>	<u>Reporter Cloning Primer Sequence</u>
2610034M16Rik promoter	<i>for: atgctagagctcAGCAAATATTTAAATAGACACC</i> <i>rev: atgctactcgagTCATTTTGGCACAGGTTTC</i>
Wdr17 promoter	<i>for: atgctagagctcGCTACAAATGAAGTTATATGGC</i>

rev: atgctactcgagGAATTGGTTTCTTGCTTTTC
Pcdh15 upstream enhancer *for: atgctaggatccTGTTGAATTTTAACTAAAG*
rev: atgctagtcgacCAAACGTTAAGAAATGTCA
Pcdh15 intronic enhancer *for: atgctaggatccTGCTTCTACGTTTTAAGCCA*
rev: atgctagtcgacTTACCAGACATTTGCCTCAA
Fscn2 intronic enhancer *for: atgctaggatccAGTTTGTGGAGGGAGCCCAA*
rev: atgctagtcgacCAACAAGGAAGCTGCTCGCA
Guca1b upstream enhancer *for: atgctaggatccGGAGCACAGAACATACATGG*
rev: atgctagtcgacTTCCTAGCCTGTGTGAGGGT
Pla2R1 intronic enhancer *for: atgctaggatccATTCAGGCTTGTCTACAAT*
rev: atgctagtcgacCTTTATCCTCACCAAGGCTA
Stard7 intronic enhancer *for: atgctaggatccGGAGCTTTGGTTAGGTGAAG*
rev: atgctagtcgacCAATACAAATGATGGAGGAG

Retinal explant luciferase reporter assays

Explant electroporation protocol adapted from (Matsuda and Cepko, 2008). Promoter or enhancer luciferase reporters were electroporated into dissected retinæ at p0 with a reporter constitutively expressing Renilla luciferase was co-electroporated as a control. Retinæ were cultured for 7 days and then washed briefly in ice cold 1x PBS and homogenized in 500µl passive lysis buffer with trituration. Homogenate was snap frozen to promote cell lysis and subsequently thawed for analysis of luciferase activity using the Dual-Glo® Luciferase Assay System (Promega). Firefly luciferase activity was normalized to renilla luciferase activity.

Chapter 3

Features of widespread MEF2D binding and differential function at enhancers

3.1 Abstract

In the previous chapter we found that MEF2D is important for normal photoreceptor development by regulating a cohort of genes critical for photoreceptor function, many of which are mutated in retinal disease. MEF2D bound broadly but preferentially activated bound regulatory elements proximal to these target genes. However, the majority of MEF2D binding throughout the retinal genome was not proximal to MEF2D target genes. The function of MEF2D at these other binding sites and how this binding contributes to gene expression remains unknown. The discrepancy between widespread TF binding and limited changes in gene expression has been previously observed in many other genome-wide studies, however a direct analysis of reasons for this discrepancy has not yet been performed. To examine the source of this discrepancy we evaluated in an unbiased manner the activity of MEF2D-bound enhancers genome-wide. We identified several classes of MEF2D-bound enhancers. Many MEF2D-bound enhancers were inactive, and of the active MEF2D-bound enhancers, only a subset was dependent on MEF2D for activity. Genes near MEF2D-dependent enhancers were more likely to be misregulated in the absence of MEF2D, however in many cases genes near MEF2D-dependent enhancers were either only slightly misregulated or not misregulated at all, suggesting that while selective activation does contribute to specifying the direct target genes of MEF2D, mechanisms beyond enhancer activation must ultimately define which MEF2D enhancers truly regulate gene expression.

3.2 Background & Significance

Transcriptional regulation of programs of gene expression provides the foundation for cellular differentiation and function. Elucidating the mechanisms by which transcription factors (TFs) bind DNA and regulate target genes is a longstanding interest in molecular biology and significant work over the past decades has demonstrated many examples of TF binding to an individual gene promoter or nearby enhancer resulting in direct regulation of the gene bound by that TF (Ptashne, 1988). However, with the advent of genome-wide ChIP-seq and RNA-seq technologies the relationship between TF binding and regulated expression of nearby genes has proven to be complex. Genome-wide analyses of transcription factor binding have suggested that only 10-25% of transcription factor occupancy relates to the expression of neighboring genes (Spitz and Furlong, 2012). Several sources of this discrepancy have been proposed, ranging from widespread non-functional binding of TFs to the inability to identify bona fide target genes that have only small changes in expression upon loss of the TF. However, an explanation for this discrepancy remains to be provided. Addressing the relationship between TF binding and gene regulation in mammalian cells should provide new insight into how regulatory elements are activated and what role any single TF plays in their activation.

The MEF2 family of TFs plays a critical role in regulating gene expression across many cell types and has been associated with cardiac, neurological and vascular disease (Bhagavatula et al., 2004; Bienvenu et al., 2013; Chasman et al., 2014; Freilinger et al., 2012; Novara et al., 2010; Wang et al., 2003). Their function at regulatory elements has been looked at on a gene-by-gene basis, particularly in myocytes (Black and Cripps, 2010). MEF2s have been suggested to bind to DNA and interact with multiple co-factors to function as repressors as well as activators (McKinsey et al., 2002). Several studies have examined MEF2 binding throughout the genome (He et al., 2011;

Schlesinger et al., 2011; Sebastian et al., 2013), though none have evaluated the functional relationship between MEF2 binding and the regulation of gene expression at a genome-wide level. Understanding how MEF2 TFs contribute to enhancer activation genome-wide should give insight into both how MEF2 TFs execute their critical functions as well as provide information regarding how TF function is determined beyond DNA binding.

We previously discovered that MEF2D regulates photoreceptor differentiation by directly activating a cohort of enhancers and promoters associated with photoreceptor-specific genes, including genes that are mutated in human forms of blindness (Chapter 2). Furthermore, MEF2D regulates these genes by being recruited to retina-specific regions of the genome partly by its co-factor CRX. However, additional regulatory mechanisms beyond retina-specific binding must modulate the action of MEF2 function because only a small subset of MEF2D binding sites are required for expression of nearby genes. MEF2D-bound enhancers that were co-bound by CRX and proximal to target genes were preferentially active. However, this alone did not account for the discrepancy between MEF2D binding and gene regulation. Other possible contributing factors include redundancy between enhancers regulating any given gene or the presence of sites where MEF2D binding is irrelevant. Alternatively, there may be many target genes subtly affected by loss of MEF2D that are difficult to appreciate due to the noise inherent in these analyses. To better understand how the MEF2 family of transcription factors regulates programs of gene expression we performed a comprehensive analysis of the activity of MEF2D-bound enhancers in our model system of retinal photoreceptor development and examined how MEF2D-bound enhancer activity relates to regulation of gene expression.

We found that approximately 1/3 of MEF2D-bound enhancers are active at postnatal day

11 (P11) as determined by histone acetylation and eRNA production. Active and inactive enhancers display differential motif enrichment, and inactive enhancers have lower levels of MEF2D binding. Furthermore, only ~1/3 of active, MEF2D-bound enhancers are dependent on MEF2D for their activity, and as might be expected, these enhancers are generally closer to genes misregulated in MEF2D KO retinæ. Enhancers dependent on MEF2D were more likely to have an MRE. Overall, we have narrowed the critical functions of MEF2D, a widely expressed and broadly bound transcription factor, to the activation of a relatively small cohort of enhancers regulating MEF2D target genes. Furthermore, we have examined determinants of regulatory element activation at multiple levels, and found that DNA accessibility and co-factor binding in particular correlate with functional TF binding, however MRE affinity or conservation does not. These results suggest that the mismatch between number of MEF2 binding sites and the number of misregulated genes is largely due to a significant amount of binding where MEF2D is not necessary for enhancer activation.

3.2 Results

MEF2D binds enhancers broadly throughout the retinal genome

Our previous study characterized 2403 high-confidence sites of MEF2D binding in P11 retinae (Chapter 2). By examining the proximity of each peak to the nearest gene transcriptional start site, we find that the majority of these MEF2D bound regions in the retina are greater than 1kb away from the nearest TSS, suggesting that MEF2D is predominantly bound to genetic enhancers (83%; 2003/2403) (**Figure 3.1A**). In order to begin to analyze enhancer activity genome-wide, we first confirmed this bias by performing ChIP-Seq for epigenetic marks of enhancers and promoters and determining the relative enrichment of each mark at MEF2D bound sites distal or proximal to a TSS (**Figure 3.1B**) (Heintzman et al., 2007). Enhancer elements can be identified by their enrichment of H3K4me1, as opposed to promoters, which have high H3K4me3 and low H3K4me1 (Heintzman et al., 2007). The small subset of MEF2D sites <1kb from a TSS is enriched for H3K4me3, a hallmark of promoter elements, while distal MEF2D sites are enriched for H3K4me1, a hallmark of enhancers (**Figure 3.1C**). These enhancer sites are also modestly enriched for H3K4me3 reflecting that a significant percentage of MEF2D-bound enhancers are located within introns of the gene body.

Identification of active, MEF2D-bound enhancers genome-wide

We previously observed that while MEF2D binds at >2400 genomic sites in the retina (Chapter 2), only 93 of these are proximal to genes that are strongly misregulated in MEF2D knockout retinae, including 75 enhancers. This observation is significant because it suggests that

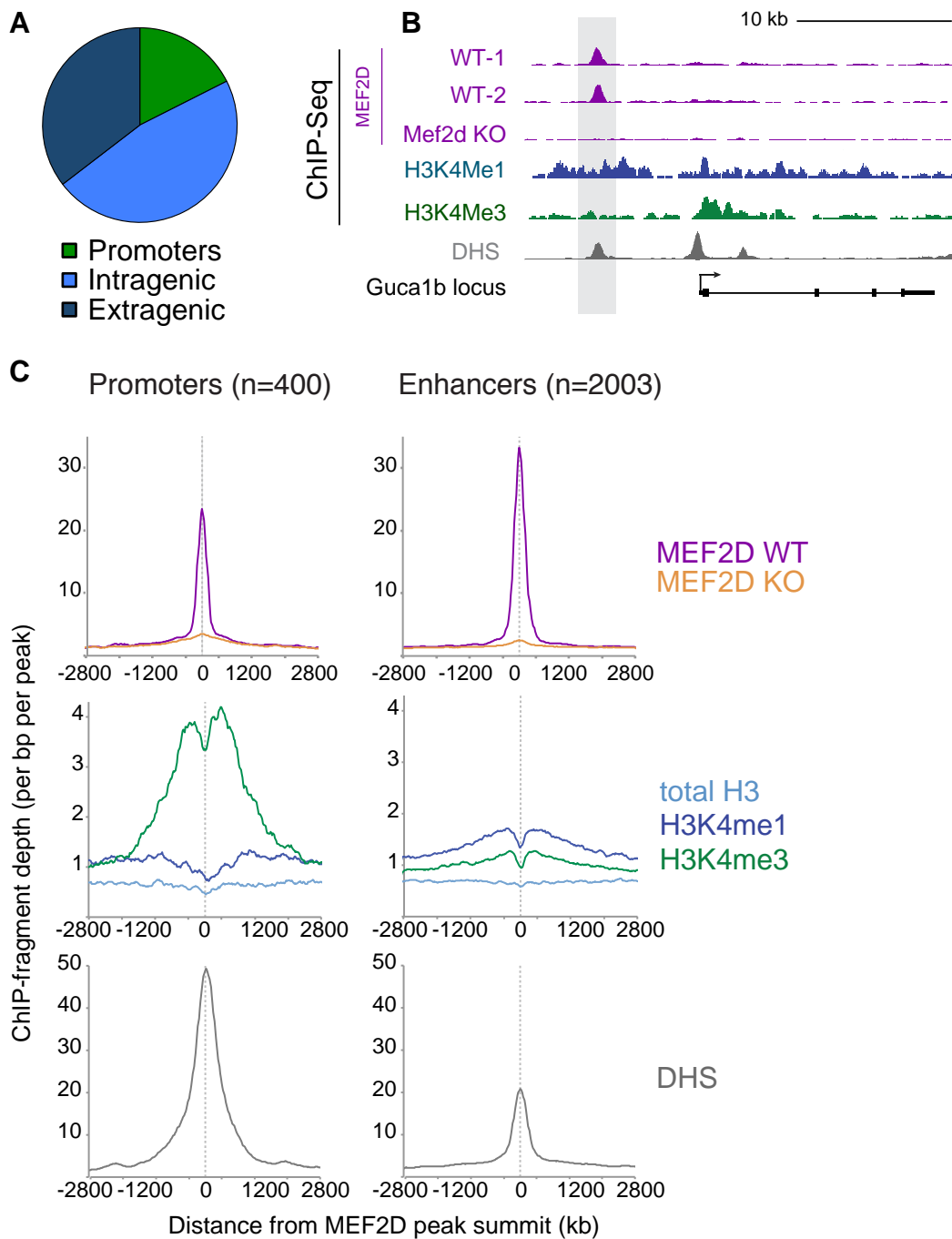
Figure 3.1. MEF2D predominantly binds enhancers throughout the retinal genome.

(A) Distribution of MEF2D binding in the retina.

(B) MEF2D, H3K4me1 and H3K4me3 ChIP-Seq tracks at the *Guca1b* genomic locus. MEF2D ChIP-Seq data are shown for 2 WT and 1 MEF2D KO sample. Arrow denotes *Guca1b* transcriptional start site (TSS). A light gray vertical bar highlights the identified MEF2D peak. DNase hypersensitivity (DHS) is also shown from the ENCODE Consortium.

(C) Aggregate plots of ChIP-Seq signal for 5.6kb region centered on summits of MEF2D-bound regions at promoters (left) or enhancers (right). Enhancers were defined as >1kb from any gene's TSS, promoters as <1kb from a gene TSS. Plots are centered on summits of MEF2D peaks and show ChIP-Seq for histone marks total H3 (light blue), H3K4ME1 (dark blue) and H3K4me3 (green) and MEF2D in MEF2D WT retinae (purple) or MEF2D KO retinae (orange). DHS data from 8-week WT retinae (ENCODE) is also shown.

Figure 3.1. (Continued) MEF2D predominantly binds enhancers throughout the retinal genome.



while MEF2D binds its targets directly, the majority of MEF2D bound elements are not actively required for regulating gene expression in the retina. Indeed we previously determined that MEF2D-bound regulatory elements proximal to target genes are far more likely to be active than those regulatory elements proximal to genes unchanged in MEF2D KO versus WT retinæ. This conclusion supports the model that while MEF2D binds broadly, only a subset of MEF2D bound enhancers are active in any given tissue. To determine why so few MEF2D-bound sites seem relevant for gene expression we sought to directly test if MEF2D-bound sites were broadly differentially active genome-wide and to identify in an unbiased manner characteristics that may determine whether or not a MEF2D-bound site is active.

Several recent studies suggest that acetylation of histone 3 lysine 27 (H3K27ac) is a hallmark of enhancers that are actively engaged in regulating transcription (Creyghton et al., 2010; Rada-Iglesias et al., 2011). Other studies have identified non-coding transcription of RNA at enhancers (eRNAs) as a mark of active enhancers (Kim et al., 2010; Li et al., 2013; Wang et al., 2011) We previously performed ChIP-Seq for H3K27Ac and analyzed eRNA production at MEF2D-bound sites in p11 WT retinæ, and confirmed that these marks of active enhancers correlated with enhancer activity in reporter assays in retinal photoreceptors (Chapter 2). To assess the levels of these marks at MEF2D-bound enhancers globally we re-examined our data sets of ChIP-Seq for H3K27Ac in p11 WT retinæ and eRNA expression in our RNA-Seq dataset (**Figure 3.2A**). To maximize specificity, we considered MEF2D-bound enhancers to be active only if they had both eRNAs and H3K27Ac ChIP signal and inactive only if they had neither eRNAs nor H3K27Ac ChIP signal. These two independent signatures of enhancer activity were well correlated (Pearson's $R=0.57$). We found that 660 MEF2D-bound enhancers had both eRNAs and H3K27Ac and so were considered active enhancers, whereas we identified 584 of

Figure 3.2. Identification of active MEF2D-bound enhancers genome-wide.

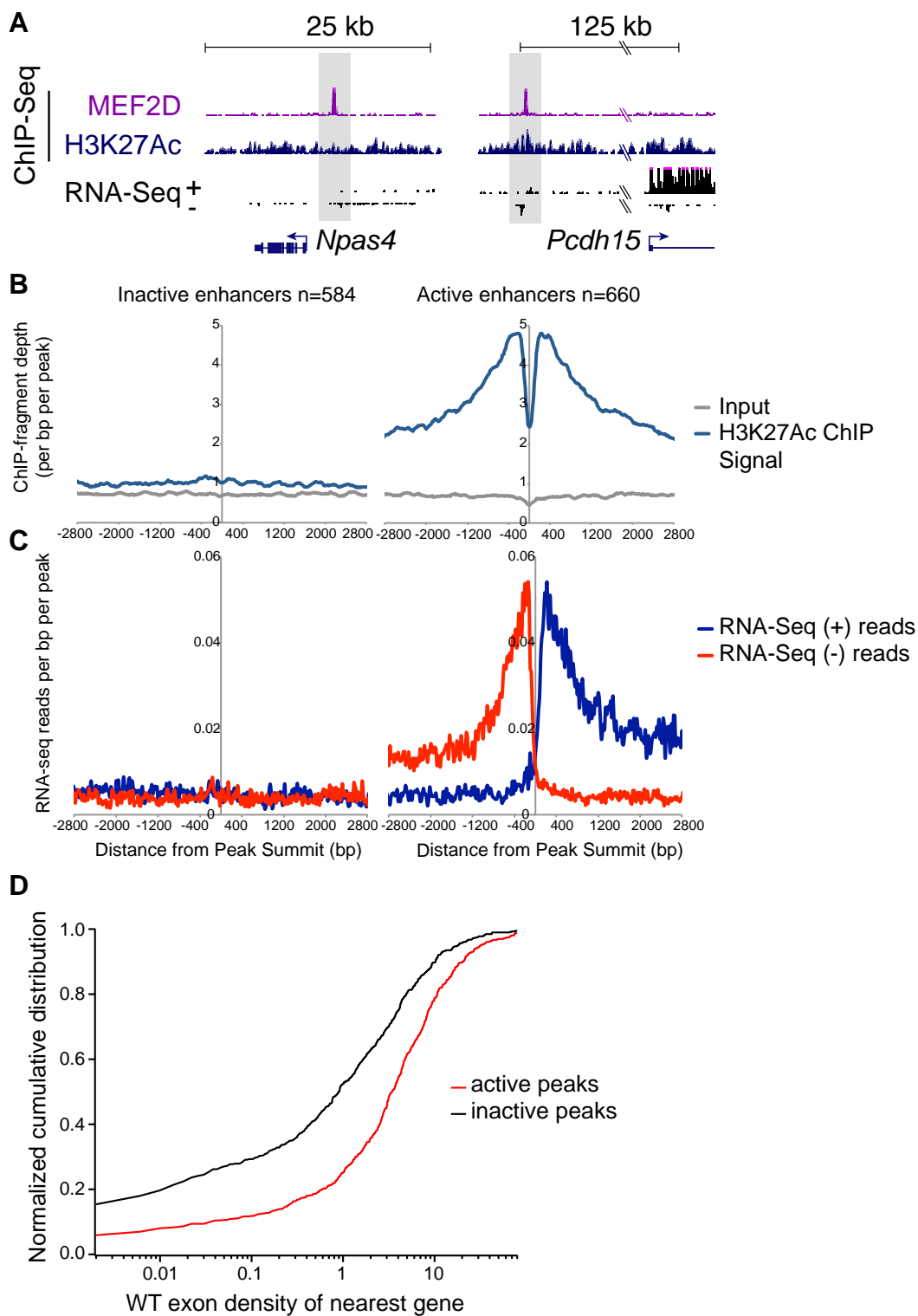
(A) Example tracks of inactive (left) and active (right) MEF2D-bound enhancers. MEF2D-bound enhancer regions are highlighted in light gray. MEF2D and H3K27Ac ChIP-Seq tracks are shown, as is an example RNA-seq track from MEF2D WT retinae. For RNA-seq, the numbers of reads aligning to forward (F, black) and reverse (R, gray) genomic strands are separately displayed.

(B) Aggregate plots of H3K27Ac ChIP-Seq signal (blue). Plots are centered on summits of MEF2D-bound regions that either had both eRNAs and H3K27Ac ChIP-seq signal (active enhancers, right) or had neither (inactive enhancers, left).

(C) Aggregate plots of RNA-seq reads (coding reads removed) for forward (dark blue) and reverse (red) strands. Plots are centered on summits of MEF2D-bound active enhancers (right) or inactive enhancers (left) as in (B).

(D) Cumulative distribution of WT average exon density (from RNA-Seq data, n=2) for genes nearest active enhancers (red) or inactive enhancers (black).

Figure 3.2. (Continued) Identification of active MEF2D-bound enhancers genome-wide



inactive MEF2D-bound sites lacking both eRNAs and H3K27Ac (**Figure 3.2B, 3.2C**). Taken together these data strongly suggest that MEF2D-bound sites are differentially activated throughout the genome.

To confirm globally that the activity of MEF2D-bound enhancers is relevant to endogenous gene expression, we looked at the correlation between the activity of MEF2D-bound enhancers and the expression level of the nearest gene. Active, MEF2D-bound enhancers were more likely to be near highly expressed genes than inactive MEF2D-bound enhancers (KS test, $p = 9.728e-17$) (**Figure 3.2D**), and in fact almost all active peaks (>80%) were near an active gene. This suggests that active MEF2D-bound enhancers globally contribute to regulating gene expression, even if they are not near a MEF2D target gene.

To find determinants of MEF2D-binding site activity, we looked for the presence of additional transcription factor binding motifs that were enriched in either active or inactive MEF2D-bound sites. We found that the top motifs enriched in active sites as compared to inactive sites were GCAACTAGGTCA ($p=1e-14$) and CTAAGCCK ($p=1e-13$), which correspond to RORA ($p=0.00003$) and CRX ($p=1e-13$) transcription factor consensus binding motifs respectively (**Figure 3.3A**). The enrichment of the CRX binding motif is consistent with our previous results where we identified a correlation between co-binding of CRX and increased activity at MEF2D-bound enhancers. The enrichment of a motif for Rora is intriguing as Rorb (a close homolog of Rora) is also an important transcription factor in photoreceptor development whose loss-of-function phenotype phenocopies the *Mef2d* KO and *Crx* KO outer segment development phenotype (Freund et al., 1997; Furukawa et al., 1999; Jia et al., 2009; Swain et al., 1997). This finding implies that MEF2D may activate enhancers in cooperation with a core set of

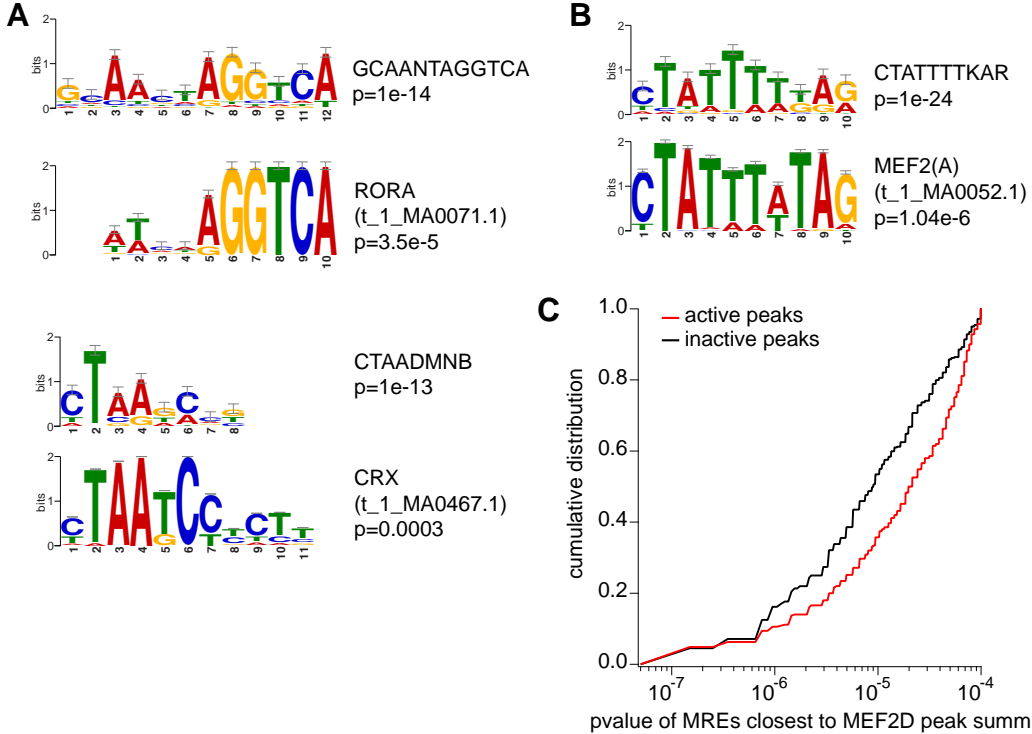
Figure 3.3. Motif enrichment in active versus inactive MEF2D-bound enhancers.

(A) Position weighted matrices (PWM) of top two enriched motifs under active MEF2D-bound enhancers as compared to inactive MEF2D-bound enhancers. Below each, high-ranking JASPAR matrix corresponding to most enriched PWM.

(B) PWM and corresponding JASPAR matrix for top motif in inactive MEF2D-bound enhancers as compared to active MEF2D-bound enhancers.

(C) Cumulative distribution of MRE strength (p-value describing similarity to canonical MRE) for all MREs with $p < 1e-4$ found in 400bp regions centered on MEF2D peak summits.

Figure 3.3. (Continued) Motif enrichment in active versus inactive MEF2D-bound enhancers



key photoreceptor transcription factors, beyond CRX. Additionally, the top *de novo* motif found in inactive as compared to active MEF2D-bound sites was CTATTTTKAG ($p=1e-24$), which is consistent with the canonical MEF2 recognition element (MRE) ($p=1e-6$) (**Figure 3.3B**). We confirmed this observation by quantifying how similar the MREs present in the two peak subsets are to the canonical MRE (**Figure 3.3C**). The inactive peaks indeed had more MREs than active peaks (80% versus 53%). Furthermore, when just the MREs between the two subsets were compared, the MREs under inactive peaks were significantly closer to the consensus MRE than those under active peaks (KS test, $p=8.7e-7$). This suggests that inactive, MEF2D-bound elements are bona fide MEF2D binding sites rather than non-specific ChIP-Seq signal which would not be expected to be enriched for the MRE motif. These inactive, MEF2D-binding sites with high affinity MREs likely have an important function in cells, though the context in which it is relevant remains to be determined.

We also noted that overall, inactive peaks are smaller than active peaks (**Figure 3.4A**). This is consistent with previous studies that have shown regions of low TF occupancy are generally nonfunctional (Fisher et al., 2012). To evaluate whether MEF2D peak size might explain the difference in regulatory element activity, we generated new subgroups of inactive and active peaks that were normalized for MEF2D ChIP peak size ($n=396$ peaks/group), and found that this did not change the differences between active and inactive peaks with respect to histone mark presence, eRNA production, enrichment of MREs (**Figure 3.4**).

The finding that a relatively small subset of MEF2D-bound enhancers is active strongly suggests that selective activation is a key aspect of MEF2D bound regulatory regions. Additionally, these results underscore that MEF2D binding to a regulatory element does not equate to activation of that element. A major reason therefore for the overrepresentation of

Figure 3.4. Properties of active and inactive enhancers normalized by size of MEF2D peak.

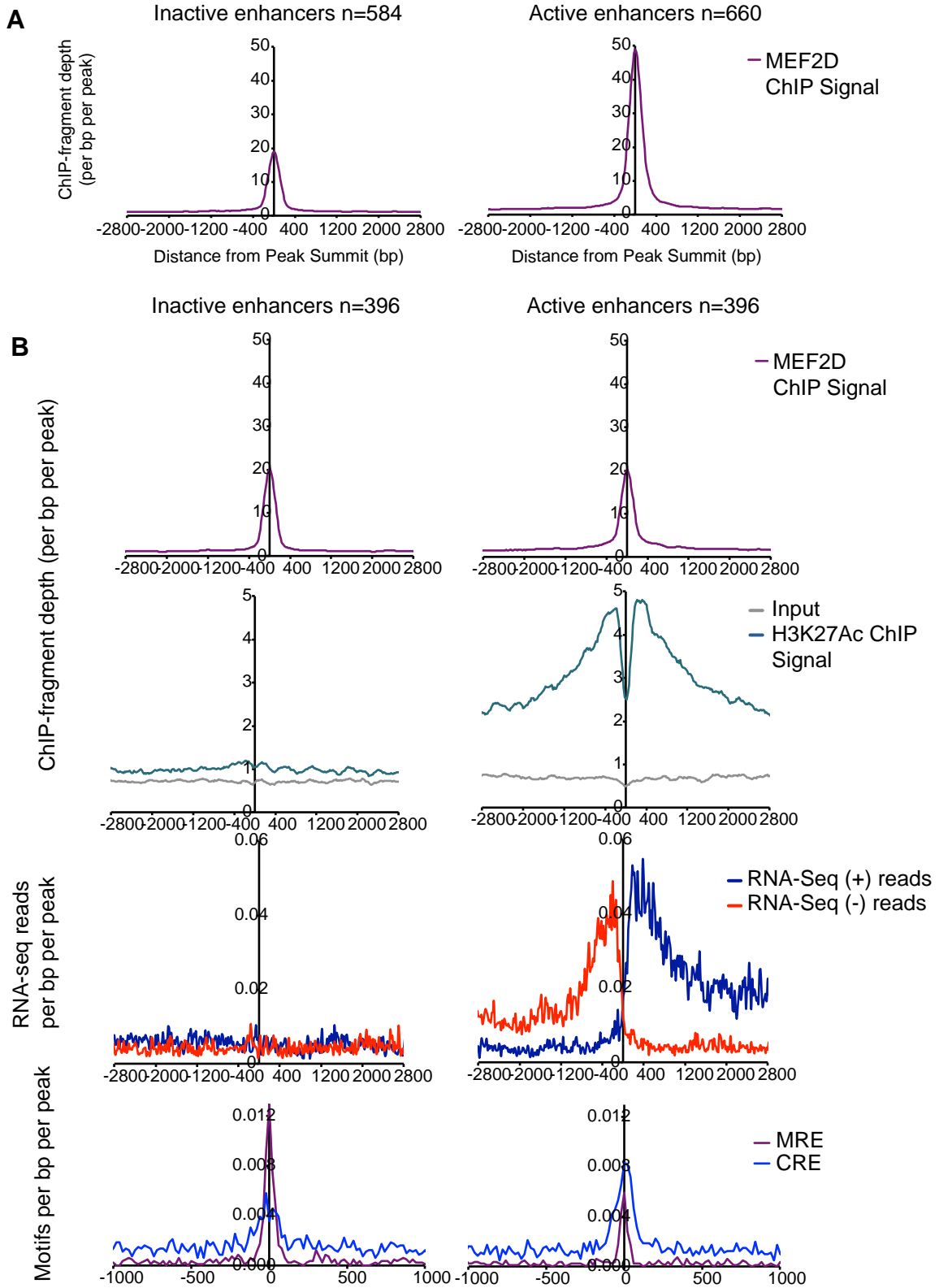
(A) Aggregate plots of MEF2D ChIP-Seq signal for 5.6kb region centered on summits of MEF2D-bound regions at all inactive (left) or active (right) enhancers. Plots are centered on summits of MEF2D peaks.

(B) Aggregate plots as described in (A) for subsets of inactive and active enhancers normalized by MEF2D peak size.

(C) Aggregate plots of H3K27Ac ChIP-Seq signal (blue, top) or RNA-seq reads (bottom) at same peak sets as in (B).

(D) Aggregate plots of DNA binding motif occurrence for the MEF2 motif (purple) or CRX motif (blue) in a 2kb window centered on summits of the same MEF2D-bound regions as in (B) and (C).

Figure 3.4. (Continued) Properties of active and inactive enhancers normalized by size of MEF2D peak



transcription factor bound sites compared to misregulated genes is because a significant percentage of transcription factor binding sites are inactive in the context of our experiments and not directly engaged in regulating gene expression. The refinement of 2003 total MEF2D-bound enhancers to 660 active enhancers represents a four-fold enrichment in fraction of enhancers near target genes. Nonetheless, only 75 enhancers are proximal to MEF2D target genes. This discrepancy suggests that while MEF2D-bound sites are differentially active, additional mechanisms must limit the number of active enhancers that are required to regulate gene expression. One possibility may be that multiple enhancers regulate each target gene (approximately 10 enhancers per gene). Another more likely possibility is that only a subset of active, MEF2D-bound enhancers functionally requires MEF2D for their activity. To test this second possibility we compared H3K27Ac and eRNA levels in WT retinæ to levels in littermate *Mef2d* KO retinæ.

MEF2D is required for enhancer activity at a subset of its bound enhancers

Just as MEF2D binding does not signify that an enhancer is active, MEF2D binding at active enhancers does not mean that those enhancers are dependent on MEF2D for their activity. We had previously observed that MEF2D bound regulatory regions near strongly misregulated genes are more active (Chapter 2), but there are still more active regulatory elements than strongly misregulated genes. MEF2D may be required at multiple enhancers for the coordinate activation of a given target gene. Alternatively (but not mutually exclusively), MEF2D may bind in many areas where it is not always necessary for an enhancer's activity, suggesting that even within a single cell type, different enhancers have varying combinations of transcription factors

and not all transcription factors are required at all regulatory elements where they are bound.

There are currently few studies that examine the change in enhancer activity upon loss of a particular transcription factor on a global level. However, we had previously demonstrated that loss of H3K27Ac and eRNAs in *Mef2d* KO retinae correlated with loss of enhancer reporter activity by mutating the MEF2 binding site (MRE) or using a MEF2D shRNA. Thus, we reasoned a global survey of changes in H3K27Ac and eRNAs in MEF2D KO retinae would be able to identify the active, MEF2D-bound enhancers that require *Mef2d* for their activity.

We defined MEF2D-dependent enhancers as distal sites that had both a greater than 50% reduction in eRNA density and a greater than 50% reduction in H3K27Ac ChIP signal at the MEF2D-bound region in *Mef2d* KO retinae compared to WT (**Figure 3.5**). Using these criteria, about 35% of active enhancers (230/660) were highly dependent on MEF2D. In contrast, about 45% of enhancers (294/660) had no change in histone acetylation or eRNAs in *Mef2d* KO retinae. These analyses suggested that only very few active, MEF2D-bound enhancers require **MEF2D** for their activity, which is consistent with our previous results that MEF2D selectively controls enhancers at target genes.

To confirm that these newly identified MEF2D-dependent enhancers are relevant for endogenous gene expression, we analyzed the change in gene expression in *Mef2d* KO retinae of genes nearest MEF2D-dependent enhancers. We found that genes nearest MEF2D-dependent enhancers changed more significantly in *Mef2d* KO retinae than genes near enhancers that were not MEF2D-dependent (KS test, $p = 9.713e-27$) (**Figure 3.5**). These genes included those previously identified as putative direct targets of MEF2D (from Chapter 2), suggesting that the contribution of MEF2D to enhancers near target genes is non-redundant and critical for their

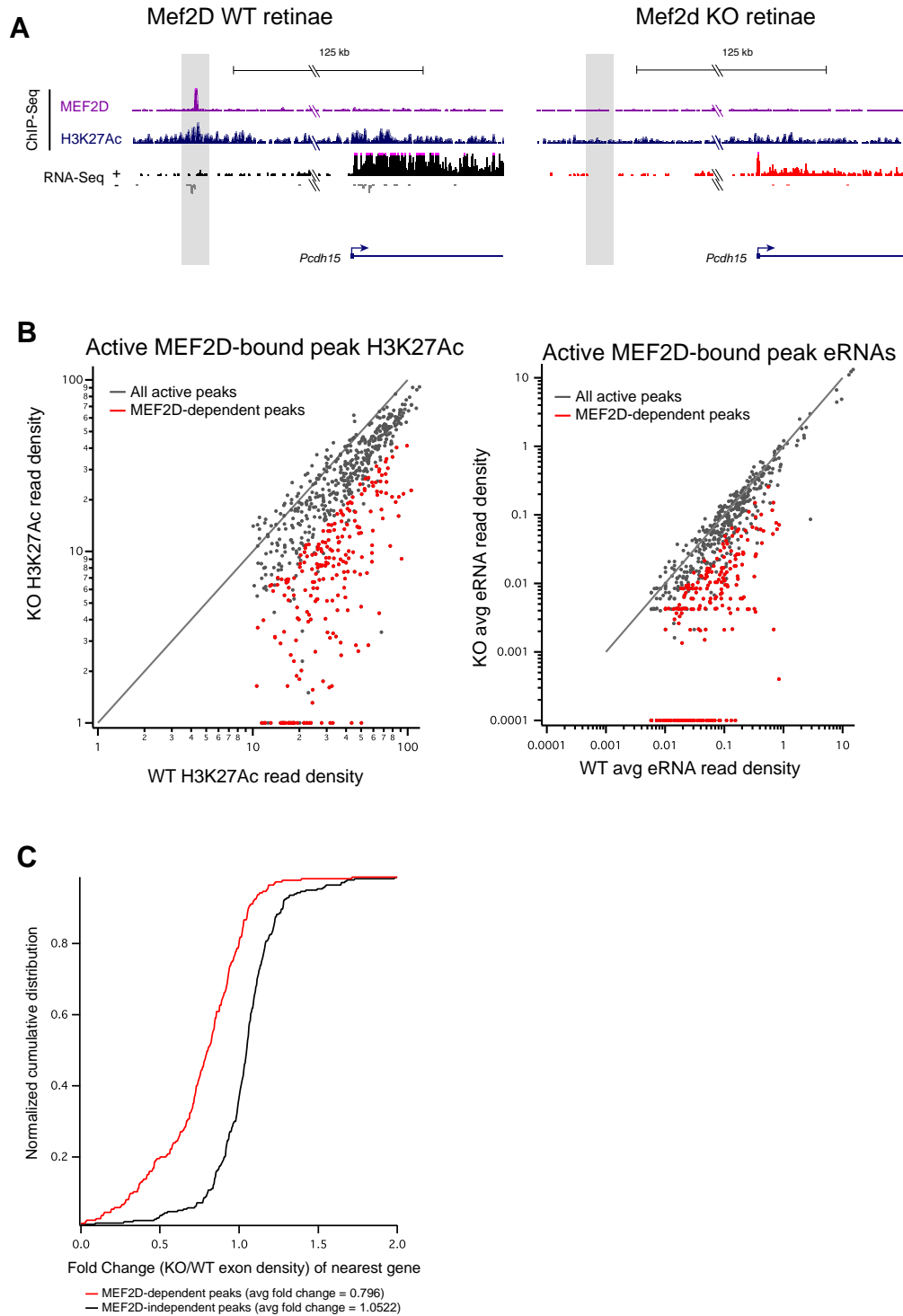
Figure 3.5. MEF2D is required for enhancer activity at a subset of its bound enhancers.

(A) Example tracks of *Pcdh15* genomic locus in MEF2D WT (left) or KO (right) retinae. MEF2D-bound enhancer regions are highlighted in light gray. MEF2D ChIP-Seq, H3K27Ac ChIP-Seq and RNA-seq in either MEF2D WT or MEF2D KO retinae are displayed.

(B) H3K27Ac ChIP-Seq read density and Average RNA-seq read density of eRNAs at all active MEF2D-bound enhancers in WT versus MEF2D KO retinae. Read density was calculated +/- 1 kb from the center of the WT MEF2D peak. Data points in red indicate the MEF2D-dependent subset of enhancers that lose both eRNAs and H3K27Ac ChIP-Seq signal by >50% in MEF2D KO retinae.

(C) Cumulative distribution of ratio of average exon read density in MEF2D KO retinae as compared to WT retinae (n=2 per genotype, RNA-Seq data) for genes nearest active enhancers that were MEF2D-dependent (red) or MEF2D-independent (black).

Figure 3.5. (Continued) MEF2D is required for enhancer activity at a subset of its bound enhancers



expression, and that this method of looking at enhancer activity effectively identifies target enhancers relevant to target gene expression.

To determine why some active, MEF2D-bound enhancers are MEF2D-dependent while others are not, we performed a differential *de novo* motif analysis on these two categories of enhancers. We hypothesized that other transcription factor motifs may be enriched near MEF2D-independent enhancers and that the presence of additional transcriptional regulators may be able to compensate for the loss of MEF2D. Unexpectedly, we did not observe strong enrichment of any single motif near MEF2D-independent enhancers. Instead, we found that enhancers that were MEF2D-dependent were more enriched for the presence of an MRE (p=1e-18; 68% of dependent peaks versus 33% of independent peaks) (**Figure 3.6**). It is unclear why this enrichment may exist, however it may suggest evolution has selected for reliable MEF2D binding at these sites to prevent loss of enhancer activity.

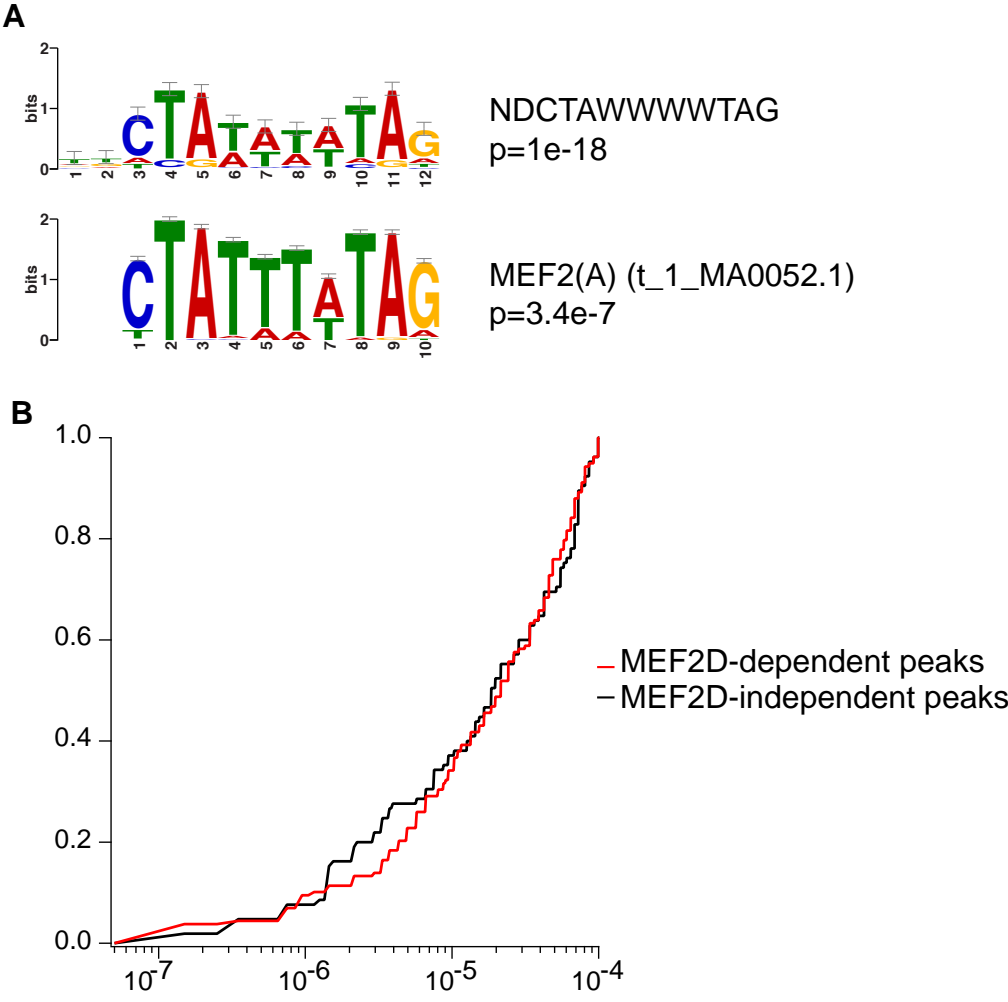
By examining the change in histone acetylation and eRNA production in *Mef2d* KO retinæ, we were able to take 2403 MEF2D-bound regions and identify the 10% of peaks (230) that are active and MEF2D-dependent. We previously observed that the 75 enhancers near target genes were preferentially MEF2D regulated and active as compared to a control 75 enhancer group. Here, we see the significance of these numbers in the context of MEF2D genome wide. These 75 enhancers near target genes are about 1/3 of the number of MEF2D-regulated enhancer elements. This narrowing to 230 MEF2D-dependent enhancers is a three-fold enrichment as compared to only looking at active enhancers that are bound by MEF2D, suggesting that the presence of active enhancers bound by a TF where that TF is not necessary for that regulatory element's activity is responsible for a great deal of the discrepancy between TF binding and gene

Figure 3.6. MEF2D-dependent regulatory elements are enriched for conserved MREs.

(A) Position weighted matrix (PWM) of top enriched motif under MEF2D-dependent enhancers as compared to MEF2D-independent enhancers. Below, high-ranking JASPAR matrix corresponding to the PWM.

(B) Cumulative distribution of MRE strength (p-value describing similarity to canonical MRE) for all MREs with $p < 1e-4$ found in 400bp regions centered on MEF2D peak summits.

Figure 3.6. (Continued) MEF2D-dependent regulatory elements are enriched for conserved MREs



regulation. Overall, this is a ten-fold enrichment for functional enhancers as compared to the 2003 total MEF2D-bound enhancers originally observed.

These analyses are significant as they make it possible to identify which MEF2D-bound enhancers are relevant for driving photoreceptor-specific gene expression. At the same time, these results provide insight into why transcription factors act specifically upon particular target genes rather than other genes near their binding sites. MEF2D binds many areas in the retinal genome, but only a subset of these sites are highly active. Among all MEF2D sites the highly active enhancers are characterized by the enrichment of additional transcription factor motifs, especially motifs for RORA/B and CRX, suggesting that these three factors work together as a suite of transcriptional regulators to coordinate photoreceptor development. This hypothesis is strengthened by the fact that MEF2D, RORB and CRX KO mice all share very similar phenotypes, a failure of retinal photoreceptor outer segment formation. Finally, among all active, MEF2D-bound elements, only a subset of these sites is dependent on MEF2D for activity and for the expression of their target genes. Together these results demonstrate that the function of a transcription factor is regulated at many levels and is strongly influenced by the transcription factor milieu of the cell.

3.4 Discussion

The function of the majority of TF binding in the regulation of programs of gene expression persists as an unsolved problem in the field of Transcription Regulation. Here we demonstrate that at a given time point only a minority of total TF-bound enhancers are active. Furthermore, only a fraction of those active regulatory elements require that TF for their activity. Not only does this identify which TF-binding sites are ultimately relevant for gene expression, but this also points to an *in vivo* mechanism for transcription factor function. In the case of MEF2D, we see that this broadly expressed transcription factor achieves its tissue specific function by regulating the activity of a relatively small number of enhancers in a manner upstream of histone acetylation and eRNA production.

Data examining TF binding is subject to experimental noise and artifact, where ChIP-seq reads do not reflect true TF occupancy. In the previous chapter we demonstrated that significant artifacts exist in assessing MEF2D binding genome-wide that could only be distinguished with careful KO studies, where only ~ 20% of our peaks reflected reproducible TF binding. This may suggest that ChIP-Seq studies performed without biological replicates or knockout controls are subject to a considerable percentage of false positive binding sites which may account for some of the discrepancy between number of TF binding sites and misregulated genes.

Of the regulatory elements where MEF2D truly binds, we found that still only a subset was actively engaged in gene regulation under our experimental conditions (**Figure 3.2**). It has been suggested that many of the smaller binding sites seen in ChIP-Seq do not affect gene expression, and instead reflect TF searching patterns, or nonproductive collisions with DNA

(Fisher et al., 2012). However, even when controlling for peak size we still find both active and inactive MEF2D-bound enhancers (**Figure 3.5**).

These inactive MEF2D-bound enhancers may only appear non-functional because MEF2D may be docked at inactive sites in anticipation of a future activation of the enhancer. Enhancer elements have recently been found to be highly dynamic over development (Nord et al., 2013). Additionally, MEF2 TFs are transcriptionally activated in response to specific stimuli in other paradigms (Flavell et al., 2008; Youn and Liu, 2000). TFs may bind to enhancers before their engagement in gene regulation, and the developmental snapshot we see with ChIP-seq and RNA-seq at p11 may capture this transitional period.

Alternatively, these inactive MEF2D-bound enhancers may never be active in the developing retina. One explanation for this would be that the amount of steady-state TF occupancy, as assessed by conventional ChIP, may not be as effective for identifying functional sites as competitive ChIP experiments which measure TF binding kinetics (Lickwar et al., 2012). A different, intriguing possibility is that sites of MEF2D binding that are not functional may be examples of evolving DNA regulatory elements, where MEF2D binding is insufficient for regulatory element activation but new DNA mutations at this site that promote the binding of other TF co-factors may license the enhancer to engage in regulating gene expression.

A significant number of MEF2D-bound enhancers are however active. We examined the function of MEF2D at these enhancers by evaluating changes in enhancer activity in *Mef2d* KO retinae. We found that many MEF2D-bound enhancers that are active do not lose activity in MEF2D KO retinae, suggesting that MEF2D may play a role at these enhancers but is not necessary for their activation (**Figure 3.6**). This may be due to redundancies for TF function

within a given enhancer, where the loss of a single TF may not be sufficient to disrupt the activity of that enhancer. Alternatively, it may be that MEF2D is important at all active enhancers where it has a function that is not read out by changes in H3K27 acetylation or eRNA production, for example facilitating long-range DNA interactions. Enhancers proximal to MEF2D target genes but not bound to MEF2D often lose marks of activity in *Mef2d* KO retinae, suggesting that multiple enhancers, not all directly bound by MEF2D, may be interacting to promote the expression of a target gene.

Redundancies between enhancers to ensure robust gene expression may account for why loss of activity at some MEF2D-bound enhancers may not correlate with changes in proximal gene expression, as 230 MEF2D-dependent enhancers is still greater than the 75 enhancers proximal to highly misregulated genes. Some enhancers may lose activity in the MEF2D KO, but fail to change target gene expression because of compensation by neighboring enhancers, or the emergence of normally inactive shadow enhancers (Spitz and Furlong, 2012). This remains an open question and will require more computational analyses as well as techniques to identify long-range interactions (e.g. Hi-C) to identify the cohort of enhancers regulating any given gene, and how this changes in MEF2D KO retinae. Identification of long-range interactions will also be important for identifying the cases where MEF2D dependent enhancers are critical for the expression of genes that are not their nearest neighbor.

An alternate explanation for why all 230 MEF2D-dependent enhancers are not proximal to MEF2D target genes is that loss of function in some MEF2D-dependent enhancers may produce only subtle changes in gene expression. Approximately 40% of the genes near MEF2D-dependent enhancers were changed by only 10-50%, and thus would not have met our two-fold

cutoff for potential MEF2D target genes. Evaluating small changes in gene expression is challenging in the face of biological and technical noise in any series of experiments, and likely leads to an underestimate of genes regulated by any given TF. In general, restricting future analyses to genes proximal to TF-dependent enhancers and promoters may facilitate the identification of direct target genes that only have small changes in expression upon TF loss-of-function. These genes can then be examined more closely and assessed for biological relevance.

3.5 Experimental Procedures

Histone mark Chromatin Immunoprecipitation, Sequencing and Data processing

H3K27Ac ChIP-Seq data was described previously (Chapter 2). ChIP was performed for other histone marks in the same manner as described in Chapter 2. Antibodies used were anti-H3 (Abcam ab1791), anti-H3K4me1 (Abcam ab8895) and anti-H3K4me3 (Abcam ab8580).

Previously published ChIP-Seq data sets

In addition to ChIP-Sequencing data we generated, DNase-Seq data from 8 week old C5JBL/6 mice was used from the ENCODE consortium (GSM1014175) (Landt et al., 2012).

ChIP- and RNA-Seq analyses

In general, analyses were performed as previously described (Chapter 2) with the specifications described below.

Differential motif enrichment (Homer 4.1; (Heinz et al., 2010)) as well as analysis of similarity of MRE motifs to canonical MRE (FIMO; (Bailey et al., 2009)) were performed for 400bp regions centered around the summits of MEF2D peaks for each group being compared. For FIMO, the MRE closest to the peak summit was used in the analysis.

Size normalization of peak subsets was performed by ranking all active and inactive peaks by average size of MEF2D ChIP-Seq peak size, and selecting adjacent pairs of active and inactive peaks.

Chapter 4

Conclusion

The results presented within this dissertation demonstrate a novel biological role for the MEF2 family member MEF2D in retinal photoreceptor development and present a comprehensive, in-depth approach to investigating the function of this TF. In this dissertation, we were able to take advantage of retinal photoreceptors as a model for understanding the role of MEF2 in neural development as well as a model in which to study the mechanisms by which MEF2D regulates target genes in the nervous system.

In Chapter 2, we identified a cell-autonomous role for MEF2D in the development of retinal photoreceptors, and elucidated a detailed mechanism for how MEF2D functions in photoreceptors. Using genome-wide loss-of-function experiments, we found that MEF2D regulates critical genes for photoreceptor development together with a novel co-factor, CRX. CRX both facilitates MEF2D binding to retina-specific enhancers and serves as a co-activator at a subset of MEF2D-bound regulatory elements proximal to target genes. Furthermore, together MEF2D and CRX regulate many critical genes and their loss-of-function leads to similar defects in photoreceptor differentiation. How MEF2D and CRX cooperate remains an open question. They may interact directly, or through a third co-factor such as p300, as discussed in Chapter 2. Alternatively, they may each make distinct contributions to the activation of their co-bound enhancers by performing separate but complementary functions, such as nucleosome remodeling, recruitment of histone acetyltransferases (HATs), or DNA looping. Future experiments to investigate these possibilities will provide greater insight into how photoreceptor-specific gene expression is established, as well as what the key role of these TFs is at their bound regulatory elements. There are several components to enhancer activation such as nucleosome remodeling, histone methylation, RNA polymerase II binding, recruitment of histone acetyltransferases (HATs) and histone acetylation, eRNA production and DNA looping to a promoter (Lam et al.,

2014). The precise order of these molecular events is unknown, and how TFs differentially contribute to these steps remains to be determined. Here, we have demonstrated that a subset of enhancers that lose MEF2D lose H3K27 acetylation and eRNA production. This provides an opportunity to evaluate how these activation components reflect the stage of enhancer activation. For example, some models have proposed that eRNAs facilitate DNA looping between enhancers and promoters (Li et al., 2013), and so one hypothesis would be that enhancers that have lost eRNAs no longer interact with the promoters of their target genes or other enhancers, which could be evaluated by chromosome conformation capture (Miele and Dekker, 2009). On the other hand, RNA polymerase II binding is thought to occur at poised enhancers and to precede eRNA production (Lam et al., 2014), so RNA polymerase II levels at these enhancers would not be expected to be affected. This could be evaluated by ChIP.

These latter analyses to dissect the mechanics of enhancer activation may benefit most from the complementary approach taken in Chapter 3 to studying the function of MEF2D in photoreceptors. While in Chapter 2 we focused on how MEF2D regulates the expression of critical target genes, in Chapter 3 we approach the function of MEF2D from the perspective of how it might be functioning at its numerous binding sites at regulatory elements genome-wide. We find that MEF2D binds many regulatory elements lacking marks of activity, and that MEF2D is not critical for enhancer activity at most of the elements where it is active. Exploring what differentiates these classes of MEF2D-bound enhancers suggested that even though some enhancers are inactive, they are still likely important sites of binding as they are highly enriched for MREs. Active enhancers in particular are enriched for motifs for photoreceptor network TFs, reinforcing the critical role MEF2D may play in this network. However, there is still a great deal to be explored regarding the differences between these classes of enhancers. For example, there

is likely to be heterogeneity among the state of enhancers within the subset of those that are inactive. Some may be poised for activity, with open chromatin and bound to RNA polymerase II. On the other hand it may be that MEF2D can also bind to closed chromatin and some of these may be inaccessible with repressive histone marks, with an unclear role in direct regulation of gene expression.

Ultimately, both approaches in Chapters 2 and 3 demonstrate that a small subset of MEF2D-bound enhancers are activated by MEF2D, and that these are enriched for regulatory elements proximal to significantly misregulated target genes. In considering the discrepancy between numerous TF binding sites and limited gene regulation, for MEF2D it seems that selective enhancer regulation will be a significant mechanism of specifying this function.

It will be interesting to examine whether the correlation between MEF2D binding and function at regulatory elements is similar to the relationship between CRX binding and regulatory element activation. CRX has been suggested to help remodel and open up chromatin to allow the binding of several other TFs such as NRL and NR2E3 (Peng and Chen, 2007), which suggests that it may play an early critical role in activating enhancers, and that sites of CRX binding may be more dependent on CRX for activation than what is seen for MEF2D. Preliminary data suggests that this is indeed the case, as more CRX-bound enhancers lose eRNAs in *Crx* KO retinae than MEF2D-bound enhancers in *Mef2d* KO retinae, consistent with the observation that more genes are misregulated in *Crx* KO retinae as well (M.M.A and T.J.C, unpublished observations). Loss of CRX also leads to an upregulation of eRNAs at some enhancers, which is consistent with loss of CRX also producing an increase in expression of

some genes (M.M.A and T.J.C, unpublished observations). Thus, enhancer activation levels and gene expression levels are likely the most consistent correlation in determining a TF's function.

These results provide a roadmap for determining the in vivo function of a TF in a relevant biological context. They also reflect the complexity of transcriptional regulation and the caution with which the study of transcriptional regulation should be approached. The specific function of a TF is regulated at many levels. Not all MREs bind MEF2, and MEF2 binding does not equal function, and even correlation between enhancer activity (H3K27Ac, eRNAs) and MEF2 binding does not imply that that transcription factor is required for functional activity of a given enhancer. Adding an assessment of how a TF affects enhancer activity by levels of H3K27Ac and eRNAs in future genome-wide studies of mechanisms of gene regulation will greatly facilitate our understanding of the role TFs play in complex gene regulatory networks.

Finally, an important aspect of this and similar studies is its relevance to genetic diseases arising from mutations in non-coding regions. Examples of non-coding mutations that affect TF binding sites are increasingly being documented (Cichocki et al., 2014; Gurnett et al., 2007; Smith and Shilatifard, 2014). For example, a recent study isolated a non-coding mutation in the first intron of *Munc13-4*, a gene previously shown to be mutated in familial hemophagocytic lymphohistiocytosis (FHL) (Cichocki et al., 2014). This point mutation disrupts the binding site for the transcription factor ELF1 and affects ELF1 binding and thus the activation of a stimulus-dependent, lymphocyte-specific alternate promoter for a different isoform of *Munc13-4*. While coding mutations in *Munc13-4* are known to exist in FHL (Sieni et al., 2014), this and other studies reflect the isolation of an emerging class of genetic diseases termed enhanceropathies (Smith and Shilatifard, 2014).

One advantage that facilitated the identification of this regulatory element mutation in *Munc13-4* was that the mutation was present within the gene locus itself, albeit in an intron. Disease mutations at extragenic regulatory regions may be quite far away from the genes they regulate (Gurnett et al., 2007). Identifying relevant regulatory elements will significantly aid in the discovery and characterization of such enhanceropathies. To this end, the analysis presented here cataloged a set of active enhancers in the developing retina and evaluated the contributions of the highly conserved TFs MEF2D and CRX in the activity of these enhancers as linked to changes in gene expression. As MEF2D and CRX have known DNA binding motifs, their motifs in these enhancers represent specific sequences of DNA that, if mutated, would be predicted to affect MEF2D or CRX binding, enhancer function and nearby gene expression. This may cause or increase relative risk for retinal disease.

Similar future studies that identify functional regulatory elements in neurons will provide two distinct advantages in the search for noncoding mutations in patients with neurological diseases. First, they narrow the regions of interest within the genome significantly, possibly allowing targeted sequencing in patients without the need of costly whole genome sequencing. Secondly, knowing how these enhancers are normally regulated facilitates distinguishing neutral mutations from possibly important point mutations that could damage TF binding and subsequent enhancer activation. Thus isolating regions of possible disease-associated mutations may have important implications for finding new mechanisms of retinal and more broadly neurological development and disease.

Bibliography

- Akhtar, M.W., Kim, M.S., Adachi, M., Morris, M.J., Qi, X., Richardson, J.A., Bassel-Duby, R., Olson, E.N., Kavalali, E.T., and Monteggia, L.M. (2012). In vivo analysis of MEF2 transcription factors in synapse regulation and neuronal survival. *PLoS One* 7, e34863.
- Amiel, J., Rio, M., de Pontual, L., Redon, R., Malan, V., Boddaert, N., Plouin, P., Carter, N.P., Lyonnet, S., Munnich, A., *et al.* (2007). Mutations in TCF4, encoding a class I basic helix-loop-helix transcription factor, are responsible for Pitt-Hopkins syndrome, a severe epileptic encephalopathy associated with autonomic dysfunction. *Am J Hum Genet* 80, 988-993.
- Amir, R.E., Van den Veyver, I.B., Wan, M., Tran, C.Q., Francke, U., and Zoghbi, H.Y. (1999). Rett syndrome is caused by mutations in X-linked MECP2, encoding methyl-CpG-binding protein 2. *Nat Genet* 23, 185-188.
- Andres, V., Cervera, M., and Mahdavi, V. (1995). Determination of the consensus binding site for MEF2 expressed in muscle and brain reveals tissue-specific sequence constraints. *J Biol Chem* 270, 23246-23249.
- Arnold, M.A., Kim, Y., Czubyrt, M.P., Phan, D., McAnally, J., Qi, X., Shelton, J.M., Richardson, J.A., Bassel-Duby, R., and Olson, E.N. (2007). MEF2C transcription factor controls chondrocyte hypertrophy and bone development. *Dev Cell* 12, 377-389.
- Bailey, T.L., Boden, M., Buske, F.A., Frith, M., Grant, C.E., Clementi, L., Ren, J., Li, W.W., and Noble, W.S. (2009). MEME SUITE: tools for motif discovery and searching. *Nucleic Acids Res* 37, W202-208.
- Baker, C.R., Booth, L.N., Sorrells, T.R., and Johnson, A.D. (2012). Protein modularity, cooperative binding, and hybrid regulatory states underlie transcriptional network diversification. *Cell* 151, 80-95.
- Banerji, J., Rusconi, S., and Schaffner, W. (1981). Expression of a beta-globin gene is enhanced by remote SV40 DNA sequences. *Cell* 27, 299-308.
- Barbosa, A.C., Kim, M.S., Ertunc, M., Adachi, M., Nelson, E.D., McAnally, J., Richardson, J.A., Kavalali, E.T., Monteggia, L.M., Bassel-Duby, R., *et al.* (2008). MEF2C, a transcription factor that facilitates learning and memory by negative regulation of synapse numbers and function. *Proc Natl Acad Sci U S A* 105, 9391-9396.
- Bessant, D.A., Payne, A.M., Mitton, K.P., Wang, Q.L., Swain, P.K., Plant, C., Bird, A.C., Zack, D.J., Swaroop, A., and Bhattacharya, S.S. (1999). A mutation in NRL is associated with autosomal dominant retinitis pigmentosa. *Nat Genet* 21, 355-356.
- Bhagavatula, M.R., Fan, C., Shen, G.Q., Cassano, J., Plow, E.F., Topol, E.J., and Wang, Q. (2004). Transcription factor MEF2A mutations in patients with coronary artery disease. *Hum Mol Genet* 13, 3181-3188.
- Biddie, S.C., John, S., Sabo, P.J., Thurman, R.E., Johnson, T.A., Schiltz, R.L., Miranda, T.B., Sung, M.H., Trump, S., Lightman, S.L., *et al.* (2011). Transcription factor AP1 potentiates chromatin accessibility and glucocorticoid receptor binding. *Mol Cell* 43, 145-155.

- Bienvenu, T., Diebold, B., Chelly, J., and Isidor, B. (2013). Refining the phenotype associated with MEF2C point mutations. *Neurogenetics* *14*, 71-75.
- Biggin, M.D. (2011). Animal transcription networks as highly connected, quantitative continua. *Dev Cell* *21*, 611-626.
- Black, B.L., and Cripps, R.M. (2010). Myocyte Enhancer Factor 2 Transcription Factors in Heart Development and Disease. In *Heart Development and Regeneration*, N. Rosenthal, and R.P. Harvey, eds. (Academic Press), pp. 673-699.
- Black, B.L., Ligon, K.L., Zhang, Y., and Olson, E.N. (1996). Cooperative transcriptional activation by the neurogenic basic helix-loop-helix protein MASH1 and members of the myocyte enhancer factor-2 (MEF2) family. *J Biol Chem* *271*, 26659-26663.
- Black, B.L., and Olson, E.N. (1998). Transcriptional control of muscle development by myocyte enhancer factor-2 (MEF2) proteins. *Annu Rev Cell Dev Biol* *14*, 167-196.
- Blaeser, F., Ho, N., Prywes, R., and Chatila, T.A. (2000). Ca²⁺-dependent gene expression mediated by MEF2 transcription factors. *J Biol Chem* *275*, 197-209.
- Boncinelli, E., Mallamaci, A., and Lavorgna, G. (1994). Vertebrate homeobox genes. *Genetica* *94*, 127-140.
- Bour, B.A., O'Brien, M.A., Lockwood, W.L., Goldstein, E.S., Bodmer, R., Taghert, P.H., Abmayr, S.M., and Nguyen, H.T. (1995). Drosophila MEF2, a transcription factor that is essential for myogenesis. *Genes Dev* *9*, 730-741.
- Boyl, P.P., Signore, M., Annino, A., Barbera, J.P., Acampora, D., and Simeone, A. (2001). Otx genes in the development and evolution of the vertebrate brain. *International journal of developmental neuroscience : the official journal of the International Society for Developmental Neuroscience* *19*, 353-363.
- Brewster, R.C., Weinert, F.M., Garcia, H.G., Song, D., Rydenfelt, M., and Phillips, R. (2014). The transcription factor titration effect dictates level of gene expression. *Cell* *156*, 1312-1323.
- Brzezinski, J.A.t., Lamba, D.A., and Reh, T.A. (2010). Blimp1 controls photoreceptor versus bipolar cell fate choice during retinal development. *Development* *137*, 619-629.
- Bulger, M., and Groudine, M. (2011). Functional and mechanistic diversity of distal transcription enhancers. *Cell* *144*, 327-339.
- Buskin, J.N., and Hauschka, S.D. (1989). Identification of a myocyte nuclear factor that binds to the muscle-specific enhancer of the mouse muscle creatine kinase gene. *Mol Cell Biol* *9*, 2627-2640.
- Cante-Barrett, K., Pieters, R., and Meijerink, J.P. (2014). Myocyte enhancer factor 2C in hematopoiesis and leukemia. *Oncogene* *33*, 403-410.

- Carter-Dawson, L.D., and LaVail, M.M. (1979). Rods and cones in the mouse retina. II. Autoradiographic analysis of cell generation using tritiated thymidine. *J Comp Neurol* *188*, 263-272.
- Cepko, C.L., Austin, C.P., Yang, X., Alexiades, M., and Ezzeddine, D. (1996). Cell fate determination in the vertebrate retina. *Proc Natl Acad Sci U S A* *93*, 589-595.
- Cepko, C.L., Ryder, E., Austin, C., Golden, J., Fields-Berry, S., and Lin, J. (1998). Lineage analysis using retroviral vectors. *Methods* *14*, 393-406.
- Chan, H.M., and La Thangue, N.B. (2001). p300/CBP proteins: HATs for transcriptional bridges and scaffolds. *J Cell Sci* *114*, 2363-2373.
- Chasman, D.I., Anttila, V., Buring, J.E., Ridker, P.M., Schurks, M., Kurth, T., and International Headache Genetics, C. (2014). Selectivity in Genetic Association with Sub-classified Migraine in Women. *PLoS Genet* *10*, e1004366.
- Chen, J., Rattner, A., and Nathans, J. (2005). The rod photoreceptor-specific nuclear receptor Nr2e3 represses transcription of multiple cone-specific genes. *J Neurosci* *25*, 118-129.
- Chen, J., Zhang, Z., Li, L., Chen, B.C., Revyakin, A., Hajj, B., Legant, W., Dahan, M., Lionnet, T., Betzig, E., *et al.* (2014). Single-molecule dynamics of enhanceosome assembly in embryonic stem cells. *Cell* *156*, 1274-1285.
- Chen, S., Wang, Q.L., Nie, Z., Sun, H., Lennon, G., Copeland, N.G., Gilbert, D.J., Jenkins, N.A., and Zack, D.J. (1997). Crx, a novel Otx-like paired-homeodomain protein, binds to and transactivates photoreceptor cell-specific genes. *Neuron* *19*, 1017-1030.
- Chen, S.X., Cherry, A., Tari, P.K., Podgorski, K., Kwong, Y.K., and Haas, K. (2012). The transcription factor MEF2 directs developmental visually driven functional and structural metaplasticity. *Cell* *151*, 41-55.
- Cherry, T.J., Wang, S., Bormuth, I., Schwab, M., Olson, J., and Cepko, C.L. (2011). NeuroD factors regulate cell fate and neurite stratification in the developing retina. *J Neurosci* *31*, 7365-7379.
- Cho, E.G., Zaremba, J.D., McKercher, S.R., Talantova, M., Tu, S., Masliah, E., Chan, S.F., Nakanishi, N., Terskikh, A., and Lipton, S.A. (2011). MEF2C enhances dopaminergic neuron differentiation of human embryonic stem cells in a parkinsonian rat model. *PLoS One* *6*, e24027.
- Cichocki, F., Schlums, H., Li, H., Stache, V., Holmes, T., Lenvik, T.R., Chiang, S.C., Miller, J.S., Meeths, M., Anderson, S.K., *et al.* (2014). Transcriptional regulation of Munc13-4 expression in cytotoxic lymphocytes is disrupted by an intronic mutation associated with a primary immunodeficiency. *J Exp Med* *211*, 1079-1091.
- Cohen, A.I., Todd, R.D., Harmon, S., and O'Malley, K.L. (1992). Photoreceptors of mouse retinas possess D4 receptors coupled to adenylate cyclase. *Proc Natl Acad Sci U S A* *89*, 12093-12097.

- Cole, C.J., Mercaldo, V., Restivo, L., Yiu, A.P., Sekeres, M.J., Han, J.H., Vetere, G., Pekar, T., Ross, P.J., Neve, R.L., *et al.* (2012). MEF2 negatively regulates learning-induced structural plasticity and memory formation. *Nat Neurosci* *15*, 1255-1264.
- Coppieters, F., Leroy, B.P., Beysen, D., Hellemans, J., De Bosscher, K., Haegeman, G., Robberecht, K., Wuyts, W., Coucke, P.J., and De Baere, E. (2007). Recurrent mutation in the first zinc finger of the orphan nuclear receptor NR2E3 causes autosomal dominant retinitis pigmentosa. *Am J Hum Genet* *81*, 147-157.
- Corbo, J.C., Lawrence, K.A., Karlstetter, M., Myers, C.A., Abdelaziz, M., Dirkes, W., Weigelt, K., Seifert, M., Benes, V., Fritsche, L.G., *et al.* (2010). CRX CHIP-seq reveals the cis-regulatory architecture of mouse photoreceptors. *Genome research* *20*, 1512-1525.
- Cosgrove, D., and Zallocchi, M. (2014). Usher protein functions in hair cells and photoreceptors. *Int J Biochem Cell Biol* *46*, 80-89.
- Creyghton, M.P., Cheng, A.W., Welstead, G.G., Kooistra, T., Carey, B.W., Steine, E.J., Hanna, J., Lodato, M.A., Frampton, G.M., Sharp, P.A., *et al.* (2010). Histone H3K27ac separates active from poised enhancers and predicts developmental state. *Proc Natl Acad Sci U S A* *107*, 21931-21936.
- Cunha, P.M., Sandmann, T., Gustafson, E.H., Ciglar, L., Eichenlaub, M.P., and Furlong, E.E. (2010). Combinatorial binding leads to diverse regulatory responses: Lmd is a tissue-specific modulator of Mef2 activity. *PLoS Genet* *6*, e1001014.
- Daiger, S.P., Sullivan, L.S., and Bowne, S.J. (2013). Genes and mutations causing retinitis pigmentosa. *Clinical genetics* *84*, 132-141.
- Dasen, J.S., and Jessell, T.M. (2009). Hox networks and the origins of motor neuron diversity. *Current topics in developmental biology* *88*, 169-200.
- Davis, R.L., Cheng, P.F., Lassar, A.B., and Weintraub, H. (1990). The MyoD DNA binding domain contains a recognition code for muscle-specific gene activation. *Cell* *60*, 733-746.
- Davis, R.L., Weintraub, H., and Lassar, A.B. (1987). Expression of a single transfected cDNA converts fibroblasts to myoblasts. *Cell* *51*, 987-1000.
- De Luca, A., Severino, A., De Paolis, P., Cottone, G., De Luca, L., De Falco, M., Porcellini, A., Volpe, M., and Condorelli, G. (2003). p300/cAMP-response-element-binding-protein ('CREB')-binding protein (CBP) modulates co-operation between myocyte enhancer factor 2A (MEF2A) and thyroid hormone receptor-retinoid X receptor. *Biochem J* *369*, 477-484.
- Della Gaspera, B., Armand, A.S., Lecolle, S., Charbonnier, F., and Chanoine, C. (2012). Mef2d acts upstream of muscle identity genes and couples lateral myogenesis to dermomyotome formation in *Xenopus laevis*. *PLoS One* *7*, e52359.

Dennis, G., Jr., Sherman, B.T., Hosack, D.A., Yang, J., Gao, W., Lane, H.C., and Lempicki, R.A. (2003). DAVID: Database for Annotation, Visualization, and Integrated Discovery. *Genome biology* 4, P3.

Downes, S.M., Holder, G.E., Fitzke, F.W., Payne, A.M., Warren, M.J., Bhattacharya, S.S., and Bird, A.C. (2001). Autosomal dominant cone and cone-rod dystrophy with mutations in the guanylate cyclase activator 1A gene-encoding guanylate cyclase activating protein-1. *Archives of ophthalmology* 119, 96-105.

Du, M., Perry, R.L., Nowacki, N.B., Gordon, J.W., Salma, J., Zhao, J., Aziz, A., Chan, J., Siu, K.W., and McDermott, J.C. (2008). Protein kinase A represses skeletal myogenesis by targeting myocyte enhancer factor 2D. *Mol Cell Biol* 28, 2952-2970.

Edmondson, D.G., Cheng, T.C., Cserjesi, P., Chakraborty, T., and Olson, E.N. (1992). Analysis of the myogenin promoter reveals an indirect pathway for positive autoregulation mediated by the muscle-specific enhancer factor MEF-2. *Mol Cell Biol* 12, 3665-3677.

Edmondson, D.G., and Olson, E.N. (1989). A gene with homology to the myc similarity region of MyoD1 is expressed during myogenesis and is sufficient to activate the muscle differentiation program. *Genes Dev* 3, 628-640.

Esau, C., Boes, M., Youn, H.D., Tattersson, L., Liu, J.O., and Chen, J. (2001). Deletion of calcineurin and myocyte enhancer factor 2 (MEF2) binding domain of Cabin1 results in enhanced cytokine gene expression in T cells. *J Exp Med* 194, 1449-1459.

Escher, P., Schorderet, D.F., and Cottet, S. (2011). Altered expression of the transcription factor Mef2c during retinal degeneration in Rpe65^{-/-} mice. *Invest Ophthalmol Vis Sci* 52, 5933-5940.

Fisher, W.W., Li, J.J., Hammonds, A.S., Brown, J.B., Pfeiffer, B.D., Weiszmann, R., MacArthur, S., Thomas, S., Stamatoyannopoulos, J.A., Eisen, M.B., *et al.* (2012). DNA regions bound at low occupancy by transcription factors do not drive patterned reporter gene expression in *Drosophila*. *Proc Natl Acad Sci U S A* 109, 21330-21335.

Flavell, S.W., Cowan, C.W., Kim, T.K., Greer, P.L., Lin, Y., Paradis, S., Griffith, E.C., Hu, L.S., Chen, C., and Greenberg, M.E. (2006). Activity-dependent regulation of MEF2 transcription factors suppresses excitatory synapse number. *Science* 311, 1008-1012.

Flavell, S.W., Kim, T.K., Gray, J.M., Harmin, D.A., Hemberg, M., Hong, E.J., Markenscoff-Papadimitriou, E., Bear, D.M., and Greenberg, M.E. (2008). Genome-wide analysis of MEF2 transcriptional program reveals synaptic target genes and neuronal activity-dependent polyadenylation site selection. *Neuron* 60, 1022-1038.

Freilinger, T., Anttila, V., de Vries, B., Malik, R., Kallela, M., Terwindt, G.M., Pozo-Rosich, P., Winsvold, B., Nyholt, D.R., van Oosterhout, W.P., *et al.* (2012). Genome-wide association analysis identifies susceptibility loci for migraine without aura. *Nat Genet* 44, 777-782.

Freund, C.L., Gregory-Evans, C.Y., Furukawa, T., Papaioannou, M., Looser, J., Ploder, L., Bellingham, J., Ng, D., Herbrick, J.A., Duncan, A., *et al.* (1997). Cone-rod dystrophy due to

mutations in a novel photoreceptor-specific homeobox gene (CRX) essential for maintenance of the photoreceptor. *Cell* *91*, 543-553.

Fuchs, S., Nakazawa, M., Maw, M., Tamai, M., Oguchi, Y., and Gal, A. (1995). A homozygous 1-base pair deletion in the arrestin gene is a frequent cause of Oguchi disease in Japanese. *Nat Genet* *10*, 360-362.

Furukawa, T., Morrow, E.M., and Cepko, C.L. (1997). Crx, a novel otx-like homeobox gene, shows photoreceptor-specific expression and regulates photoreceptor differentiation. *Cell* *91*, 531-541.

Furukawa, T., Morrow, E.M., Li, T., Davis, F.C., and Cepko, C.L. (1999). Retinopathy and attenuated circadian entrainment in Crx-deficient mice. *Nat Genet* *23*, 466-470.

Gaudilliere, B., Shi, Y., and Bonni, A. (2002). RNA interference reveals a requirement for myocyte enhancer factor 2A in activity-dependent neuronal survival. *J Biol Chem* *277*, 46442-46446.

Gerber, S., Rozet, J.M., Takezawa, S.I., dos Santos, L.C., Lopes, L., Gribouval, O., Penet, C., Perrault, I., Ducroq, D., Souied, E., *et al.* (2000). The photoreceptor cell-specific nuclear receptor gene (PNR) accounts for retinitis pigmentosa in the Crypto-Jews from Portugal (Marranos), survivors from the Spanish Inquisition. *Hum Genet* *107*, 276-284.

Gertz, J., Savic, D., Varley, K.E., Partridge, E.C., Safi, A., Jain, P., Cooper, G.M., Reddy, T.E., Crawford, G.E., and Myers, R.M. (2013). Distinct properties of cell-type-specific and shared transcription factor binding sites. *Mol Cell* *52*, 25-36.

Gong, X., Tang, X., Wiedmann, M., Wang, X., Peng, J., Zheng, D., Blair, L.A., Marshall, J., and Mao, Z. (2003). Cdk5-mediated inhibition of the protective effects of transcription factor MEF2 in neurotoxicity-induced apoptosis. *Neuron* *38*, 33-46.

Gossett, L.A., Kelvin, D.J., Sternberg, E.A., and Olson, E.N. (1989). A new myocyte-specific enhancer-binding factor that recognizes a conserved element associated with multiple muscle-specific genes. *Mol Cell Biol* *9*, 5022-5033.

Gramzow, L., and Theissen, G. (2010). A hitchhiker's guide to the MADS world of plants. *Genome biology* *11*, 214.

Gurnett, C.A., Bowcock, A.M., Dietz, F.R., Morcuende, J.A., Murray, J.C., and Dobbs, M.B. (2007). Two novel point mutations in the long-range SHH enhancer in three families with triphalangeal thumb and preaxial polydactyly. *Am J Med Genet A* *143*, 27-32.

Haberland, M., Arnold, M.A., McAnally, J., Phan, D., Kim, Y., and Olson, E.N. (2007). Regulation of HDAC9 gene expression by MEF2 establishes a negative-feedback loop in the transcriptional circuitry of muscle differentiation. *Mol Cell Biol* *27*, 518-525.

- Haider, N.B., Jacobson, S.G., Cideciyan, A.V., Swiderski, R., Streb, L.M., Searby, C., Beck, G., Hockey, R., Hanna, D.B., Gorman, S., *et al.* (2000). Mutation of a nuclear receptor gene, NR2E3, causes enhanced S cone syndrome, a disorder of retinal cell fate. *Nat Genet* 24, 127-131.
- Hao, H., Kim, D.S., Klocke, B., Johnson, K.R., Cui, K., Gotoh, N., Zang, C., Gregorski, J., Gieser, L., Peng, W., *et al.* (2012). Transcriptional regulation of rod photoreceptor homeostasis revealed by in vivo NRL targetome analysis. *PLoS Genet* 8, e1002649.
- Hao, H., Tummala, P., Guzman, E., Mali, R.S., Gregorski, J., Swaroop, A., and Mitton, K.P. (2011). The transcription factor neural retina leucine zipper (NRL) controls photoreceptor-specific expression of myocyte enhancer factor Mef2c from an alternative promoter. *J Biol Chem* 286, 34893-34902.
- Hatakeyama, J., Tomita, K., Inoue, T., and Kageyama, R. (2001). Roles of homeobox and bHLH genes in specification of a retinal cell type. *Development* 128, 1313-1322.
- He, A., Kong, S.W., Ma, Q., and Pu, W.T. (2011). Co-occupancy by multiple cardiac transcription factors identifies transcriptional enhancers active in heart. *Proc Natl Acad Sci U S A* 108, 5632-5637.
- Heidenreich, K.A., and Linseman, D.A. (2004). Myocyte enhancer factor-2 transcription factors in neuronal differentiation and survival. *Mol Neurobiol* 29, 155-166.
- Heintzman, N.D., Stuart, R.K., Hon, G., Fu, Y., Ching, C.W., Hawkins, R.D., Barrera, L.O., Van Calcar, S., Qu, C., Ching, K.A., *et al.* (2007). Distinct and predictive chromatin signatures of transcriptional promoters and enhancers in the human genome. *Nat Genet* 39, 311-318.
- Heinz, S., Benner, C., Spann, N., Bertolino, E., Lin, Y.C., Laslo, P., Cheng, J.X., Murre, C., Singh, H., and Glass, C.K. (2010). Simple combinations of lineage-determining transcription factors prime cis-regulatory elements required for macrophage and B cell identities. *Mol Cell* 38, 576-589.
- Hobert, O. (2008). Regulatory logic of neuronal diversity: terminal selector genes and selector motifs. *Proc Natl Acad Sci U S A* 105, 20067-20071.
- Hong, E.J., McCord, A.E., and Greenberg, M.E. (2008). A biological function for the neuronal activity-dependent component of Bdnf transcription in the development of cortical inhibition. *Neuron* 60, 610-624.
- Hsiau, T.H., Diaconu, C., Myers, C.A., Lee, J., Cepko, C.L., and Corbo, J.C. (2007). The cis-regulatory logic of the mammalian photoreceptor transcriptional network. *PLoS One* 2, e643.
- Huang da, W., Sherman, B.T., and Lempicki, R.A. (2009a). Bioinformatics enrichment tools: paths toward the comprehensive functional analysis of large gene lists. *Nucleic Acids Res* 37, 1-13.
- Huang da, W., Sherman, B.T., and Lempicki, R.A. (2009b). Systematic and integrative analysis of large gene lists using DAVID bioinformatics resources. *Nat Protoc* 4, 44-57.

- Huang, J., Weintraub, H., and Kedes, L. (1998). Intramolecular regulation of MyoD activation domain conformation and function. *Mol Cell Biol* *18*, 5478-5484.
- Ikeshima, H., Imai, S., Shimoda, K., Hata, J., and Takano, T. (1995). Expression of a MADS box gene, MEF2D, in neurons of the mouse central nervous system: implication of its binary function in myogenic and neurogenic cell lineages. *Neurosci Lett* *200*, 117-120.
- Irwin, S.A., Patel, B., Idupulapati, M., Harris, J.B., Crisostomo, R.A., Larsen, B.P., Kooy, F., Willems, P.J., Cras, P., Kozlowski, P.B., *et al.* (2001). Abnormal dendritic spine characteristics in the temporal and visual cortices of patients with fragile-X syndrome: a quantitative examination. *Am J Med Genet* *98*, 161-167.
- Jeon, C.J., Strettoi, E., and Masland, R.H. (1998). The major cell populations of the mouse retina. *J Neurosci* *18*, 8936-8946.
- Jia, L., Oh, E.C., Ng, L., Srinivas, M., Brooks, M., Swaroop, A., and Forrest, D. (2009). Retinoid-related orphan nuclear receptor RORbeta is an early-acting factor in rod photoreceptor development. *Proc Natl Acad Sci U S A* *106*, 17534-17539.
- Johnson, D.S., Mortazavi, A., Myers, R.M., and Wold, B. (2007). Genome-wide mapping of in vivo protein-DNA interactions. *Science* *316*, 1497-1502.
- Junion, G., Spivakov, M., Girardot, C., Braun, M., Gustafson, E.H., Birney, E., and Furlong, E.E. (2012). A transcription factor collective defines cardiac cell fate and reflects lineage history. *Cell* *148*, 473-486.
- Kao-Huang, Y., Revzin, A., Butler, A.P., O'Conner, P., Noble, D.W., and von Hippel, P.H. (1977). Nonspecific DNA binding of genome-regulating proteins as a biological control mechanism: measurement of DNA-bound Escherichia coli lac repressor in vivo. *Proc Natl Acad Sci U S A* *74*, 4228-4232.
- Katoh, K., Omori, Y., Onishi, A., Sato, S., Kondo, M., and Furukawa, T. (2010). Blimp1 suppresses Chx10 expression in differentiating retinal photoreceptor precursors to ensure proper photoreceptor development. *J Neurosci* *30*, 6515-6526.
- Kaushal, S., Schneider, J.W., Nadal-Ginard, B., and Mahdavi, V. (1994). Activation of the myogenic lineage by MEF2A, a factor that induces and cooperates with MyoD. *Science* *266*, 1236-1240.
- Kim, T.K., Hemberg, M., Gray, J.M., Costa, A.M., Bear, D.M., Wu, J., Harmin, D.A., Laptewicz, M., Barbara-Haley, K., Kuersten, S., *et al.* (2010). Widespread transcription at neuronal activity-regulated enhancers. *Nature* *465*, 182-187.
- Kim, Y., Phan, D., van Rooij, E., Wang, D.Z., McAnally, J., Qi, X., Richardson, J.A., Hill, J.A., Bassel-Duby, R., and Olson, E.N. (2008). The MEF2D transcription factor mediates stress-dependent cardiac remodeling in mice. *J Clin Invest* *118*, 124-132.

- Kohl, S., Coppieters, F., Meire, F., Schaich, S., Roosing, S., Brennenstuhl, C., Bolz, S., van Genderen, M.M., Riemsdag, F.C., European Retinal Disease, C., *et al.* (2012). A nonsense mutation in PDE6H causes autosomal-recessive incomplete achromatopsia. *Am J Hum Genet* *91*, 527-532.
- Kolpakova, A., Katz, S., Keren, A., Rojtlat, A., and Bengal, E. (2013). Transcriptional regulation of mesoderm genes by MEF2D during early *Xenopus* development. *PLoS One* *8*, e69693.
- Lam, B.Y., and Chawla, S. (2007). MEF2D expression increases during neuronal differentiation of neural progenitor cells and correlates with neurite length. *Neurosci Lett* *427*, 153-158.
- Lam, M.T., Li, W., Rosenfeld, M.G., and Glass, C.K. (2014). Enhancer RNAs and regulated transcriptional programs. *Trends in biochemical sciences* *39*, 170-182.
- Landt, S.G., Marinov, G.K., Kundaje, A., Kheradpour, P., Pauli, F., Batzoglou, S., Bernstein, B.E., Bickel, P., Brown, J.B., Cayting, P., *et al.* (2012). ChIP-seq guidelines and practices of the ENCODE and modENCODE consortia. *Genome research* *22*, 1813-1831.
- Lassar, A.B., Buskin, J.N., Lockshon, D., Davis, R.L., Apone, S., Hauschka, S.D., and Weintraub, H. (1989). MyoD is a sequence-specific DNA binding protein requiring a region of myc homology to bind to the muscle creatine kinase enhancer. *Cell* *58*, 823-831.
- Lee, Y., Nadal-Ginard, B., Mahdavi, V., and Izumo, S. (1997). Myocyte-specific enhancer factor 2 and thyroid hormone receptor associate and synergistically activate the alpha-cardiac myosin heavy-chain gene. *Mol Cell Biol* *17*, 2745-2755.
- Lettice, L.A., Heaney, S.J., Purdie, L.A., Li, L., de Beer, P., Oostra, B.A., Goode, D., Elgar, G., Hill, R.E., and de Graaff, E. (2003). A long-range *Shh* enhancer regulates expression in the developing limb and fin and is associated with preaxial polydactyly. *Hum Mol Genet* *12*, 1725-1735.
- Li, H., Radford, J.C., Ragusa, M.J., Shea, K.L., McKercher, S.R., Zaremba, J.D., Soussou, W., Nie, Z., Kang, Y.J., Nakanishi, N., *et al.* (2008a). Transcription factor MEF2C influences neural stem/progenitor cell differentiation and maturation in vivo. *Proc Natl Acad Sci U S A* *105*, 9397-9402.
- Li, W., Notani, D., Ma, Q., Tanasa, B., Nunez, E., Chen, A.Y., Merkurjev, D., Zhang, J., Ohgi, K., Song, X., *et al.* (2013). Functional roles of enhancer RNAs for oestrogen-dependent transcriptional activation. *Nature* *498*, 516-520.
- Li, Z., McKercher, S.R., Cui, J., Nie, Z., Soussou, W., Roberts, A.J., Sallmen, T., Lipton, J.H., Talantova, M., Okamoto, S., *et al.* (2008b). Myocyte enhancer factor 2C as a neurogenic and antiapoptotic transcription factor in murine embryonic stem cells. *J Neurosci* *28*, 6557-6568.
- Lickwar, C.R., Mueller, F., Hanlon, S.E., McNally, J.G., and Lieb, J.D. (2012). Genome-wide protein-DNA binding dynamics suggest a molecular clutch for transcription factor function. *Nature* *484*, 251-255.

- Lilly, B., Galewsky, S., Firulli, A.B., Schulz, R.A., and Olson, E.N. (1994). D-MEF2: a MADS box transcription factor expressed in differentiating mesoderm and muscle cell lineages during *Drosophila* embryogenesis. *Proc Natl Acad Sci U S A* *91*, 5662-5666.
- Lilly, B., Zhao, B., Ranganayakulu, G., Paterson, B.M., Schulz, R.A., and Olson, E.N. (1995). Requirement of MADS domain transcription factor D-MEF2 for muscle formation in *Drosophila*. *Science* *267*, 688-693.
- Lin, Q., Schwarz, J., Bucana, C., and Olson, E.N. (1997). Control of mouse cardiac morphogenesis and myogenesis by transcription factor MEF2C. *Science* *276*, 1404-1407.
- Lin, Y., Bloodgood, B.L., Hauser, J.L., Lapan, A.D., Koon, A.C., Kim, T.K., Hu, L.S., Malik, A.N., and Greenberg, M.E. (2008). Activity-dependent regulation of inhibitory synapse development by Npas4. *Nature* *455*, 1198-1204.
- Liu, X., Wu, B., Szary, J., Kofoed, E.M., and Schaufele, F. (2007). Functional sequestration of transcription factor activity by repetitive DNA. *J Biol Chem* *282*, 20868-20876.
- Lu, J., McKinsey, T.A., Nicol, R.L., and Olson, E.N. (2000). Signal-dependent activation of the MEF2 transcription factor by dissociation from histone deacetylases. *Proc Natl Acad Sci U S A* *97*, 4070-4075.
- Luo, D.G., Xue, T., and Yau, K.W. (2008). How vision begins: an odyssey. *Proc Natl Acad Sci U S A* *105*, 9855-9862.
- Lyons, G.E., Micales, B.K., Schwarz, J., Martin, J.F., and Olson, E.N. (1995). Expression of *mef2* genes in the mouse central nervous system suggests a role in neuronal maturation. *J Neurosci* *15*, 5727-5738.
- Lyons, M.R., Schwarz, C.M., and West, A.E. (2012). Members of the myocyte enhancer factor 2 transcription factor family differentially regulate *Bdnf* transcription in response to neuronal depolarization. *J Neurosci* *32*, 12780-12785.
- Ma, K., Chan, J.K., Zhu, G., and Wu, Z. (2005). Myocyte enhancer factor 2 acetylation by p300 enhances its DNA binding activity, transcriptional activity, and myogenic differentiation. *Mol Cell Biol* *25*, 3575-3582.
- Mao, Z., Bonni, A., Xia, F., Nadal-Vicens, M., and Greenberg, M.E. (1999). Neuronal activity-dependent cell survival mediated by transcription factor MEF2. *Science* *286*, 785-790.
- Mao, Z., and Nadal-Ginard, B. (1996). Functional and physical interactions between mammalian achaete-scute homolog 1 and myocyte enhancer factor 2A. *J Biol Chem* *271*, 14371-14375.
- Masland, R.H. (2001). The fundamental plan of the retina. *Nat Neurosci* *4*, 877-886.
- Matsuda, T., and Cepko, C.L. (2004). Electroporation and RNA interference in the rodent retina in vivo and in vitro. *Proc Natl Acad Sci U S A* *101*, 16-22.

- Matsuda, T., and Cepko, C.L. (2008). Analysis of gene function in the retina. *Methods Mol Biol* 423, 259-278.
- Mazzoni, E.O., Mahony, S., Closser, M., Morrison, C.A., Nedelec, S., Williams, D.J., An, D., Gifford, D.K., and Wichterle, H. (2013). Synergistic binding of transcription factors to cell-specific enhancers programs motor neuron identity. *Nat Neurosci* 16, 1219-1227.
- McKinsey, T.A., Zhang, C.L., Lu, J., and Olson, E.N. (2000). Signal-dependent nuclear export of a histone deacetylase regulates muscle differentiation. *Nature* 408, 106-111.
- McKinsey, T.A., Zhang, C.L., and Olson, E.N. (2002). MEF2: a calcium-dependent regulator of cell division, differentiation and death. *Trends in biochemical sciences* 27, 40-47.
- McLean, C.Y., Bristor, D., Hiller, M., Clarke, S.L., Schaar, B.T., Lowe, C.B., Wenger, A.M., and Bejerano, G. (2010). GREAT improves functional interpretation of cis-regulatory regions. *Nat Biotechnol* 28, 495-501.
- Mears, A.J., Kondo, M., Swain, P.K., Takada, Y., Bush, R.A., Saunders, T.L., Sieving, P.A., and Swaroop, A. (2001). Nrl is required for rod photoreceptor development. *Nat Genet* 29, 447-452.
- Merika, M., and Thanos, D. (2001). Enhanceosomes. *Curr Opin Genet Dev* 11, 205-208.
- Merika, M., Williams, A.J., Chen, G., Collins, T., and Thanos, D. (1998). Recruitment of CBP/p300 by the IFN beta enhanceosome is required for synergistic activation of transcription. *Mol Cell* 1, 277-287.
- Miele, A., and Dekker, J. (2009). Mapping cis- and trans- chromatin interaction networks using chromosome conformation capture (3C). *Methods Mol Biol* 464, 105-121.
- Mikkelsen, T.S., Ku, M., Jaffe, D.B., Issac, B., Lieberman, E., Giannoukos, G., Alvarez, P., Brockman, W., Kim, T.K., Koche, R.P., *et al.* (2007). Genome-wide maps of chromatin state in pluripotent and lineage-committed cells. *Nature* 448, 553-560.
- Molkentin, J.D., Black, B.L., Martin, J.F., and Olson, E.N. (1995). Cooperative activation of muscle gene expression by MEF2 and myogenic bHLH proteins. *Cell* 83, 1125-1136.
- Molkentin, J.D., Black, B.L., Martin, J.F., and Olson, E.N. (1996a). Mutational analysis of the DNA binding, dimerization, and transcriptional activation domains of MEF2C. *Mol Cell Biol* 16, 2627-2636.
- Molkentin, J.D., Li, L., and Olson, E.N. (1996b). Phosphorylation of the MADS-Box transcription factor MEF2C enhances its DNA binding activity. *J Biol Chem* 271, 17199-17204.
- Moreau, P., Hen, R., Wasylyk, B., Everett, R., Gaub, M.P., and Chambon, P. (1981). The SV40 72 base repair repeat has a striking effect on gene expression both in SV40 and other chimeric recombinants. *Nucleic Acids Res* 9, 6047-6068.

- Morin, S., Charron, F., Robitaille, L., and Nemer, M. (2000). GATA-dependent recruitment of MEF2 proteins to target promoters. *EMBO J* 19, 2046-2055.
- Morrow, E.M., Furukawa, T., Lee, J.E., and Cepko, C.L. (1999). NeuroD regulates multiple functions in the developing neural retina in rodent. *Development* 126, 23-36.
- Morrow, E.M., Yoo, S.Y., Flavell, S.W., Kim, T.K., Lin, Y., Hill, R.S., Mukaddes, N.M., Balkhy, S., Gascon, G., Hashmi, A., *et al.* (2008). Identifying autism loci and genes by tracing recent shared ancestry. *Science* 321, 218-223.
- Mullen, A.C., Orlando, D.A., Newman, J.J., Loven, J., Kumar, R.M., Bilodeau, S., Reddy, J., Guenther, M.G., DeKoter, R.P., and Young, R.A. (2011). Master transcription factors determine cell-type-specific responses to TGF-beta signaling. *Cell* 147, 565-576.
- Mylona, A., Nicolas, R., Maurice, D., Sargent, M., Tuil, D., Daegelen, D., Treisman, R., and Costello, P. (2011). The essential function for serum response factor in T-cell development reflects its specific coupling to extracellular signal-regulated kinase signaling. *Mol Cell Biol* 31, 267-276.
- Naidu, P.S., Ludolph, D.C., To, R.Q., Hinterberger, T.J., and Konieczny, S.F. (1995). Myogenin and MEF2 function synergistically to activate the MRF4 promoter during myogenesis. *Mol Cell Biol* 15, 2707-2718.
- Nakazawa, M., Wada, Y., and Tamai, M. (1998). Arrestin gene mutations in autosomal recessive retinitis pigmentosa. *Archives of ophthalmology* 116, 498-501.
- Naya, F.J., Black, B.L., Wu, H., Bassel-Duby, R., Richardson, J.A., Hill, J.A., and Olson, E.N. (2002). Mitochondrial deficiency and cardiac sudden death in mice lacking the MEF2A transcription factor. *Nat Med* 8, 1303-1309.
- Ng, L., Hurley, J.B., Dierks, B., Srinivas, M., Salto, C., Vennstrom, B., Reh, T.A., and Forrest, D. (2001). A thyroid hormone receptor that is required for the development of green cone photoreceptors. *Nat Genet* 27, 94-98.
- Nir, I., Harrison, J.M., Haque, R., Low, M.J., Grandy, D.K., Rubinstein, M., and Iuvone, P.M. (2002). Dysfunctional light-evoked regulation of cAMP in photoreceptors and abnormal retinal adaptation in mice lacking dopamine D4 receptors. *J Neurosci* 22, 2063-2073.
- Nishida, A., Furukawa, A., Koike, C., Tano, Y., Aizawa, S., Matsuo, I., and Furukawa, T. (2003). Otx2 homeobox gene controls retinal photoreceptor cell fate and pineal gland development. *Nat Neurosci* 6, 1255-1263.
- Nishiguchi, K.M., Friedman, J.S., Sandberg, M.A., Swaroop, A., Berson, E.L., and Dryja, T.P. (2004). Recessive NRL mutations in patients with clumped pigmentary retinal degeneration and relative preservation of blue cone function. *Proc Natl Acad Sci U S A* 101, 17819-17824.

- Nord, A.S., Blow, M.J., Attanasio, C., Akiyama, J.A., Holt, A., Hosseini, R., Phouanavong, S., Plajzer-Frick, I., Shoukry, M., Afzal, V., *et al.* (2013). Rapid and pervasive changes in genome-wide enhancer usage during mammalian development. *Cell* *155*, 1521-1531.
- Norman, C., Runswick, M., Pollock, R., and Treisman, R. (1988). Isolation and properties of cDNA clones encoding SRF, a transcription factor that binds to the c-fos serum response element. *Cell* *55*, 989-1003.
- Novara, F., Beri, S., Giorda, R., Ortibus, E., Nageshappa, S., Darra, F., Dalla Bernardina, B., Zuffardi, O., and Van Esch, H. (2010). Refining the phenotype associated with MEF2C haploinsufficiency. *Clinical genetics* *78*, 471-477.
- Nurrish, S.J., and Treisman, R. (1995). DNA binding specificity determinants in MADS-box transcription factors. *Mol Cell Biol* *15*, 4076-4085.
- Olney, J.W. (1968). An electron microscopic study of synapse formation, receptor outer segment development, and other aspects of developing mouse retina. *Investigative ophthalmology* *7*, 250-268.
- Ornatsky, O.I., Andreucci, J.J., and McDermott, J.C. (1997). A dominant-negative form of transcription factor MEF2 inhibits myogenesis. *J Biol Chem* *272*, 33271-33278.
- Pan, F., Ye, Z., Cheng, L., and Liu, J.O. (2004). Myocyte enhancer factor 2 mediates calcium-dependent transcription of the interleukin-2 gene in T lymphocytes: a calcium signaling module that is distinct from but collaborates with the nuclear factor of activated T cells (NFAT). *J Biol Chem* *279*, 14477-14480.
- Payne, A.M., Downes, S.M., Bessant, D.A., Taylor, R., Holder, G.E., Warren, M.J., Bird, A.C., and Bhattacharya, S.S. (1998). A mutation in guanylate cyclase activator 1A (GUCA1A) in an autosomal dominant cone dystrophy pedigree mapping to a new locus on chromosome 6p21.1. *Hum Mol Genet* *7*, 273-277.
- Peng, G.H., and Chen, S. (2007). Crx activates opsin transcription by recruiting HAT-containing co-activators and promoting histone acetylation. *Hum Mol Genet* *16*, 2433-2452.
- Pfeiffer, B.E., Zang, T., Wilkerson, J.R., Taniguchi, M., Maksimova, M.A., Smith, L.N., Cowan, C.W., and Huber, K.M. (2010). Fragile X mental retardation protein is required for synapse elimination by the activity-dependent transcription factor MEF2. *Neuron* *66*, 191-197.
- Piri, N., Gao, Y.Q., Danciger, M., Mendoza, E., Fishman, G.A., and Farber, D.B. (2005). A substitution of G to C in the cone cGMP-phosphodiesterase gamma subunit gene found in a distinctive form of cone dystrophy. *Ophthalmology* *112*, 159-166.
- Pollock, R., and Treisman, R. (1991). Human SRF-related proteins: DNA-binding properties and potential regulatory targets. *Genes Dev* *5*, 2327-2341.

- Potthoff, M.J., Arnold, M.A., McAnally, J., Richardson, J.A., Bassel-Duby, R., and Olson, E.N. (2007). Regulation of skeletal muscle sarcomere integrity and postnatal muscle function by Mef2c. *Mol Cell Biol* 27, 8143-8151.
- Potthoff, M.J., and Olson, E.N. (2007). MEF2: a central regulator of diverse developmental programs. *Development* 134, 4131-4140.
- Ptashne, M. (1988). How eukaryotic transcriptional activators work. *Nature* 335, 683-689.
- Pulipparacharuvil, S., Renthal, W., Hale, C.F., Taniguchi, M., Xiao, G., Kumar, A., Russo, S.J., Sikder, D., Dewey, C.M., Davis, M.M., *et al.* (2008). Cocaine regulates MEF2 to control synaptic and behavioral plasticity. *Neuron* 59, 621-633.
- Quinn, Z.A., Yang, C.C., Wrana, J.L., and McDermott, J.C. (2001). Smad proteins function as co-modulators for MEF2 transcriptional regulatory proteins. *Nucleic Acids Res* 29, 732-742.
- Rada-Iglesias, A., Bajpai, R., Swigut, T., Brugmann, S.A., Flynn, R.A., and Wysocka, J. (2011). A unique chromatin signature uncovers early developmental enhancers in humans. *Nature* 470, 279-283.
- Ramanan, N., Shen, Y., Sarsfield, S., Lemberger, T., Schutz, G., Linden, D.J., and Ginty, D.D. (2005). SRF mediates activity-induced gene expression and synaptic plasticity but not neuronal viability. *Nat Neurosci* 8, 759-767.
- Rao, R.C., Hennig, A.K., Malik, M.T., Chen, D.F., and Chen, S. (2011). Epigenetic regulation of retinal development and disease. *Journal of ocular biology, diseases, and informatics* 4, 121-136.
- Rashid, A.J., Cole, C.J., and Josselyn, S.A. (2014). Emerging roles for MEF2 transcription factors in memory. *Genes, brain, and behavior* 13, 118-125.
- Rivera, V.M., Sheng, M., and Greenberg, M.E. (1990). The inner core of the serum response element mediates both the rapid induction and subsequent repression of c-fos transcription following serum stimulation. *Genes Dev* 4, 255-268.
- Roberts, M.R., Hendrickson, A., McGuire, C.R., and Reh, T.A. (2005). Retinoid X receptor (gamma) is necessary to establish the S-opsin gradient in cone photoreceptors of the developing mouse retina. *Invest Ophthalmol Vis Sci* 46, 2897-2904.
- Robertson, G., Hirst, M., Bainbridge, M., Bilenky, M., Zhao, Y., Zeng, T., Euskirchen, G., Bernier, B., Varhol, R., Delaney, A., *et al.* (2007). Genome-wide profiles of STAT1 DNA association using chromatin immunoprecipitation and massively parallel sequencing. *Nat Methods* 4, 651-657.
- Rodriguez-Tornos, F.M., San Aniceto, I., Cubelos, B., and Nieto, M. (2013). Enrichment of conserved synaptic activity-responsive element in neuronal genes predicts a coordinated response of MEF2, CREB and SRF. *PLoS One* 8, e53848.

- Salma, J., and McDermott, J.C. (2012). Suppression of a MEF2-KLF6 survival pathway by PKA signaling promotes apoptosis in embryonic hippocampal neurons. *J Neurosci* 32, 2790-2803.
- Sandmann, T., Girardot, C., Brehme, M., Tongprasit, W., Stolc, V., and Furlong, E.E. (2007). A core transcriptional network for early mesoderm development in *Drosophila melanogaster*. *Genes Dev* 21, 436-449.
- Sandmann, T., Jensen, L.J., Jakobsen, J.S., Karzynski, M.M., Eichenlaub, M.P., Bork, P., and Furlong, E.E. (2006). A temporal map of transcription factor activity: mef2 directly regulates target genes at all stages of muscle development. *Dev Cell* 10, 797-807.
- Sartorelli, V., Huang, J., Hamamori, Y., and Kedes, L. (1997). Molecular mechanisms of myogenic coactivation by p300: direct interaction with the activation domain of MyoD and with the MADS box of MEF2C. *Mol Cell Biol* 17, 1010-1026.
- Sato, M., Nakazawa, M., Usui, T., Tanimoto, N., Abe, H., and Ohguro, H. (2005). Mutations in the gene coding for guanylate cyclase-activating protein 2 (GUCA1B gene) in patients with autosomal dominant retinal dystrophies. *Graefes Arch Clin Exp Ophthalmol* 243, 235-242.
- Savignac, M., Mellstrom, B., and Naranjo, J.R. (2007). Calcium-dependent transcription of cytokine genes in T lymphocytes. *Pflugers Arch* 454, 523-533.
- Schlesinger, J., Schueler, M., Grunert, M., Fischer, J.J., Zhang, Q., Krueger, T., Lange, M., Tonjes, M., Dunkel, I., and Sperling, S.R. (2011). The cardiac transcription network modulated by Gata4, Mef2a, Nkx2.5, Srf, histone modifications, and microRNAs. *PLoS Genet* 7, e1001313.
- Sebastian, S., Faralli, H., Yao, Z., Rakopoulos, P., Palii, C., Cao, Y., Singh, K., Liu, Q.C., Chu, A., Aziz, A., *et al.* (2013). Tissue-specific splicing of a ubiquitously expressed transcription factor is essential for muscle differentiation. *Genes Dev* 27, 1247-1259.
- Shalizi, A., Gaudilliere, B., Yuan, Z., Stegmuller, J., Shirogane, T., Ge, Q., Tan, Y., Schulman, B., Harper, J.W., and Bonni, A. (2006). A calcium-regulated MEF2 sumoylation switch controls postsynaptic differentiation. *Science* 311, 1012-1017.
- Shore, P., and Sharrocks, A.D. (1995). The MADS-box family of transcription factors. *Eur J Biochem* 229, 1-13.
- Sieni, E., Cetica, V., Hackmann, Y., Coniglio, M.L., Da Ros, M., Ciambotti, B., Pende, D., Griffiths, G., and Arico, M. (2014). Familial Hemophagocytic Lymphohistiocytosis: When Rare Diseases Shed Light on Immune System Functioning. *Frontiers in immunology* 5, 167.
- Skerjanc, I.S., and Wilton, S. (2000). Myocyte enhancer factor 2C upregulates MASH-1 expression and induces neurogenesis in P19 cells. *FEBS Lett* 472, 53-56.
- Slepek, T.I., Webster, K.A., Zang, J., Prentice, H., O'Dowd, A., Hicks, M.N., and Bishopric, N.H. (2001). Control of cardiac-specific transcription by p300 through myocyte enhancer factor-2D. *J Biol Chem* 276, 7575-7585.

- Smith, E., and Shilatifard, A. (2014). Enhancer biology and enhanceropathies. *Nat Struct Mol Biol* *21*, 210-219.
- Sohocki, M.M., Sullivan, L.S., Mintz-Hittner, H.A., Birch, D., Heckenlively, J.R., Freund, C.L., McInnes, R.R., and Daiger, S.P. (1998). A range of clinical phenotypes associated with mutations in CRX, a photoreceptor transcription-factor gene. *Am J Hum Genet* *63*, 1307-1315.
- Spitz, F., and Furlong, E.E. (2012). Transcription factors: from enhancer binding to developmental control. *Nature reviews Genetics* *13*, 613-626.
- Stehling-Sun, S., Dade, J., Nutt, S.L., DeKoter, R.P., and Camargo, F.D. (2009). Regulation of lymphoid versus myeloid fate 'choice' by the transcription factor Mef2c. *Nat Immunol* *10*, 289-296.
- Swain, P.K., Chen, S., Wang, Q.L., Affatigato, L.M., Coats, C.L., Brady, K.D., Fishman, G.A., Jacobson, S.G., Swaroop, A., Stone, E., *et al.* (1997). Mutations in the cone-rod homeobox gene are associated with the cone-rod dystrophy photoreceptor degeneration. *Neuron* *19*, 1329-1336.
- Swaroop, A., Kim, D., and Forrest, D. (2010). Transcriptional regulation of photoreceptor development and homeostasis in the mammalian retina. *Nature reviews Neuroscience* *11*, 563-576.
- Tapscott, S.J., Davis, R.L., Thayer, M.J., Cheng, P.F., Weintraub, H., and Lassar, A.B. (1988). MyoD1: a nuclear phosphoprotein requiring a Myc homology region to convert fibroblasts to myoblasts. *Science* *242*, 405-411.
- Thompson, D.A., Gyurus, P., Fleischer, L.L., Bingham, E.L., McHenry, C.L., Apfelstedt-Sylla, E., Zrenner, E., Lorenz, B., Richards, J.E., Jacobson, S.G., *et al.* (2000). Genetics and phenotypes of RPE65 mutations in inherited retinal degeneration. *Invest Ophthalmol Vis Sci* *41*, 4293-4299.
- Treisman, R., and Ammerer, G. (1992). The SRF and MCM1 transcription factors. *Curr Opin Genet Dev* *2*, 221-226.
- Untergasser, A., Nijveen, H., Rao, X., Bisseling, T., Geurts, R., and Leunissen, J.A. (2007). Primer3Plus, an enhanced web interface to Primer3. *Nucleic Acids Res* *35*, W71-74.
- Verzi, M.P., Agarwal, P., Brown, C., McCulley, D.J., Schwarz, J.J., and Black, B.L. (2007). The transcription factor MEF2C is required for craniofacial development. *Dev Cell* *12*, 645-652.
- Vetere, G., Restivo, L., Cole, C.J., Ross, P.J., Ammassari-Teule, M., Josselyn, S.A., and Frankland, P.W. (2011). Spine growth in the anterior cingulate cortex is necessary for the consolidation of contextual fear memory. *Proc Natl Acad Sci U S A* *108*, 8456-8460.
- Wada, Y., Abe, T., Itabashi, T., Sato, H., Kawamura, M., and Tamai, M. (2003). Autosomal dominant macular degeneration associated with 208delG mutation in the FSCN2 gene. *Archives of ophthalmology* *121*, 1613-1620.

- Wada, Y., Abe, T., Takeshita, T., Sato, H., Yanashima, K., and Tamai, M. (2001). Mutation of human retinal fascin gene (FSCN2) causes autosomal dominant retinitis pigmentosa. *Invest Ophthalmol Vis Sci* 42, 2395-2400.
- Wang, D., Garcia-Bassets, I., Benner, C., Li, W., Su, X., Zhou, Y., Qiu, J., Liu, W., Kaikkonen, M.U., Ohgi, K.A., *et al.* (2011). Reprogramming transcription by distinct classes of enhancers functionally defined by eRNA. *Nature* 474, 390-394.
- Wang, L., Fan, C., Topol, S.E., Topol, E.J., and Wang, Q. (2003). Mutation of MEF2A in an inherited disorder with features of coronary artery disease. *Science* 302, 1578-1581.
- Wang, X., She, H., and Mao, Z. (2009). Phosphorylation of neuronal survival factor MEF2D by glycogen synthase kinase 3beta in neuronal apoptosis. *J Biol Chem* 284, 32619-32626.
- White, M.A., Myers, C.A., Corbo, J.C., and Cohen, B.A. (2013). Massively parallel in vivo enhancer assay reveals that highly local features determine the cis-regulatory function of ChIP-seq peaks. *Proc Natl Acad Sci U S A* 110, 11952-11957.
- Xia, Z., Dudek, H., Miranti, C.K., and Greenberg, M.E. (1996). Calcium influx via the NMDA receptor induces immediate early gene transcription by a MAP kinase/ERK-dependent mechanism. *J Neurosci* 16, 5425-5436.
- Yanagi, Y., Masuhiro, Y., Mori, M., Yanagisawa, J., and Kato, S. (2000). p300/CBP acts as a coactivator of the cone-rod homeobox transcription factor. *Biochem Biophys Res Commun* 269, 410-414.
- Yang, Q., She, H., Gearing, M., Colla, E., Lee, M., Shacka, J.J., and Mao, Z. (2009). Regulation of neuronal survival factor MEF2D by chaperone-mediated autophagy. *Science* 323, 124-127.
- Yee, S.P., and Rigby, P.W. (1993). The regulation of myogenin gene expression during the embryonic development of the mouse. *Genes Dev* 7, 1277-1289.
- Yokokura, S., Wada, Y., Nakai, S., Sato, H., Yao, R., Yamanaka, H., Ito, S., Sagara, Y., Takahashi, M., Nakamura, Y., *et al.* (2005). Targeted disruption of FSCN2 gene induces retinopathy in mice. *Invest Ophthalmol Vis Sci* 46, 2905-2915.
- Yoshida, S., Mears, A.J., Friedman, J.S., Carter, T., He, S., Oh, E., Jing, Y., Farjo, R., Fleury, G., Barlow, C., *et al.* (2004). Expression profiling of the developing and mature Nrl^{-/-} mouse retina: identification of retinal disease candidates and transcriptional regulatory targets of Nrl. *Hum Mol Genet* 13, 1487-1503.
- Youn, H.D., Chatila, T.A., and Liu, J.O. (2000a). Integration of calcineurin and MEF2 signals by the coactivator p300 during T-cell apoptosis. *EMBO J* 19, 4323-4331.
- Youn, H.D., Grozinger, C.M., and Liu, J.O. (2000b). Calcium regulates transcriptional repression of myocyte enhancer factor 2 by histone deacetylase 4. *J Biol Chem* 275, 22563-22567.

- Youn, H.D., and Liu, J.O. (2000). Cabin1 represses MEF2-dependent Nur77 expression and T cell apoptosis by controlling association of histone deacetylases and acetylases with MEF2. *Immunity* 13, 85-94.
- Youn, H.D., Sun, L., Prywes, R., and Liu, J.O. (1999). Apoptosis of T cells mediated by Ca²⁺-induced release of the transcription factor MEF2. *Science* 286, 790-793.
- Young, R.W. (1985). Cell differentiation in the retina of the mouse. *The Anatomical record* 212, 199-205.
- Young, T.L., and Cepko, C.L. (2004). A role for ligand-gated ion channels in rod photoreceptor development. *Neuron* 41, 867-879.
- Zhang, X., Serb, J.M., and Greenlee, M.H. (2011). Mouse retinal development: a dark horse model for systems biology research. *Bioinformatics and biology insights* 5, 99-113.
- Zhang, Y., Liu, T., Meyer, C.A., Eeckhoute, J., Johnson, D.S., Bernstein, B.E., Nusbaum, C., Myers, R.M., Brown, M., Li, W., *et al.* (2008). Model-based analysis of ChIP-Seq (MACS). *Genome biology* 9, R137.
- Zhou, Z., Hong, E.J., Cohen, S., Zhao, W.N., Ho, H.Y., Schmidt, L., Chen, W.G., Lin, Y., Savner, E., Griffith, E.C., *et al.* (2006). Brain-specific phosphorylation of MeCP2 regulates activity-dependent Bdnf transcription, dendritic growth, and spine maturation. *Neuron* 52, 255-269.
- Zweier, M., Gregor, A., Zweier, C., Engels, H., Sticht, H., Wohlleber, E., Bijlsma, E.K., Holder, S.E., Zenker, M., Rossier, E., *et al.* (2010). Mutations in MEF2C from the 5q14.3q15 microdeletion syndrome region are a frequent cause of severe mental retardation and diminish MECP2 and CDKL5 expression. *Human mutation* 31, 722-733.
- Zweier, M., and Rauch, A. (2012). The MEF2C-Related and 5q14.3q15 Microdeletion Syndrome. *Molecular syndromology* 2, 164-170.